SOVIET PHYSICS USPEKHI VOLUME 5, NUMBER 5 MARCH-APRIL, 1963

HIGH POWER ELECTRONICS

P. L. KAPITZA

Usp. Fiz. Nauk 78, 181—265 (October, 1962)

CONTENTS

INTRODUCTION

ALTHOUGH electronic processes are finding increasing use in modern electrical engineering, it is easy to see that there is nevertheless a field where electronics has barely penetrated. To be sure, electronic processes are used most extensively at present in measurements (cathode ray oscillographs, photocells, high frequency measurements, amplifiers, etc.), in cybernetics (automation, computers, stabilizers, etc.), and in communication (radio, television, radar, etc.). But the application of microwave electronics to the solution of power problems is still in its initial stage.

I have named this branch "high-power electronics." This name, of course, is arbitrary, since it is impossible to delineate the boundary at which "high power" begins. It therefore seems to me that the term "high-power electronics" should be used to describe that branch of electrical engineering in which microwave electronics is used for direct power generation, i.e., to produce electromagnetic oscillations which are transformed not only into electromagnetic waves but also into heat, into the energy of accelerated corpuscular beams, and into other forms of energy.

It seems to me that large-scale power generation at microwave frequencies is one of the most promising trends in modern electrical engineering. The main advantages of microwave power are by now quite clearly manifest, and consist in the possibility of concentrating a large amount of electromagnetic energy in small volumes, and also in the exceeding flexibility with which the high-frequency energy is transformed into other types of energy (concentrated heat supply; acceleration of elementary particles; production, heating, and containment of plasma, etc.). The reason why electronics is not extensively used in power applications is that there is at present no effective and reliable method for generating microwave energy and for converting it into other forms of energy.

In order to develop high-power electronics it is necessary to start with scientifically sound solutions of these problems.

My co-workers and I have engaged in these questions during the last few years, and accumulated much scientific material which we are now able to publish. Inasmuch as most of the work was done several years ago, we have decided to print the material in the form in which it was recorded at that time, without reference to the literature.

Our work began with a theoretical investigation of the processes involved in the generation of high-power microwave oscillations. We started from the premise that high power oscillations can be produced effectively only by electronic processes which occur in constant (crossed) magnetic and electric fields, and developed a method for a theoretical analysis of such processes. This method, as will be shown below, is sufficiently general and complete; it can be successfully used, in particular, to develop a lucid quantitative theory of the processes that occur in magnetron oscillators.

This method and the most important results are contained in our large paper "High-power Electronics," which was completed in April 1952 and after which the entire topic was named. Following that work, our research on high-power electronics expanded in scope. Our next theoretical paper "Natural Oscillations of Cavity Resonators with Latticed Partition," completed in 1955, is contained in a collection separately published by the press of the U.S.S.R. Academy of Sciences.

Later reports of our laboratory will be published in the subsequent collections.

The initial stage of this work (both experimental and theoretical) was carried out by myself in closest collaboration with S. I. Filimonov and S. P. Kapitza. Unflagging interest in the theoretical problems was shown by V. A. Fock, who offered many valuable suggestions. I am grateful to my friends and co-workers for participating in my scientific work, in spite of the difficult conditions under which it was carried out in 1946—1952.

I wish to note also that much of the editorial work was undertaken by L. A. Vaĭnshteĭn, to whom all the authors are deeply grateful.

PROBLEMS OF HIGH-POWER ELECTRONICS

Electronics deals with many physical phenomena connected with the flow of electric current through gases. Noteworthy among the physical properties of an electric current flowing through a gas are two important and interesting attributes which uncover entirely new possibilities for electrical engineering and are therefore extensively used in practice.

The first property of electrical processes accompanying the flow of current through a gas is that their inertia is exceedingly small and that they can therefore be readily controlled. The physical reason for this property has been understood ever since the discovery of electrons: the charge is transported by electrons, the mass of which is several thousand times smaller than the mass of the ions. When electric current flows through a gas (in contrast to a metal), it is possible to control the motion of the electrons rapidly and effectively.

The second important physical property of electric currents in gases is that if the gas is sufficiently rarefied, the motion of the electron in the gas occurs with very low "friction," and therefore with low losses; this makes it possible to impart very high velocities to the electrons that produce the current. In a metal, large current with low ohmic losses is produced by a large number of slowly moving electrons. In the gas, to the contrary, a current with the same amount of loss can be produced by a small number of fast electrons, owing to the fact that the losses practically disappear at sufficiently low pressures.

The freedom of motion of the electrons in a gas and their inertia had been long made use of in vacuum tubes, which made possible the successful development of modern radio (particularly at microwave frequencies); but electronic processes are as yet not efficient enough for use in power. The capabilities afforded by the flow of current through gases are employed in power engineering only to solve secondary problems.*

One might think that the reason for it is that there is no need for fast processes in power. Such a thought must be rejected, for many very important problems in electrical engineering are still unsolved and cannot be solved without electronics. We need merely mention among these problems the transmission of large amounts of power over waveguides through long distances at low losses, the production of intense highly-directional beams of electromagnetic waves and corpuscular beams, the direct utilization of atomic energy, and effective methods of isotope separation. Even this far from complete list is sufficient to show the prospects latent in the development of high-power electronics.

any principal reasons preventing the development of high-power electronics? I believe that this question must be answered in the affirmative: such reasons do exist; although at first glance they seem to be insignificant, they have in effect been the decisive obstacles so far. Only by overcoming these obstacles can electronic processes at high powers be made feasible.

If electrons move in vacuum (in the absence of ions), they form a negatively charged cloud. Because the charges are of like sign, they repel one another, so that their motion cannot be regular. If the cloud has low density, the repulsion due to the space charge will hardly distort the motion, but with increasing power the cloud density increases and with it the repulsive forces. These forces can become so large as to completely disturb the character of the electron motion as the power is increased. In ordinary electronic devices, say vacuum tubes, this phenomenon occurs at relatively low powers. Not much can be done to raise the permissible power by increasing the dimensions of the apparatus, for it can be shown that the linear dimensions must increase as the square of the power, so that at sufficiently high power all dimensions become unattainably large.

The disturbing action of the space charge is the principal factor limiting the use of electronic processes at high powers.

What are the means of combatting the limiting action of space charge? There are two such means, which are frequently very effective.

The first has already been extensively used: this is neutralization of space charge by positive ions in the gas. It is well known that at low vacuum, the negatively charged electron cloud contains positive ions, which have too high an inertia to participate in the dynamics of the process, but neutralize the mutual repulsion of the electrons. This makes feasible electronic processes of appreciable power. This is done, for example, in mercury arc rectifiers, in thyratrons, and in other gas-filled tubes.

This measure, however, has two essential and unavoidable shortcomings, which offset to a considerable degree the main advantages of the electronic processes. The first shortcoming is the additional loss due to the presence in the working space of gas molecules with which the rapidly moving electrons collide. The sec-

*This was written in 1952.

ond and principal shortcoming is that the possibility of effective electric control of the electron motion is greatly limited in the presence of extraneous ions.

The second means of combatting space charge is more effective: the space charge is neutralized by forces due to motion of the electrons in a constant magnetic field. By way of an example illustrating the mechanism of this process, let us analyze one of the simplest and best known cases of neutralization of the harmful action of space charge by means of a magnetic field, wherein the electron cloud moves parallel to the force lines of the magnetic field. Under the influence of the space charge, the electrons acquire transverse velocities perpendicular to the magnetic field. The resultant Lorentz force twists the electron trajectories in a plane perpendicular to the principal motion, and returns the electrons to the cloud. As a result, the cloud does not spread out as it moves and maintains a constant transverse cross section.

The focusing action of the constant magnetic field is well known and is extensively used in practice to compensate for the repulsion of the space charges. This remarkable property of magnetic fields is manifest also in other more complicated cases, when it frequently escapes attention in spite of the fact that the physical mechanism is analogous to that just analyzed. The magnetron is the clearest example of an instrument in which the focusing action of the magnetic field on the electronic process is realized in masked form.

As is well known, the magnetron generates microwave oscillations, which are excited by the uniform motion of an electron cloud with periodic charge-density distribution. A beam with clearly outlined boundaries and with high charge density is feasible only if the repulsion forces between the electrons are neutralized by a constant magnetic field. This is attained by a process, called phase focusing, which will be investigated in detail in the present paper. This process explains why such exceedingly high power can be realized in modern magnetrons in pulsed modes, reaching hundreds of kilowatts per cm^2 of working surface of the cathode around which the electron cloud moves. To be sure, this power is produced in pulses of not more than several microseconds, but this does not change the principal aspect of the problem, since the time necessary to establish the electronic processes is a negligible fraction of the pulse duration.

The production of such power shows that the limitations imposed by space charge on the high-power electronic processes can be eliminated if the electrons move in a permanent magnetic field.

It is appropriate to raise here the question: why have electronic processes in a magnetic field not been used hitherto for high-power microwave electrical engineering? I believe that there are three reasons for it.

The first reason is that the great possibilities offered by electronics for the development of high-power electrical engineering have not yet been fully recognized.

Second: no sufficient scientific foundation has yet been developed for the problems that can be solved by high-power electronics.

Third: the physical theory of the phenomena occurring in the corresponding electronic devices is not sufficiently understood; the difficulties connected with the calculations for such phenomena and devices have not yet been overcome.

Our investigations have been aimed at solving these three problems, both theoretically and experimentally.

Before proceeding to a detailed exposition, I wish to present a general description of the path followed in the research.

I believed that the most important was to find a clear and readily realizable method for the theoretical analysis of the electronic processes that occur in a constant magnetic field. The unsatisfactory status of the existing theoretical level can be illustrated by the calculation method usually employed in the design of magnetrons: after many years of (essentially empirical) work, a large number of various magnetrons are produced, from which the specimens with the best characteristics are chosen; mathematical formulas obtained by similarity theory are then used to recalculate the performance of these magnetrons under other operating conditions, in which case they retain the same basic characteristics. The magnetrons obtained in such an empirical way are satisfactory devices, with efficiencies reaching 60—70%. This method enables the design engineers to satisfy current demands, but of course cannot lead to an understanding or utilization of all the possibilities latent in the electronics of the magnetron.

In our researches we attempted first of all to discover the mechanism of the electronic processes occurring in the presence of a magnetic field, and then developed methods for their calculation.

This problem reduces to solving equations of motion which, although well formulated, are rather complicated. So far they were amenable only to numerical integration, so that it was difficult to elucidate the physical picture of the studied phenomena. The method of solving these equations, described in Chapter I, is based on the periodicity of the developing processes, which are due both to the permanent magnetic field and to the high frequency oscillations. When this periodicity is eliminated by the mathematical averaging operation, a simple and sufficiently accurate solution is obtained, which makes possible an understanding of the physical picture of the phenomena and which leads to mathematical equations that are suitable for practical calculations. The electron trajectories, which were hitherto determined by numerical integration, are obtained by this method in explicit form in terms of elementary functions.

In the subsequent chapters it is shown how this method is used to solve various specific electronic

problems and how the results obtained are experimentally confirmed. We have investigated in detail the processes that occur in the planotron and in the magnetron. The planotron is similar to the magnetron, except that the magnetron closes on itself, as it were, while the planotron is a magnetron which is cut open and unrolled in a plane, hence its name (a detailed description is found in Chapter VII). In Chapters II–IV we give a detailed theoretical investigation of the planotron. In Chapter VI we apply our method to ordinary multicavity magnetrons and compare the obtained theoretical results with the published experimental data.

In Chapter VIII we investigate the resonant action of a high frequency field on the circular (Larmor) motion of charged particles and consider theoretically in this connection an isotope-separation process which makes use of this action. The calculation is by the averaging method and leads to a quantitative description of the process, which has other applications, too.

Chapter IX is devoted to a general analysis of other problems of high-power electronics, which for the time being are rather problematic, and which may be solved by using a planotron. It is shown that power transmission over large distances is possible in principle. The point is that the theory implies the reversibility of the electronic processes in the planotron and in the magnetron, so that they can be used not only to convert direct current into high frequency oscillations, as at present, but also change high frequency oscillations into direct current. This makes feasible transmission of electricity over waveguides in the form of high-frequency waves. We then describe a possible device in which high-power beams of fast electrons or ions can be obtained with the aid of a planotron.

The arguments advanced in Chapter IX are still moot and merely illustrate the premise that the development of high power electronics is of great importance to science and technology.

In conclusion, I wish to recall that before electrical engineering turned to power, it engaged extensively in the past century only in problems of electric communication (telegraph, signalization, etc.). It is quite probable that history will repeat: now electronics is principally used for radio communication, but its future lies in the solution of the most important problems of power engineering.

I. SOLUTION OF THE FUNDAMENTAL EQUATION OF MOTION OF CHARGED PARTICLES BY THE TIME-AVERAGING METHOD

As was indicated in the introduction, an important factor in the high-power electronic problems of interest to us is the motion of charged particles under the simultaneous influence of electric and magnetic fields.*

*We consider essentially the motion of electrons, and only in Chapter VIII will the averaging method developed below be applied to the motion of ions.

Since we can confine ourselves in most cases to a consideration of the two-dimensional problem, the classical equations for a charge e with mass m have the form

$$\left.\begin{aligned} m\ddot{x} - \frac{e}{c}H\dot{y} &= eE_x, \\ m\ddot{y} + \frac{e}{c}H\dot{x} &= eE_y. \end{aligned}\right\} \tag{1.01}$$

The electric field projections E_x and E_y along the x and y axes can depend both on x and on y, and also on the time t. As to the magnetic field, in the problems of interest to us we can regard it as constant in time and in space, with only one component H perpendicular to the x, y plane.

Inasmuch as Eqs. (1.01) contain the accelerations $\ddot{x}$ and $\ddot{y}$ and the velocities $\dot{x}$ and $\dot{y}$, we have a fourth-order system of differential equations, which has been solved in final form only for very simple motions. For the cases of practical significance, for example for the motion of electrons in a magnetron, numerical integration is customarily used, but the results obtained in this way are of little help in the understanding of the mechanism of the electronic processes and do not permit the calculation of the main characteristics of electron devices of this type. The method which we developed for solving (1.01), by averaging over the time, is effective for the study of electronic processes in which so-called resonance phenomena take place. Although this method is approximate, it does cast light on the physical nature of the processes and turns out to be convenient for quantitative interpretation of the experimental material.

To abbreviate the notation we introduce the following symbols:

$$f_x = \frac{e}{m}E_x, \quad f_y = \frac{e}{m}E_y, \quad \Omega = \frac{eH}{mc}, \tag{1.02}$$

where f_x and f_y obviously have the dimension of acceleration and Ω has the dimension of angular velocity (Larmor frequency), and we rewrite (1.01) in the form

$$\left.\begin{aligned} \ddot{x} - \Omega\dot{y} &= f_x, \\ \ddot{y} + \Omega\dot{x} &= f_y. \end{aligned}\right\} \tag{1.03}$$

The next simplification consists of changing over to the complex quantities

$$\left.\begin{aligned} z &= x + iy, & z^* &= x - iy, \\ f &= f_x + if_y, & f^* &= f_x - if_y. \end{aligned}\right\} \tag{1.04}$$

The asterisk denotes the conjugate. By virtue of the relations

$$x = \frac{z+z^*}{2}, \qquad y = \frac{z-z^*}{2i} \tag{1.05}$$

we obtain in lieu of the system (1.03) the single complex equation

$$\ddot{z} + i\Omega\dot{z} = f(z,\ z^*,\ t). \tag{1.06}$$

This equation has an especially simple solution in the following three cases, which we shall call the fun-

damental cases. We denote by α and β the constant complex quantities determined by the initial conditions, and by z_0 the solution of (1.06) in the fundamental cases.

The first fundamental case of motion occurs when there is no acceleration

$$z_0 = \alpha + \beta e^{-i\Omega t} \qquad (f = f_0 = 0). \tag{1.07}$$

This is the case of free motion of the electrons in a magnetic field, when the motion has angular velocity Ω along a circular orbit with radius $|\beta|$ and with center at the point with complex coordinate α.

The second fundamental case of motion corresponds to constant acceleration $f = f_0$; then

$$z_0 = \alpha - \frac{if_0}{\Omega} t + \beta e^{-i\Omega t} \qquad (f = f_0 = \text{const}) \tag{1.08}$$

and the motion is along a circular orbit with angular velocity $-\Omega$, the center of the circular orbit moving with uniform velocity $-if_0/\Omega$ in a direction perpendicular to the acceleration f_0. This is the classical motion of an electron along a cycloid or trochoid (when $\beta = 0$ the trochoid degenerates into a straight line); it is particularly significant in the theory of the planotron (planar magnetron). It is obvious that the first fundamental case of motion can be treated as a particular case of the second fundamental case of motion by putting $f_0 = 0$.

The third fundamental case of motion is obtained when the acceleration f depends linearly on z; then

$$z_0 = \alpha e^{-i\Omega_1 t} + \beta e^{-i\Omega_2 t} \qquad (f = f_0 = Cz). \tag{1.09}$$

Substituting z_0 in (1.05) we obtain Ω_1 and Ω_2 as the roots of a quadratic equation; they are

$$\left.\begin{aligned} \Omega_1 &= \frac{\Omega}{2}\left(1 - \sqrt{1 - \frac{4C}{\Omega^2}}\right), \\ \Omega_2 &= \frac{\Omega}{2}\left(1 + \sqrt{1 - \frac{4C}{\Omega^2}}\right). \end{aligned}\right\} \tag{1.10}$$

The solution (1.09) represents an epitrochoid, which can be regarded as a superposition of two circular motions: the electrons move along a circle of radius $|\beta|$ with angular velocity $-\Omega_2$, and the center of this circle moves about the origin with angular velocity $-\Omega_1$ along a circle of radius $|\alpha|$. This case is important for magnetron theory (see Chapter VI).

In all these three fundamental cases we can regard the motion of the electron as consisting of two parts, motion along a circular orbit and the motion of the center of this circular orbit. In the first fundamental case the center of the circular orbit is stationary, in the second case it moves uniformly on a straight line, and in the third case it moves uniformly along a circle.

Our approximate method is based on the fact that in the majority of cases of interest to us the character of motion of the particle does not change much even in the presence of an additional acceleration (apart from the acceleration f_0) which depends in more complicated fashion on the coordinates x and y and on the time t.

Let us assume that this additional acceleration, which we shall denote by F, is produced by an electric field $E = E_x + iE_y$. Then the total acceleration of the particles has in complex notation the form

$$f = f_0 + F(z, z^*, t), \qquad F = \frac{e}{m} E, \tag{1.11}$$

where f_0 is the acceleration in one of the three fundamental cases.

In those cases when the additional acceleration F does not distort the character of the particle motion, we obtain an approximate solution of Eq. (1.06) by using the following averaging method. In most problems of practical interest, the value of the constant magnetic field is large, and this makes the term $i\Omega\dot{z}$ in (1.06) large compared with $\ddot{z}$. Therefore at large values of Ω the displacement of the center of the orbit during the time of a complete period of revolution of the particle is small and the influence of the orbital motion of the charged particles on the motion of the center of their orbit can be regarded with sufficient accuracy as an "average" over a short period of time.*

Mathematically this method is formulated in the following manner. We introduce the acceleration (1.12) into Eq. (1.06) and the coordinates of the particle, which moves in accordance with the resultant equation

$$\ddot{z} + i\Omega\dot{z} = f_0 + F \tag{1.12}$$

will be denoted by z, to distinguish them from the particle coordinates z_0 in the fundamental cases of motion, when there is no acceleration F.

Let us consider particle motion which can be regarded as a perturbation of the first or second fundamental case of motion. We seek a solution in the same form as given in (1.08) for z_0, but we now assume that the quantities α and β are no longer constant. We then obtain the following values for z and its time derivatives:

$$\left.\begin{aligned} z &= \alpha - \frac{if_0}{\Omega} t + \beta e^{-i\Omega t} = z_0, \\ \dot{z} &= \dot{\alpha} + \dot{\beta} e^{-i\Omega t} + \dot{z}_0, \\ \ddot{z} &= \ddot{\alpha} + (\ddot{\beta} - 2i\Omega\dot{\beta}) e^{-i\Omega t} + \ddot{z}_0. \end{aligned}\right\} \tag{1.13}$$

According to these formulas, the motion can be regarded for a certain short time interval, for certain definite values of α and β and their derivatives, as a somewhat distorted first or second fundamental case of motion. Inasmuch as we have two variables α and β, we can, without violating (1.13), impose additional

*When high-frequency oscillations are superimposed on smooth motion of a material point, it is possible to obtain an approximate solution of certain problems of mechanics by an averaging method similar to that described in the present paper. Thus, the method described has enabled the author to obtain a simple and lucid solution of the problem of a pendulum with vibrating support (the solution of this problem was hitherto very complicated). See the article "Dynamic Stability of a Pendulum with Oscillating Point of Suspension" [JETP 21 (5), 588 (1951)] or "Pendulum with Vibrating Suspension" [UFN 44 (1), 7 (1951)].

conditions on α and β. As will be seen from the subsequent averaging, it is important that the values of z and z_0 be as close to each other as possible during the averaging time T. This condition can be satisfied by choosing α and β in such a way that at each instant of time we have agreement not only between z and z_0 but also between their first derivatives $\dot{z}$ and $\dot{z}_0$. For this purpose it is necessary to impose on $\dot{\alpha}$ and $\dot{\beta}$ the following condition:

$$\dot{\alpha}+\dot{\beta}e^{-i\Omega t}=0. \tag{1.14}$$

By virtue of this condition the expressions in (1.13) assume the form

$$\left.\begin{aligned} &z=z_0,\\ &\dot{z}=\dot{z}_0,\\ &\ddot{z}=-\ddot{\alpha}-\ddot{\beta}e^{-i\Omega t}+\ddot{z}_0=-i\Omega\dot{\beta}e^{-i\Omega t}+\ddot{z}_0. \end{aligned}\right\} \tag{1.15}$$

Substituting these values into the fundamental equation (1.12) and using (1.14) we obtain

$$\left.\begin{aligned} \dot{\alpha}&=-\frac{i}{\Omega}F(z,\ z^*,\ t),\\ \dot{\beta}&=\frac{i}{\Omega}F(z,\ z^*,\ t)\,e^{i\Omega t}. \end{aligned}\right\} \tag{1.16}$$

In the problem of interest to us F will be a rapidly oscillating function of the time, so that $\dot{\alpha}$ and $\dot{\beta}$ will also contain rapidly oscillating terms. In order for the sought-for motion to acquire the simple and clear analytic form necessary for practical use, we must smooth out these rapid small oscillations; for this purpose we replace $\dot{\alpha}$ and $\dot{\beta}$ by their averages $\bar{\dot{\alpha}}$ and $\bar{\dot{\beta}}$ over the time interval T:

$$\left.\begin{aligned} \bar{\dot{\alpha}}&=-\frac{i}{\Omega}\frac{1}{T}\int_{t-T/2}^{t+T/2}F(z,\ z^*,\ t)\,dt,\\ \bar{\dot{\beta}}&=\frac{i}{\Omega}\frac{1}{T}\int_{t-T/2}^{t+T/2}F(z,\ z^*,\ t)\,e^{i\Omega t}\,dt. \end{aligned}\right\} \tag{1.17}$$

It is clear that along with smoothing of the derivatives it is necessary to smooth the values of α and β themselves. This is done in the following fashion: in order to carry out the averaging, it is necessary to know the time dependence of z and z* under the integral sign; since this is not known, we can replace them by the known values z_0 and z_0^* (with constant α and β). As can be seen from (1.15) we can, in view of the condition (1.14), replace z by z_0 with a high degree of approximation (discarding only $\ddot{\alpha}$ and $\ddot{\beta}$). The averaging time T is chosen in accordance with the periodicity of the integrand such that after averaging the integrand does not depend on the time, but only on α and β, which we identify with the average values $\bar{\alpha}$ and $\bar{\beta}$ (we assume here $\dot{\bar{\alpha}}=\bar{\dot{\alpha}}$ and $\dot{\bar{\beta}}=\bar{\dot{\beta}}$). Thus we obtain ultimately

$$\left.\begin{aligned} \dot{\bar{\alpha}}&=-\frac{i}{\Omega}\overline{F(z_0,\ z_0^*,\ t)},\\ \dot{\bar{\beta}}&=\frac{i}{\Omega}\overline{F(z_0,\ z_0^*,\ t)\,e^{i\Omega t}}. \end{aligned}\right\} \tag{1.18}$$

We reason analogously in the case when the motion of the particle can be conveniently regarded as a perturbation to the third fundamental case. The fundamental equation is written

$$\ddot{z}+i\Omega\dot{z}=Cz+F(z,\ z^*,\ t) \tag{1.19}$$

and we seek its solution in the form

$$z=\alpha e^{-i\Omega_1 t}+\beta e^{-i\Omega_2 t},$$

where, unlike (1.09), α and β depend on t. For a more effective agreement between the perturbed motion z and the fundamental motion z_0 we introduce the condition

$$\dot{\alpha}e^{-i\Omega_1 t}+\dot{\beta}e^{-i\Omega_2 t}=0, \tag{1.20}$$

which is analogous to (1.14). We then obtain the following values for z and its derivatives:

$$\left.\begin{aligned} &z=z_0,\\ &\dot{z}=\dot{z}_0,\\ &\ddot{z}=-\ddot{\alpha}e^{-i\Omega_1 t}-\ddot{\beta}e^{-i\Omega_2 t}+z_0\\ &\quad=-i\Omega_1\dot{\alpha}e^{-i\Omega_1 t}-i\Omega_2\dot{\beta}e^{-i\Omega_2 t}+\ddot{z}_0. \end{aligned}\right\} \tag{1.21}$$

Substituting these quantities into the fundamental equation (1.19), using (1.10) and condition (1.20), and reasoning as in the preceding case, we obtain for the averaged (slowly varying) quantities $\bar{\alpha}$ and $\bar{\beta}$ the following equations:

$$\left.\begin{aligned} \dot{\bar{\alpha}}&=-\frac{i}{\sqrt{\Omega^2-4C}}\overline{F(z_0,\ z_0^*,\ t)\,e^{i\Omega_1 t}},\\ \dot{\bar{\beta}}&=\frac{i}{\sqrt{\Omega^2-4C}}\overline{F(z_0,\ z_0^*,\ t)\,e^{i\Omega_2 t}}. \end{aligned}\right\} \tag{1.22}$$

The average time T is again determined from the periodicity of the various terms of the averaged function.*

The variables in (1.22) can be written in the form

$$\left.\begin{aligned} \bar{\alpha}&=Re^{i\theta},\quad \dot{\bar{\alpha}}=(\dot{R}+iR\dot{\theta})\,e^{i\theta},\\ \bar{\beta}&=ae^{i\varphi},\quad \dot{\bar{\beta}}=(\dot{a}+ia\dot{\varphi})\,e^{i\varphi}. \end{aligned}\right\} \tag{1.23}$$

Equating real and imaginary parts in each equation of (1.22), we obtain four equations, from which we determine the radial velocities $\dot{R}$ and $\dot{a}$ and the angular velocities $\dot{\theta}$ and $\dot{\varphi}$ associated with them. By determining the time dependence of $\bar{\alpha}$ and $\bar{\beta}$ we can find the sought motion of the particles. We obtain here separately the trajectory of the center of the circular or-

*The derivation of (1.13) and (1.22) has been modified somewhat compared with the derivation contained in the original manuscript (1952). The conditions of slow variation were imposed on the quantities α and β over the averaging period T from the very beginning, in place of the conditions (1.14) and (1.20). Both methods lead to the same equations and to the same error estimates. The possibility of using conditions (1.14) and (1.20) and that this simplifies the derivation was graciously pointed out by L. A. Vaĭnshteĭn.

bit and the variation of the radius and phase of the orbital motion.

The complexity of the mathematical calculations depends on the integration connected with the time averaging. The form of the integrand determines the method of calculating the right halves of the equation; sometimes they can be reduced to certain forms of definite integrals, and then the integration limits are determined by the averaging period T. The averaging greatly simplifies if the integrand can be expanded in powers of the frequencies. Then the constant time-independent term of the expansion gives the averaged value, and terms with the lowest frequencies determine the period T of the values of $\dot{\alpha}$ and $\dot{\beta}$ necessary for the "smoothing." An example of such an averaging will be given in the next chapter.

The accuracy with which the motion is calculated is determined by the following factors. The first and principal error reduces to the difference that arises as a result of replacing $\dot{\alpha}$ and $\dot{\beta}$ by the smoothed quantities $\bar{\dot{\alpha}}$ and $\bar{\dot{\beta}}$. This difference can be estimated only for specific functions F. But it is easy to see that for any function the uncertainty in the coordinates of the particle for any time cannot exceed

$$\Delta\alpha = |\dot{\alpha}|T \quad \text{and} \quad \Delta\beta = |\dot{\beta}|T, \tag{1.24}$$

where T is the necessary averaging time. Usually

$$T \sim \frac{2\pi}{\Omega}, \quad |\dot{\alpha}| \sim \frac{|F|}{\Omega}.$$

Therefore

$$\Delta\alpha \sim \frac{2\pi|F|}{\Omega^2}. \tag{1.25}$$

Thus, the uncertainty in the position of the particles at a given instant of time decreases with the square of the magnetic field, increases in proportion to the additional acceleration F, and does not depend on the constant acceleration f_0.

Another factor which limits the accuracy of averaging is the substitution of z_0 for z in the integrand. As was already mentioned, the difference between z and z_0 is small, owing to the conditions (1.14) and (1.20) superimposed on $\dot{\alpha}$ and $\dot{\beta}$; it depends only on the second derivatives. We shall not consider it here. The actual degree of approximation can be determined reliably only on the basis of an analysis of specific examples (see Chapter III). We merely note here that both the feasibility of averaging itself, and the possibility of replacing z by z_0 during the averaging are determined by the fact that the quantity (1.25) must be small compared with the characteristic geometrical dimensions which determine the path of the particle (for example, the distance between the cathode and the anode) or the spatial variation of the field (for example, the periodicity of the resonant structure or the wavelength).

Further development of the method makes it possible to study, without special difficulties, the distortion and, in final analysis, the stability of the obtained trajectories under the influence of perturbing factors. Such factors, which influence the motion under real conditions, are: the field produced by the space charge, the inhomogeneity of the magnetic field, the inaccuracy in the manufacture or adjustment of the device, etc. A general method for taking these disturbing factors into account reduces to the following calculations.

As can be seen from (1.18) and (1.22), in order for $\bar{\dot{\alpha}}$ and $\bar{\dot{\beta}}$ not to vanish it is necessary that the averaged function have a constant term. For this purpose it is necessary that F have a periodicity which is matched both in time and in space. The mode under which such matching is produced accurately will be called the "resonant" mode. To solve the electronics problems of interest to us, only such "resonant modes" are of interest, for only in such modes does even a small additional acceleration F change appreciably the motion of the charged particles.

In practice, great interest attaches to the stability of such resonant modes. Usually the problem is formulated as follows. Let us assume that the motion occurs in accord with Eq. (1.12) and a resonant mode sets in for certain values of accelerations f_0 and of the Larmor frequency Ω. Then the velocity is determined by the first equation of (1.18). Let us assume that such a disturbing factor has changed the acceleration f_0 by a small amount Δf_0; the question is how this affects the velocity $\bar{\dot{\alpha}}$. We write Eq. (1.12) in the form

$$\ddot{z} + i\Omega\dot{z} = f_0 + \Delta f_0 + F \tag{1.26}$$

and consider Δf_0 + F as a supplementary acceleration. Using the same arguments as before, we can replace (1.18) immediately by the following equation for the perturbed acceleration $\bar{\dot{\alpha}}'$:

$$\bar{\dot{\alpha}}' = -\frac{i}{\Omega}(\Delta f_0 + \bar{F}); \tag{1.27}$$

Inasmuch as Δf_0 is constant and F remains the same as before, we obtain by substituting the value of $\bar{\dot{\alpha}}$ from (1.18)

$$\bar{\dot{\alpha}}' = \bar{\dot{\alpha}} - i\frac{\Delta f_0}{\Omega}. \tag{1.28}$$

We thus obtain a simple result: the velocity $\bar{\dot{\alpha}}$ has changed by an amount $-i\,\Delta f_0/\Omega$. Expanding the real and imaginary parts of Δf_0, $\bar{\dot{\alpha}}$, and $\bar{\dot{\alpha}}'$ we obtain each velocity component. In this way we can determine the distortion of the initial trajectory, and also the stability of the process. It is usually disturbed when $\bar{\dot{\alpha}}$ and $\Delta f_0/\Omega$ become comparable in absolute magnitude.

As another example, let us consider the account of the disturbing factors in the third fundamental case of motion. We assume that in (1.20) the acceleration Cz, produced by the constant electric field, changes by an amount ΔCz. Then the equation of motion can be

written in the form

$$\ddot{z} + i\Omega\dot{z} = Cz + \Delta Cz = F. \qquad (1.29)$$

Let us determine $\dot{\bar{\alpha}}'$ in the same way as $\dot{\bar{\alpha}}$ before; we then obtain

$$\dot{\bar{\alpha}}' = -\frac{i}{\sqrt{\Omega^2 - 4C}}\left(\overline{\Delta C z_0 e^{i\Omega_1 t}} + \overline{F e^{i\Omega_1 t}}\right). \qquad (1.30)$$

Carrying out the averaging, substituting z_0 from (1.09), we obtain

$$\dot{\bar{\alpha}}' = \dot{\bar{\alpha}} - \frac{i}{\sqrt{\Omega^2 - 4C}}\Delta C\bar{\alpha}. \qquad (1.31)$$

Substituting the values of $\dot{\bar{\alpha}}$ and $\dot{\bar{\alpha}}'$ from (1.23) and comparing real and imaginary parts we obtain

$$\left.\begin{aligned} \dot{\theta}' &= \theta - \frac{\Delta C}{\sqrt{\Omega^2 - 4C}}, \\ \dot{R}' &= \dot{R}. \end{aligned}\right\} \qquad (1.32)$$

Using these relations, we can calculate the trajectory of the perturbed motion. In this case $\overline{F}$, $\overline{F\exp(i\Omega_1 t)}$, and the other right halves depend on the new variables $\bar{\alpha}'$ and $\bar{\alpha}$ in the same way as they depended on the old variables $\bar{\alpha}$ and $\bar{\beta}$ in the case of unperturbed motion (for $\Delta f_0 = 0$).

In conclusion we note that in the calculation of the trajectories the following well known properties of a two-dimensional function satisfying the Laplace equation are useful. We present them here, since we need them later on.

If Φ is an electric potential, it can always be represented in the form

$$\Phi = \frac{W(z) + W^*(z)}{2}, \qquad (1.33)$$

where $W(z)$ is a corresponding analytic function of the complex variable z; the extreme function corresponding to this potential is

$$\Psi = \frac{W(z) - W^*(z)}{2i}. \qquad (1.34)$$

The complex intensity E of the electric field $\mathbf{E} = \operatorname{grad}\Phi$ corresponding to the potential (1.33) is

$$E = E_x + iE_y = \frac{dW^*(z)}{dz}. \qquad (1.35)$$

II. MOTION OF ELECTRONS IN A PLANOTRON

In this chapter we shall show how to apply the method developed in Chapter I to the planotron (planar magnetron).* It turns out that in this case we obtain a simple and illustrative expression for the motion of the electron, from which we can derive the principal characteristics of microwave generators of this type. Figure 1 shows schematically the working space of the planotron and the notation employed: the width of the working space D, the pitch of the resonant structure l, and the gaps between resonator plates h.

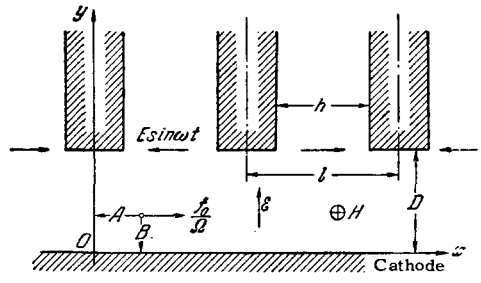

FIG. 1

The constant electric field $\mathscr{E}$ of the working space has a fundamental component along the y axis and we assume in our initial calculations that this component is constant. The acceleration corresponding to the inhomogeneous field $\mathscr{E}_{0y}$ will be denoted by

$$f_{0y} = \frac{e}{m}\mathscr{E}_{0y}. \qquad (2.01)$$

The components of the electric field $\mathbf{E}$ produced by the oscillations in the resonators will be denoted by E_x and E_y, the angular frequency of the natural oscillations of the resonator system will be denoted by ω, and the corresponding wavelength by λ. The wave number k, and the quantity g are defined by

$$\left.\begin{aligned} k &= \frac{\omega}{c} = \frac{2\pi}{\lambda}, \\ g &= \frac{\pi}{l}, \end{aligned}\right\} \qquad (2.02)$$

where c is the velocity of light. The magnetic field H is perpendicular to the plane of the figure and is constant in time and in space.

The complex amplitude of the scalar potential Φ in the interaction space will obviously satisfy the wave equation

$$\frac{\partial^2\Phi}{\partial x^2} + \frac{\partial^2\Phi}{\partial y^2} + k^2\Phi = 0. \qquad (2.03)$$

The overall form of the periodic solution of this equation will be (assuming that the electric field in the neighboring resonators is of opposite sign)

$$\Phi = \sum_{n=1}^{\infty} M_n e^{g(inx + my)}. \qquad (2.04)$$

Substituting this expression in (2.03) we have

$$n^2 - m^2 = \left(\frac{2l}{\lambda}\right)^2. \qquad (2.05)$$

In practice λ is always appreciably larger than the pitch l, so that we can put with sufficient accuracy

$$n^2 = m^2 \quad (\text{for } \lambda \gg l). \qquad (2.06)$$

This condition is equivalent to stating that in the working space we can replace with sufficient accuracy Eq.

*A more detailed description of the planotron will be given in Chapter VII.

(2.03) for the potential Φ by the Laplace equation

$$\frac{\partial^2\Phi}{\partial x^2}+\frac{\partial^2\Phi}{\partial y^2}=0. \tag{2.07}$$

We can simultaneously neglect the vector potential in calculating the electric field. We determine the coefficients M_n from the following simplified boundary conditions: $\Phi = 0$ when $y = 0$ (on the plane of the cathode); the derivative $\partial\Phi/\partial x$ vanishes everywhere on the upper limit of the interaction space, where $y = D$, except in the gap h between the sides of the resonator, where we assume that it has a constant value E_1. This simplification is fully justified by the degree of approximation of the solution which we need. We then obtain by the usual method employed to calculate the Fourier-series coefficients the following expression for the amplitude of the scalar potential:

$$\Phi=\frac{4E_1}{\pi h}\sum_{n=1}^{\infty}(-1)^{n+1}\frac{\sin\frac{(2n-1)gh}{2}}{(2n-1)^2\operatorname{sh}(2n-1)gD}$$
$$\times\cos(2n-1)gx\operatorname{sh}(2n-1)gy. \tag{2.08}*$$

We confine ourselves henceforth to the first term only ($n = 1$). This is perfectly permissible in view of the presence of the term $\sinh(2n-1)gD$ in the denominator. Thus, the periodic electric field acting on the electron in the interaction space has components

$$\left.\begin{aligned}E_x&=\frac{\partial\Phi}{\partial x}\sin\omega t,\\ E_y&=\frac{\partial\Phi}{\partial y}\sin\omega t,\end{aligned}\right\} \tag{2.09}$$

and we retain only the first term in the series $\partial\Phi/\partial x$ and $\partial\Phi/\partial y$. If we introduce the notation

$$U=\frac{e}{m}\frac{4E_1}{\pi}\frac{\sin\frac{gh}{2}}{\operatorname{sh}gD} \tag{2.10}$$

and change over from forces to accelerations, we obtain

$$\left.\begin{aligned}F_x&=\frac{e}{m}E_x=-U\operatorname{sh}gy\sin gx\sin\omega t,\\ F_y&=\frac{e}{m}E_y=U\operatorname{ch}gy\cos gx\sin\omega t.\end{aligned}\right\} \tag{2.11}\dagger$$

In order to find the motion of the electrons in the interaction space, it is necessary to solve the fundamental equation of motion (1.03) at a constant acceleration if$_{0y}$ and a variable acceleration F. For this purpose we use the second fundamental case, when the solution of (1.06) has the form (1.08). This solution is now conveniently written in the form

$$z=\bar{\alpha}+\frac{f_{0y}}{\Omega}t+\bar{\beta}e^{-i\Omega t}, \tag{2.12}$$

where

$$\left.\begin{aligned}\bar{\alpha}&=A+iB,\quad \dot{\bar{\alpha}}=\dot{A}+i\dot{B},\\ \bar{\beta}&=-iae^{-i\varphi},\quad \dot{\bar{\beta}}=-(i\dot{a}+a\dot{\varphi})e^{-i\varphi},\end{aligned}\right\} \tag{2.13}$$

*sh = sinh.

†ch = cosh.

a is the radius of the orbit and φ is the phase angle; positive values of $\Omega+\dot{\varphi}$ correspond to clockwise rotation of the electrons along a circular orbit.

The motion of the electron under the influence of the acceleration F is determined from Eqs. (1.18), which now assume the form

$$\left.\begin{aligned}\dot{A}+i\dot{B}&=-\frac{i}{\Omega}\overline{F(z_0,z_0^*,t)},\\ \dot{a}-ia\dot{\varphi}&=-\frac{1}{\Omega}\overline{F(z_0,z_0^*,t)e^{i(\Omega t+\varphi)}},\end{aligned}\right\} \tag{2.14}$$

where

$$z=A+iB+\frac{f_{0y}}{\Omega}t-iae^{-i(\Omega t+\varphi)}. \tag{2.15}$$

The complex acceleration $F(z, z^*, t)$ is determined with the aid of expressions (2.11) in the form

$$F=F_x+iF_y=iU\cos gz^*\sin\omega t. \tag{2.16}$$

We are interested in motions for which the averaged quantities $\dot{\bar{\alpha}}$ and $\dot{\bar{\beta}}$ do not vanish. This occurs if the angular frequency of the electron Ω, the natural frequency of the resonators ω, and the drift velocity f_{0y}/Ω are connected by a definite relation which we shall call the "resonance condition." This condition can be determined by substituting the value of z^* from (2.15) into the right halves of (2.14). Inasmuch as $\cos gz^*$ can be represented in the form

$$\cos gz^*=\sum_{m=0}^{\infty}C_m^+e^{i\left(m\Omega+\frac{gf_{0y}}{\Omega}\right)t}+\sum_{m=0}^{\infty}C_m^-e^{i\left(m\Omega-\frac{gf_{0y}}{\Omega}\right)t},$$

where

$$C_m^{\pm}=\frac{1}{2}\frac{(\mp ga)^m}{m!}e^{im\varphi}e^{\pm g(B+iA)},$$

and C_m^+ and C_m^- decrease rapidly with increasing m and do not depend explicitly on t, the terms appearing under the averaging sign are proportional to $\exp[i(m\Omega \pm gf_{0y}/\Omega \pm \omega)t]$, and the result of the averaging of the individual terms of the series differs from zero under one of the following conditions (then the corresponding term will not depend on the time):

$$\left.\begin{aligned}m_1\Omega&=\frac{gf_{0y}}{\Omega}+\omega\quad (1\text{st condition}),\\ m_2\Omega&=\frac{gf_{0y}}{\Omega}-\omega\quad (2\text{d condition}),\\ m_3\Omega&=-\frac{gf_{0y}}{\Omega}+\omega\quad (3\text{d condition}),\end{aligned}\right\} \tag{2.17}$$

where m_1, m_2, and m_3 are arbitrary positive integers, including zero.

Of greatest interest to us is the resonant condition in the form

$$\frac{gf_{0y}}{\Omega}=\omega \text{ and } m_1\Omega\neq 2\omega,\qquad m_2=m_3=0. \tag{2.18}$$

The averaging (under the condition $m_2 = 0$) yields

$$\left.\begin{aligned}\bar{F}&=-\frac{i}{2}U\sin g\bar{\alpha}^*,\\ \overline{Fe^{i\Omega t}}&=0.\end{aligned}\right\} \tag{2.19}$$

We need to determine the averaging time T.

Inasmuch as a/l (the ratio of the radius of the orbit to the pitch of the resonant system) is small, it is necessary to include in the expansion of $\cos gz^*$ only the terms proportional to $C_0^{\pm}$. When $m_2 = 0$ one of these terms will not depend explicitly on the time, while the other will oscillate with frequency 2ω. We therefore choose an averaging time $T = \pi/\omega$.

Substituting these expressions into (2.14) and separating imaginary and real parts, we obtain

$$\left.\begin{aligned} \dot{A} &= -\frac{U}{2\Omega}\operatorname{ch} gB \sin gA, \\ \dot{B} &= \frac{U}{2\Omega}\operatorname{sh} gB \cos gA, \\ \dot{a} &= 0, \\ \dot{\varphi} &= 0. \end{aligned}\right\} \qquad (2.20)$$

These expressions describe the motion of the electrons in the planotron in the fundamental working process; we note that in this case $\dot{a} = 0$ so that consequently, the radii a of the circular orbits of the electrons remain constant in time as they move in the interaction space. This is not always the case; if the electron revolution frequency Ω is a rational multiple of the frequency 2ω, and consequently

$$\frac{gf_{0y}}{\Omega} = \omega, \quad m_1\Omega = 2\omega, \quad m_2 = m_3 = 0, \qquad (2.21)$$

then $\dot{a}$ and $\dot{\varphi}$ become different from zero. Let us consider by way of an example (see also Chapter V) the motion under the condition $m_1 = 2$, i.e., when the angular velocity Ω of the electron revolution is equal to the angular frequency ω of the resonators. In order to take into account the influence of the terms $C_1^{\pm}$ and $C_2^{\pm}$ the averaging must be carried out in this case over the time $T = 2\pi/\omega$; the averaging yields

$$\left.\begin{aligned} \overline{F} &= -\frac{i}{2}U \sin g\bar{\alpha}^* - \frac{1}{2}U\left(\frac{ga}{2}\right)^2 e^{-i(gA+2\varphi)}e^{-gB}, \\ \overline{Fe^{i\Omega t}} &= \frac{1}{2}U\frac{ga}{2}e^{-i(gA+2\varphi)}e^{-gB}. \end{aligned}\right\} \qquad (2.22)$$

Substituting these expressions into (2.14) and separating imaginary and real parts, we obtain

$$\left.\begin{aligned} \dot{A} &= -\frac{U}{2\Omega}\left[\operatorname{ch} gB \sin gA + \left(\frac{ga}{2}\right)^2 e^{-gB}\sin(gA+2\varphi)\right], \\ \dot{B} &= \frac{U}{2\Omega}\left[\operatorname{sh} gB \cos gA + \left(\frac{ga}{2}\right)^2 e^{-gB}\cos(gA+2\varphi)\right], \\ \dot{a} &= \frac{U}{2\Omega}\frac{ga}{2}e^{-gB}\cos(gA+2\varphi), \\ a\dot{\varphi} &= -\frac{U}{2\Omega}\frac{ga}{2}e^{-gB}\sin(gA+2\varphi), \\ \Omega &= \omega = \frac{gf_{0y}}{\Omega}. \end{aligned}\right\} \qquad (2.23)$$

It is seen from these equations that the orbits of the electrons can either increase or decrease, depending on the values of the phase 2φ for a given gA. The influence of this phenomenon on the efficiency will be considered in detail below. For the time being we point out only that the efficiency will deteriorate as a net result of the variation of the orbit radius a, so that the operation of the planotron in the $\Omega = \omega$ mode is undesirable. Usually the operating mode is chosen in accordance with conditions (2.18). Converting from acceleration to field values, we can write these conditions in a form suitable for practical use:

$$\frac{\mathscr{E}_{0y}}{cH} = \frac{2l}{\lambda}, \quad H \neq \frac{m}{e}\frac{2\pi c^2}{\lambda}. \qquad (2.24)$$

In considering the mechanism of the electronic processes in the planotron, we confine ourselves henceforth, unless specially stipulated, to the modes determined by these resonant conditions, when the radius of the orbit a remains constant. The velocities $\dot{A}$ and $\dot{B}$ of the centers of the electron orbits are given in this case by (2.20). We call them the phase velocities. In order to explain their physical meaning, we introduce an observer who moves at the drift velocity f_{0y}/Ω. It is then seen from (2.15) that such an observer sees only the velocities $\dot{A}$ and $\dot{B}$ of the orbit centers, and in addition, a file of resonators moving past him with velocity $-f_{0y}/\Omega$. In order to make the electron motion pattern as seen by the observer more definite, the observer must refer the velocity to a definite phase Ωt, we choose it to be a multiple of 2π and refer the position and velocity of the electrons to the location of the resonators at that instant. This is why we call the velocities $\dot{A}$ and $\dot{B}$ the phase velocities and call the corresponding trajectory of the electron-orbit centers the phase trajectory. All the phase trajectories fill the three-dimensional phase space, of which the (A, B) plane is a section.

We eliminate the time from the equations in (2.20) by integration and obtain an equation for the trajectories of the electron-orbit centers in phase space

$$\operatorname{sh} gB \sin gA = R. \qquad (2.25)$$

By varying the constant R, we obtain the entire family of trajectories. They are plotted in Fig. 2 for R = 1.0, 0.5, 0.25, and 0.1; the arrows indicate the directions of the velocities $\dot{A}$ and $\dot{B}$.

To visualize the motion of a large number of electron-orbit centers, we assume that the orbits emerge

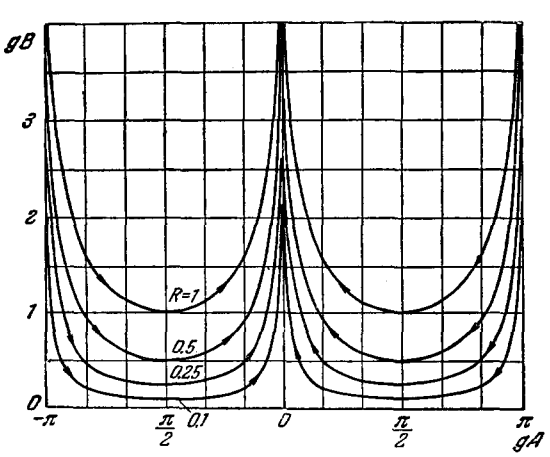

FIG. 2

constantly from a uniform layer in the plane y = d, parallel to the cathode and located a distance d away from it. We call this plane the supply plane. Then, if we draw the corresponding trajectory for each electron (as in Fig. 2), we obtain the flow pattern of the centers, as shown in Fig. 3. Thus, all the electron centers gather in tongues at the phase gA = 0 (and also gA = ± 2π, gA = ± 4π etc.). The boundaries of these tongues are determined by the equation

$$\operatorname{sh} gB \sin gA = \operatorname{sh} gd. \tag{2.26}$$

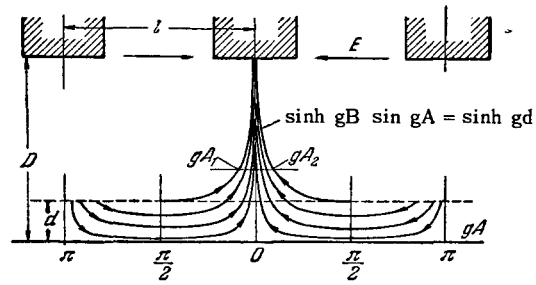

FIG. 3

We have arrived at a mechanism called in the case of the magnetron, "phase focusing." We see from Fig. 3 directly the principal feature of the electron motion: one half of all the electrons (generated with phase gA between $-\pi/2$ and $\pi/2$) is directed straight into the tongues and reaches the anode, while the other half must first approach the cathode. Inasmuch as we are considering not the motion of the electrons themselves but the motion of the centers of their orbits, it is obvious that the electrons cannot come closer to the cathode than a distance equal to the radius of the orbit. Therefore the electrons generated, for example, with $\pi/2 < gA < 3\pi/2$ or $-3\pi/2 < gA < 3\pi/2$, may return to the cathode rather than go into the tongues with excess energy drawn from the oscillating system. This is the well known phenomenon of backward current, which is used in the magnetron to keep the cathode hot.

We shall deal in greater detail with these phenomena and the losses associated with them in Chapter IV. For the time being we indicate only two limiting cases. If the orbit radius a is equal to the height of the supply plane d, then obviously half the electrons will return to the cathode and half will go to the anode; thus, the maximum backward current due to this mechanism can be equal to the forward current to the anode. On the other hand, if the orbit radius a is equal to zero, then all the electrons can enter the tongues and there will be no backward current.

The center of the electron orbit entering into one of the tongues will move towards the anode in the tongue and, because this motion is synchronized with the oscillations of the electric field in the interaction space, it will give up the potential energy acquired in the transverse electric field $\mathscr{E}_{0y}$, to the oscillations of the resonant system.

An examination of the obtained pattern of electron motion in the interaction space discloses clearly the physical nature of the "phase focusing" mechanism. Under the influence of the high-frequency electric field, the centers of the electron orbits acquire as they move in phase space a velocity $\dot{A}$ along the x axis, under the influence of which the phase difference between the passage of the electrons under the resonator gaps and the electric field changes. It is seen from Fig. 3 that no matter what the phase gA of the center of the electron orbit is in the supply plane B = d, its velocity $\dot{A}$ will always be directed such as to guide the electron to the tongue, in which it will move towards the anode. Thus, were it not for the interference of the orbit radius a, sooner or later all the electrons on the supply plane B = d would enter the tongues. The velocity $\dot{A}$ will be called from now on the "phasing velocity." It has a maximum when the phase gA is equal to $\pm \pi/2$. In this case the velocity $\dot{B}$ is equal to zero.

When the electron moves with velocity $\dot{A}$ parallel to the plane of the cathode and perpendicular to the constant electric field $\mathscr{E}_{0y}$, no energy is exchanged between the electrons and the oscillating system. On the other hand, when the electrons move along the y axis with a velocity $\dot{B}$, energy is exchanged with the oscillating system. Obviously, the power transferred to the system by one electron is

$$P_e = e\mathscr{E}_{0y}\dot{B}. \tag{2.27}$$

When the velocity $\dot{B}$ is positive and the electron moves towards the anode, the power is transferred to the oscillating system; to the contrary, when $\dot{B}$ is negative, power is drawn from the oscillating system. It is seen from (2.20) that $\dot{B}$ will have a maximum positive value when gA = 0, and a maximum negative value when $gA = \pm \pi$. The direction of the phasing velocity $\dot{A}$ is always such as to lead the electron to a phase gA = 0, at which $\dot{B}$ has a maximum positive value and the oscillations are generated in the system most effectively. It is important to note that the electrons are phased to correspond to the generation condition near the cathode in a space bounded by the plane B = d. If d is small, then even when part of the electrons return to the cathode no appreciable energy losses are needed and thus the entire phase-focusing process is "cheaply obtained." This is the major advantage of this generation process.

The picture considered discloses the mechanism that guarantees stability of generation in the planotron. As will be shown below, the expressions obtained also make it possible to investigate quantitatively the stability of the process and to calculate those basic indices, which determine the efficiency of such systems.

Before we proceed to these questions, let us dwell on one very important consequence of the analysis of the motion of the electron-orbit centers. We refer here to the reversibility of the generation process and to the possible existence of processes in which the planotron transforms the oscillation energy into direct-

current energy. For this purpose we examine the motion of electrons in a constant electric field $\mathscr{E}_{0y}$ of opposite sign. Then (unlike Fig. 1) the lower plate y = 0 will be the anode, and the lower resonator surface y = D will be the cathode. We see that upon reversal of the sign of $\mathscr{E}_{0y}$, the acceleration f_{0y} also reverses sign. Inasmuch as expression (2.12) and all the following expressions contain the acceleration f_{0y} in the form of the ratio f_{0y}/Ω reversal of the sign of f_{0y} and simultaneous reversal of the sign of the angular velocity Ω (i.e., reversal of the direction of the magnetic field H) leaves all further relations (2.20) for $\dot{A}$ and $\dot{B}$ and the resonance condition (2.18) unchanged. Thus we obtain the same trajectories (see Figs. 2 and 3) for the electron-orbit centers in phase space. The phase-focusing pattern, and consequently the stability mechanism also remain the same; however owing to the reversal of the sign of $\mathscr{E}_{0y}$, when the electron moves in the working space with positive velocity $\dot{B}$ it moves from the anode to the cathode, i.e., against the electric field, and such motion can be effected only by drawing energy from the oscillating system. Thus, the power generated (2.27) reverses sign and the system will operate as a dc generator with a potential difference

$$V = \mathscr{E}_{0y} D. \tag{2.28}$$

The stability and many other characteristics which we derive below for the planotron will be valid independently of the mode in which the instrument operates—as a generator of electromagnetic oscillations of high frequency or as a dc generator. The slight difference in the mechanism of the process arises only when the direction of rotation of the electron in its circular orbit comes into play. In the two foregoing generation processes the sign of this rotation will be different, since the direction of the magnetic field was reversed. Consequently in the case of a planotron operating as a high-frequency generator the electrons move from the cathode to the resonators along cycloids whose convex parts face the anode (the resonators), while in the generation of direct current the electrons move along cycloids whose convex parts face away from the resonators, which act as the cathode in this case (for more details see Chapter IV, Fig. 7). This difference is essential in the consideration of the efficiencies of the two modes: owing to the reversed position of the cycloid in the planotron operating as a dc generator, the losses will be distributed among the anode and the cathode, in different fashion than in the case of a high-frequency generator.

The foregoing conclusion concerning the complete reversibility of the electronic processes in planotrons apply also to magnetrons. Consequently both planotrons and magnetrons can be used not only to transform dc into high-frequency electromagnetic oscillations, but can be used, with equal stability and with the same characteristics, for the conversion of high-frequency electromagnetic energy into dc. This conclusion is important for the future development of electronic high-power processes, for this uncovers the possibility of transforming high frequency energy, and consequently transmission of large power over long distances both in free space and through waveguides.

We shall return to this question in Chapter IX.

III. PRINCIPAL CHARACTERISTICS OF THE PLANOTRON

In this chapter we investigate the operating stability of the planotron and find its power limit. The simple formulas obtained in the preceding chapter for the trajectories of electrons moving in the working space of the planotron yield all the data necessary for the calculation of the stability of the electronic processes against disturbing factors produced by the inhomogeneity of the fields, by space charge, etc.

Let us establish first the connection between the current and the space charge it produces. From (2.20) we find that the components of the phase velocities $\dot{A}$ and $\dot{B}$ satisfy the solenoidal condition

$$\frac{\partial \dot{A}}{\partial A} + \frac{\partial \dot{B}}{\partial B} = 0. \tag{3.01}$$

Consequently, the motion of the centers of the orbits in phase space is like the flow of an incompressible liquid. The velocities $\dot{A}$ and $\dot{B}$ have a velocity potential. The corresponding stream function is

$$\Psi = \frac{U}{2\Omega g} \operatorname{sh} gB \sin gA. \tag{3.02}$$

It is easy to check that $\dot{A}$ and $\dot{B}$ satisfy the following relations:

$$\dot{A} = -\frac{\partial \Psi}{\partial B}, \quad \dot{B} = \frac{\partial \Psi}{\partial A}. \tag{3.03}$$

Let us denote the number of the centers of the electron orbits per unit volume by μ and regard μ as a density. Along any current line, both the function Ψ and the density μ remain constant [in accord with Eq. (3.01)]. If the density μ has a specified distribution in the supply plane B = d (see Fig. 3), where the formation of the tongues begins, then this distribution will remain the same in any other plane B = const. If the initial distribution in the supply plane is homogeneous, the density μ remains constant over the entire tongue. We confine ourselves henceforth to an examination of motion for a homogeneous density μ. As can be seen, a homogeneous density is obtained in two cases. The first case occurs when d = a (where a is the radius of the electron orbits) under the condition that the centers of the electron orbits are uniformly generated in the supply plane itself; then they can enter into the tongue only from the interval $-\pi/2 < gA < \pi/2$, i.e., from half the total length of the cathode, and continue to move with constant density along

the tongues. The second case will occur when a = 0, when electrons enter into the tongue from the entire supply: half of the electrons goes directly into the tongue, the other half travels under the supply plane. Then the density in the tongues is again uniform, but it is twice as large as in the preceding case. In the intermediate cases, when 0 < a < d, bands (bounded by the current lines) are produced along the edges of the tongue, with double density, while the density has its usual value in the center of the tongue.

Revolving around each center is an electron with charge e, and inasmuch as the orbit is small and its radius is smaller than d, we can assume with sufficient accuracy that the space charge density in the cluster is $\rho = e\mu$. Therefore when μ is constant the charge density ρ is also constant. If we denote by J the average current density (the current per unit electrode surface), then the current strength per pair of resonators will be

$$2lJ = \int_{A_1}^{A_2} \varrho \dot{B}\, dA, \qquad (3.04)$$

where A_1 and A_2 are the values of A at the extreme points of the tongue (see Fig. 3). Substituting the value of $\dot{B}$ from (3.03) and assuming ρ to be constant, we have

$$J = \frac{\varrho}{2l}(\Psi_2 - \Psi_1) = \frac{\varrho U}{2\pi\Omega} \operatorname{sh} gd. \qquad (3.05)$$

Thus, a connection is established between the current and the space-charge density in the tongues. In all the modes the space charge of the electron cloud is contained within definite limits, specified by the form of the tongues; the charge density in the tongues can usually be regarded as constant, and the value of the space charge can be assumed proportional to the current.

From the value and distribution of the space charges we can calculate their disturbing action on the motion of the electrons and determine both the stability of the process and the limiting generation power. In addition to the space charges, there are other factors which disturb the electronic process in the planotron. Principal among them in practice are the lack of complete homogeneity of the magnetic field, the variability of the static field $\mathscr{E}_{0y}$, and inaccuracy in the manufacture of the device. It will be shown below that the stability of the electronic processes depends on the intensity of the oscillations in the resonator; for a planotron and magnetron under operating conditions, this stability, as will be shown below, is quite high.

Let us consider first the simplest case, when along with the electric field $\mathscr{E}_{0y}$, satisfying the resonance condition, there exists also a small perturbing field, directed along the y axis, the intensity of which will be denoted by $\Delta\mathscr{E}_{0y}$; the acceleration corresponding to it is

$$\Delta f_{0y} = \frac{e}{m} \Delta \mathscr{E}_{0y}. \qquad (3.06$$

The additional acceleration Δf_{0y} increases the drift velocity by an amount $\Delta f_{0y}/\Omega$ and disturbs the resonance condition (2.18).

At the end of Chapter I we described a method for calculating the perturbed motion. In the present simple case it is likewise easy to carry out the calculations anew, namely, on going over from formula (2.16) to formula (2.19) it is necessary to take into account in the expression for gz* the additional term $g\Delta f_{0y}t/\Omega$, which (for sufficiently small Δf_{0y}) can be regarded constant over the averaging time. Then

$$\bar{F} = -\frac{i}{2} U \sin g\left(\bar{\alpha}^* + \frac{\Delta f_{0y}}{\Omega} t\right), \quad \overline{Fe^{i\Omega t}} = 0.$$

Introducing a new complex quantity

$$\bar{\alpha}' = \bar{\alpha} + \frac{\Delta f_{0y}}{\Omega} t, \quad \bar{\alpha}' = A' + iB', \quad A' = A + \frac{\Delta f_{0y}}{\Omega} t, \quad B' = B,$$

we obtain the equation

$$\dot{A}' - \frac{\Delta f_{0y}}{\Omega} + i\dot{B}' = \frac{U}{2\Omega} \sin g(A' - iB'). \qquad (3.07)$$

The same relations are obtained directly from (1.28) by putting $\Delta f_0 = i\Delta f_{0y}$. Separating the real and imaginary parts, we obtain

$$\left.\begin{aligned} \dot{A}' &= -\frac{U}{2\Omega} \operatorname{ch} gB' \sin gA' + \frac{\Delta f_{0y}}{\Omega}, \\ \dot{B}' &= \frac{U}{2\Omega} \operatorname{sh} gB' \cos gA', \end{aligned}\right\} \qquad (3.08)$$

which are analogous to (2.20) and differ from them only in the presence of a term $\Delta f_{0y}/\Omega$, which changes the phase velocity $\dot{A}$. It is easy to see that the perturbed motion remains potential in character and the components $\dot{A}'$ and $\dot{B}'$ satisfy as before the solenoidal condition (3.01). Consequently, all the kinematic properties of the unperturbed motion (the existence of a velocity potential and a stream function, homogeneous density of the space charge, etc.) remain in force for the perturbed motion. The stream function of the perturbed motion will be

$$\Psi' = \frac{U}{2\Omega g} \operatorname{sh} gB' \sin gA' - \frac{\Delta f_{0y}}{\Omega} B'. \qquad (3.09)$$

Our problem consists of finding those limiting values of $\Delta f_{0y}/\Omega$, at which the stream lines Ψ' = const retain a tongue-like character and the electrons produced in the supply plane reach the anode.

For convenience in analysis we introduce the notation

$$x = gA', \quad y = yB', \quad \sigma = \frac{2\Delta f_{0y}}{U}. \qquad (3.10)$$

Then the trajectory equation assumes the form

$$\operatorname{sh} y \sin x = \sigma(y - y_0). \qquad (3.11)$$

Figure 4b shows the stream lines Ψ' = const (trajectories) for σ = 4. It is seen from Fig. 4b that the centers of the orbits situated above or on the horizontal line $y = y_1$ all enter into the tongues and reach the anode. The centers of the orbits situated below the horizontal line $y = y_2$ will move along curves similar

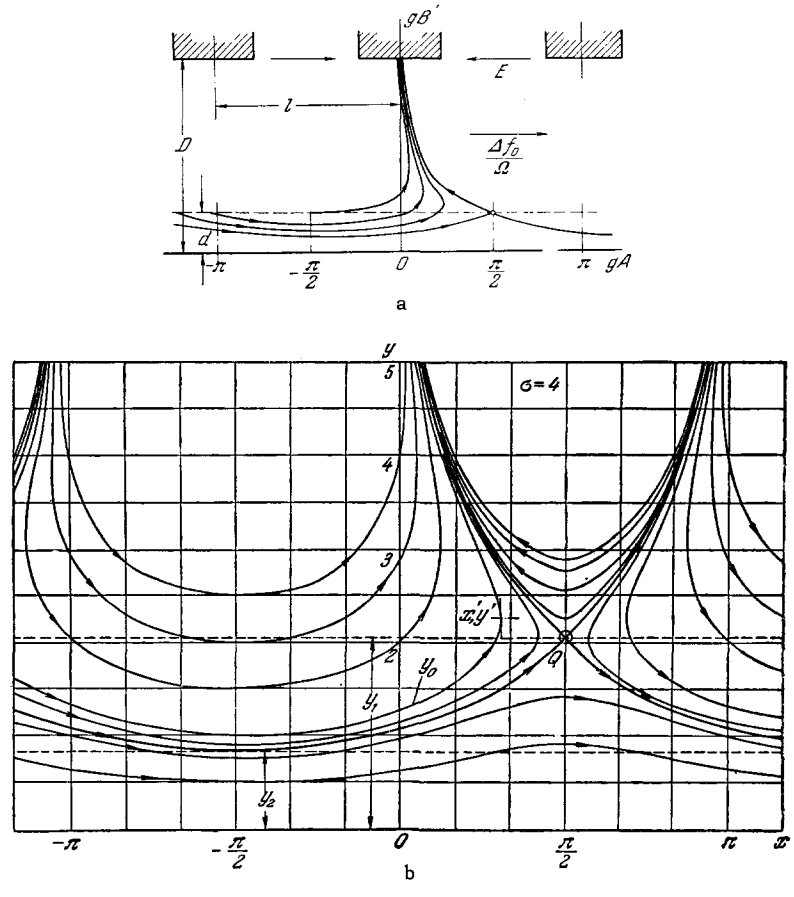

FIG. 4

to sin x without entering the tongues. The centers of the orbits lying in the band $y_2 < y < y_1$ will only partly enter into the tongues. The values of y_1 and y_2 are determined in the following manner.

Let us consider two points on one and the same phase trajectory. At the point with the coordinates $x = -\pi/2$, $y = y_2$ this trajectory is closest to the plane of the cathode $y = 0$. The point with the coordinates $x = \pi/2$, $y = y_1$ on Fig. 4b is denoted by Q. The main distinguishing property of this point is as follows: on the vertical $x = \pi/2$ this is the only point at which the approaching trajectories have a vertical tangent. Therefore the point Q is determined by the condition

$$\left.\frac{\partial x}{\partial y}\right|_{x\to\frac{\pi}{2}} = 0, \quad y = y_1. \tag{3.12}$$

Differentiating (3.11) we obtain

$$\operatorname{ch} y_1 = \sigma. \tag{3.13}$$

Eliminating y_0 and σ from (3.11) we obtain a connection between y_1 and y_2 in the form

$$\operatorname{sh} y_1 + \operatorname{sh} y_2 = (y_1 - y_2)\operatorname{ch} y_1. \tag{3.14}$$

In order to maintain the character of the motion completely unchanged, it is necessary that the supply plane be higher than the plane $y = y_1$, i.e., it is necessary to have $gd \geq y_1$ and consequently $\cosh gd \geq \cosh y_1$. Returning to the previous notation, we obtain the following stability condition for the tongue

$$\Delta f_{0y} \leqslant \frac{U}{2} \operatorname{ch} gd. \tag{3.15}$$

If Δf_{0y} does not satisfy this condition, then the formation of the tongues is disturbed and the anode current decreases or even drops to zero.

The boundaries of the tongue corresponding to the perturbed current lines are shown in Fig. 4a. The perturbed tongues can be imagined by visualizing a wind blowing through the unperturbed tongues (Fig.3) in the direction of $\Delta f_{0y}/\Omega$. From the expression from the extreme lines we see that the width of the tongues $A_2 - A_1$ is the same at a given altitude in the unperturbed and perturbed motion [subject to condition (3.15)], so that the areas of the tongues and the space charge density in the perturbed motion remain unchanged.

The meaning of condition (3.15) becomes physically clear if one determines from (2.11) the amplitude of the acceleration along the y axis, produced by an alternating electric field in the supply plane. This amplitude is equal to

$$F'_y = U \operatorname{ch} gd \qquad (A = 0,\ B = d). \tag{3.16}$$

Substituting this value into the condition (3.15), we can rewrite it in the form

$$\Delta f_{0y} \leqslant \frac{F'_y}{2}. \qquad (3.17)$$

Changing from acceleration to fields we get

$$\Delta \mathscr{E}_{0y} \leqslant \frac{E'_y}{2} \qquad (A=0,\ B=d). \qquad (3.18)$$

Thus, the motion remains stable if the constant perturbing field is directed along the y axis and does not exceed half the amplitude of the alternating field in the supply plane. The special role of the component E_y can be seen from the first equation of (3.08): it determines the phasing velocity, which under condition (3.15) or (3.18) neutralizes the action of the "dephasing" velocity $\Delta f_{0y}/\Omega$.

A similar stability analysis of the electronic process can be carried out in those cases when the disturbing factor upsets the resonance condition. It is seen from formula (3.18) that the resonance can be influenced by three factors: change in the electric field $\mathscr{E}_{0y}$, change in the magnetic field H, and change in the period (pitch) of the structure l.

Let us denote the relative perturbations by γ. In the case of a perturbation of the electric field

$$\gamma = \frac{\Delta \mathscr{E}_{0y}}{\mathscr{E}_{0y}}. \qquad (3.19)$$

If an inhomogeneity equal to ΔH arises in the magnetic field, then the relative perturbation is

$$\gamma = -\frac{\Delta H}{H}. \qquad (3.20)$$

If the manufacturing inaccuracy causes the pitch of the resonators to change by Δl, then

$$\gamma = -\frac{\Delta l}{l}. \qquad (3.21)$$

Employing in all these three cases (3.08) and the equations that follow, we can show that the perturbations do not disturb the electronic process if

$$|\gamma| \leqslant \frac{E'_y}{2\mathscr{E}_{0y}}. \qquad (3.22)$$

In this case γ can be any of the foregoing quantities.

Under ordinary generation conditions, the ratio of the fields E'_y and $\mathscr{E}_{0y}$ is not a small quantity, so that the system displays good stability against perturbations. The relative perturbation γ can amount to many per cent and still not upset the generation, so that there is no need for very precise manufacture of the system or for great homogeneity of the magnetic field in the operation of the planotron.

However, exact satisfaction of the resonance condition may be important for self-excitation. The initial oscillations in the system are excited as a result of fluctuations occurring in the cloud of electrons drifting around the cathode. Therefore the initial oscillations in the system cannot be large and the field E'_y corresponding to them in the supply plane will be weak; it follows therefore that in the case of self-excitation the ratio (3.22) imposes more stringent conditions on γ.*

Exact satisfaction of the resonance conditions is necessary only at the instant of self-excitation: the more precise the manufacture of the device and the more homogeneous the electric and magnetic fields, the easier it is to produce self-excitation.

Were the initial value of E'_y known, one could establish with assurance the necessary tolerances for the values of γ in the case of self-excitation. It is apparently difficult to calculate the initial oscillation intensity, but it is quite feasible to measure it; this is an interesting experiment which should be performed.

The most appreciable influences on the operation of all electronic devices are the disturbances due to space charges which occur during the flow of the current. Their action determines essentially the energy characteristics of the planotron as well as of the magnetron, klystron, and other electronic devices. The physical picture of the disturbing action of the space charge in the planotron is very simple: the electrons filling the tongues are repelled and thus oppose the phasing action of the velocity $\dot{A}$. It is obvious that the field produced by the space charge will affect most strongly the electrons whose orbit centers lie on the boundaries of the tongue, for it is there that the repulsion is a maximum. The strongest perturbation will be introduced in the electron motion by the component $\mathscr{E}'_y$ of the electric field due to the space charges: this follows from the fact that in a magnetic field the velocity acquired by the electrons under the influence of the electric field is directed towards that field, at a right angle, precisely in the direction of the A axis in which the phasing velocity $\dot{A}$ acts.

The largest value of the component $\mathscr{E}'_y$ due to the space charges will be at the root of the tongue, at the point with coordinates A = 0 and B = d (the point O′ on Fig. 5). Knowing the density of the homogeneous space charge ρ and the form of the tongue it is possible to calculate the field at the point O′; these calculations lead to complicated integrals. The problem can be simplified by replacing the tongue with a triangle of the same area, which obviously produces (for the same density ρ) at the point O′ approximately the same field. Such a triangle is shown in Fig. 5. We make the base of the triangle equal to νl, where ν is

*In the study of self-excitation it is necessary to take account of the fact that it is guaranteed by the excitation of a chain of resonators, so that it is necessary to introduce into consideration the summary perturbation factor $\Sigma\gamma$. In addition, it is necessary to recognize that in the unexcited state the electron cloud will diffuse in the working space from the cathode to the anode and consequently the height d of the supply plane seemingly increases. This brings the electrons into a region with larger values of E'_y, which makes the onset of oscillations easier.

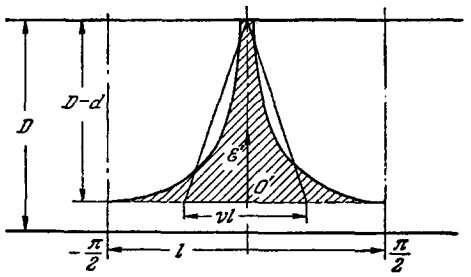

FIG. 5

obviously less than unity; this quantity can be estimated in simple fashion by means of a planimeter. Regarding the problem as a two-dimensional one, we calculate the space-charge field at the point O′ in the method usually employed in such problems, namely by integration of the fields produced by each area element. As a result of the calculation we obtain for the component $\mathcal{E}'_y$ of the space-charge field at the point O′ the following expression:

$$\mathcal{E}'_y = \varrho \frac{vl(D-d)^2}{(D-d)^2 + \left(\frac{vl}{2}\right)^2} \left[\ln \frac{2(D-d)}{vl} + \frac{\pi}{4} \frac{vl}{D-d} \right]. \quad (3.23)$$

Inasmuch as d is small compared with D and ν is less than unity, we can approximately put

$$\mathcal{E}'_y = \varrho v l \ln \frac{2D}{vl}. \quad (3.24)$$

If we put

$$\chi = \nu \ln \frac{2D}{vl}, \quad (3.25)$$

we obtain ultimately

$$\mathcal{E}'_y = \varrho \chi l. \quad (3.26)$$

The corresponding acceleration will be

$$\Delta f'_y = \frac{e}{m} \varrho \chi l. \quad (3.27)$$

More detailed calculations show that the coefficient differs little from unity; it is little sensitive to a variation of the parameters D, d, and l. This is confirmed by the fact that expression (3.26) can be obtained in simple fashion by assuming the entire charge concentrated at the centroid of the triangle.

The field $\mathcal{E}'_y$ moves together with the tongues, so that it will exert the same influence on the electrons as if the field were constant. We can therefore use the stability condition (3.15), which we introduce for a constant perturbing field, and the maximum possible charge density in the tongue (which we denote by ρ_c) is obtained from the relation

$$\frac{e}{m} \varrho_c \chi l = \frac{U}{2} \operatorname{ch} gd. \quad (3.28)$$

Substituting the value of ρ_c in expression (3.05) for the current density, we obtain its critical value

$$J_c = \frac{m}{e} \frac{U^2}{4\pi\Omega\chi l} \operatorname{ch} gd \operatorname{sh} gd. \quad (3.29)$$

The specific power, i.e., the power removed from a unit cathode surface and converted into oscillating energy of the system, will obviously consist of the work carried out by all the electrons, so that we obtain for the specific power the expression

$$P = \eta_e J \mathcal{E}_{0y} D, \quad (3.30)$$

which is analogous to (2.27); here η_e is the efficiency of the electronic process. From this expression we obtain the critical specific power if we substitute in it the critical current (3.29). Making this substitution and using the resonance condition (2.24) we obtain

$$P_c = \eta_e \left(\frac{m}{e}\right)^2 \frac{\omega D U^2}{4\pi^2} \operatorname{ch} gd \operatorname{sh} gd. \quad (3.31)$$

We obtained two important characteristics of the generation process: the critical (limiting) current J_c and the critical power P_c, determined by the perturbing action of the space charges. These quantities, as can be seen from (3.29) and (3.31), are proportional to U^2, which according to (2.10) is in turn proportional to the energy of the alternating electric field in the resonators. Thus, the specific power generated in the interaction space is proportional to the energy of the oscillating system, which is also maintained by the generated power. Obviously, the power drawn from the resonators and the Joule power loss should be chosen such that the generated power does not exceed the critical value P_c. This choice determines the degree of stability of the generator.

Let us consider the electromagnetic oscillations in the resonators. The energy in the resonators, as is well known, is concentrated alternately in the electric and the magnetic fields. For generation of the oscillations, only the electric field is important, and furthermore that part of the field which acts in the working space. All the other electric fields (except for the small field corresponding to the power drawn) do not participate usefully in the process. The presence of these fields in the resonators is not only useless but harmful, since they are maintained at the expense of current flowing in the resonator walls, which involves additional Joule losses. Therefore an important characteristic of the resonator system is a quantity which we designate ψ and call the coefficient of utilization of the electric field in the resonators. If the total electric energy per unit area of the interaction space is W in the resonators and in the working space, and W_0 in the interaction space only, then

$$\psi = \frac{W_0}{W}. \quad (3.32)$$

The better the construction of the resonant system, the higher the utilization coefficient ψ. But even in the best resonator systems ψ does not exceed one-third; usually this quantity is much smaller.

A second quantity characterizing the operation of the resonators is their total Q, which includes the

loaded Q_l and the loss Q_j, determined by the Joule losses. For Q, Q_l, and Q_j we have the usual relation

$$\frac{1}{Q}=\frac{1}{Q_l}+\frac{1}{Q_j}. \tag{3.33}$$

From the definition of Q we have the following relation between the power P delivered to the system and the energy W stored in it:

$$Q=\frac{\omega W}{P}=\psi\frac{\omega W_0}{P}. \tag{3.34}$$

The electric energy of the alternating field per unit length in the interaction space can be determined by integration. It is equal to

$$W_0=\frac{1}{16\pi l}\int_0^D\int_{-l}^{l}\left[\left(\frac{\partial\Phi}{\partial x}\right)^2+\left(\frac{\partial\Phi}{\partial y}\right)^2\right]dy\,dx. \tag{3.35}$$

Substituting expression (2.08) for the potential Φ and confining ourselves to the first term of the series, we obtain after integration

$$W_0=\left(\frac{m}{e}\right)^2\frac{lU^2}{32\pi^2}\operatorname{sh}2gD. \tag{3.36}$$

Substituting this value in (3.34), and also substituting in place of P_c the critical power (3.31), we obtain the critical Q of the system

$$Q_c=\frac{1}{\eta_e\psi}=\frac{\pi\chi l}{4D}\frac{\operatorname{sh}2gD}{\operatorname{sh}2gd}. \tag{3.37}$$

This very important expression gives the smallest value of the total Q for which a stable electronic process is still possible. This is fundamental for the establishment of the dimension of the working space in the planotron and the magnetron. The three coefficients in this expression are determined in the following fashion. The first is the efficiency η_e of the electronic process, which will be calculated in the next chapter. The second is the utilization coefficient ψ and is calculated from the distribution of the electric field in the resonator, and is determined even more easily by experiment.* The coefficient χ is determined by the form of the tongue and, as was already pointed out, its value varies little and is close to unity.

The importance of (3.37) lies in the fact that it establishes, together with the expression for the efficiency which will be given in the next chapter, those relationships between the parameters D, l, and d of the working space, which are necessary to obtain the most stable and most effective operating mode. We note that the values of Q_c, calculated from (3.37) are close to those obtained in experiment (of order 10^2).

In practice it is also important to know the limiting power which can be obtained in the planotron per unit cathode area. Expression (3.37) yields P_c—the maximum specific power for a given value of U^2, which is proportional to the energy of the alternating electric field in the resonators. Thus, the power is limited by the same factor which limits the intensity of oscillation in the resonators. In practice this factor is usually simply electric breakdown, but there is also another principal limitation on the power. It is obvious that with increasing U the phase velocities $\dot{A}$ and $\dot{B}$ will increase in accordance with (2.20), and theoretically they can reach values at which the generation mechanism becomes disturbed. Thus, for example, at large values of $\dot{B}$ the electrons will reach the anode within the averaging time (during which the electrons have time to shift from one resonator to the other in the operation mode); this is not realistic, for they cannot have time to gather into tongues.

We can derive the conditions that limit $\dot{A}$ and $\dot{B}$; they are mathematically identical to the conditions under which our approximate method of solving the fundamental equation of motion can be employed.

In Chapter I it was pointed out in the description of the method [see formula (1.24)] that the uncertainty in the position of the electron on the trajectory does not exceed $\Delta\alpha=|\dot{\bar{\alpha}}|\,T$. It is obvious that phase focusing can be realized only when ΔA is much less than the value of l—the pitch of the resonant system. In the case considered by us, in the derivation of Eqs. (2.20), we chose an averaging time $T=\pi/\omega$. The condition necessary for realization of phase focusing will have the form

$$\frac{\Delta A}{l}=\frac{|\dot{A}|g}{\omega}\ll 1. \tag{3.38}$$

Using (2.18) and (2.20) we get

$$f_{0y}\gg\frac{U}{2}\operatorname{ch}gB\,|\sin gA|. \tag{3.39}$$

These inequalities should be realized first of all in the plane B = d, where the main phasing of the electrons takes place. Taking the largest value on the right side, we obtain

$$U\ll\frac{2f_{0y}}{\operatorname{ch}gd}. \tag{3.40}$$

Substituting this value into (3.31) and changing from acceleration to field values, we obtain an inequality for the limiting power P_c per unit surface:

$$P_c\ll\eta_e c\mathcal{E}_{0y}^2\frac{2D}{\pi\lambda}\tanh gd. \tag{3.41}$$

We can obtain a similar relation by considering *

*We have used the following simple method of measuring ψ in cold tests of the generator: the interaction space is filled with an insulator (usually Plexiglas) and the shift $\Delta\omega$ of the resonant frequency of the system is measured. The coefficient of utilization is calculated from the formula $\psi=2\Delta\omega/\epsilon\omega$, where ϵ is the dielectric constant of the insulator.

*More accurately, this condition can be written in the form $\Delta B/D'\ll 1$, where D′ is the shortest path covered by the center of the electron orbit in the working space (D′ = D − d − a, where d is the distance from the supply plane to the cathode and a is the radius of the orbit). Usually D′ ~ l and $\Delta A\sim\Delta B$, so that the condition does not yield anything new. However, if the magnetic field is only slightly larger than critical, then D′ is small

the condition $\Delta B/D \ll 1$ for vertical motion of the electrons (D is the distance between the cathode and anode).

From this we can derive the dependence of the generated power on the wavelength and on the other parameters of the generator. If we substitute into this expression the parameters of the experimental planotron, then we find that the limiting power which can be drawn from a unit surface reaches exceedingly high values—tens and hundreds of kilowatts per square centimeter of cathode area. Such large values, as is well known, have already been realized in magnetrons operating in pulsed modes. In the case of continuous generation, it is necessary to draw much less power. The main limitation on the continuous mode is the difficulty in cooling the resonators and the cathode; neither the space charge nor the violation of the character of motion will be limiting factors hindering the production of large continuous power with the aid of a planotron and a magnetron designed for continuous operation.

We note in conclusion that the method we have employed for an approximate calculation of the space charge yields an exaggerated value of the perturbations due to them. In fact, the electric field produced by the space charges has a complicated distribution in space, and we confine ourselves to the calculation of the field only at the point O′ (see Fig. 5), where it has a maximum value. Further, we have assumed that the perturbation carried out by the space charges is equal to the perturbation caused by the field (3.26), as if this field were to have a constant value over the entire interaction space. This method of reasoning leads, of course, to too high an estimate of the perturbation, but the error associated with this is apparently not very large, since the electrons most sensitive to the perturbations are located near the supply plane. We have thus obtained the critical current J_c and the limiting power P_c as a function of the parameters of the interaction space and the wavelength; this dependence can serve as the basis of the similarity theory necessary for the construction of generators with various parameters.

All that can be expected from a more complete calculation method is merely more precise values for some of the coefficients. It would be interesting to obtain more exact expressions for the limiting values of the power and the current, to investigate the deformation of the tongues due to the space charges, and to compare the obtained results with the experimental research.

and the condition $\Delta B/D' \ll 1$ greatly limits the amplitude of the high-frequency field. This example shows once more that the averaging method is applicable when effective generation takes place.

IV. ANODE AND CATHODE LOSSES IN THE PLANOTRON

The electronic efficiency of the planotron, which we have designated η_e, is the ratio of the power fed into the resonators from the electron cloud, to the power received from the dc source. In addition to the losses occurring in the electronic process, it is necessary to take into account also the Joule losses in the resonators. The calculation of the efficiency from the Q of the resonators is well known and will not be discussed here. If we denote the resonator efficiency by η_r, then the over-all resonator efficiency is

$$\eta = \eta_e \eta_r. \tag{4.01}$$

On the basis of the results obtained above for the electronic processes in the planotron, we now consider the electronic losses in this device. There are three principal types of losses. The first and unavoidable losses are connected with the fact that at the instant when the electron completes its working path from the cathode to the anode and transfers energy to the oscillations, it arrives at the anode with a certain velocity, the loss of which heats the anode. These will be called "anode losses" and the efficiency corresponding to them will be designated η_a. The second form of losses—losses on the cathode—were already mentioned in Chapter II (see p. 787). They are caused by the excess energy with which the electron with improper phase gA returns to the cathode. The efficiency corresponding to these losses will be designated η_k. The third type of losses will be called the "edge losses," since they are connected with phenomena occurring on the edges of the cathode and the anode and consist in the fact that in the absence of oscillations in the generator the current is not completely blocked and has sometimes an appreciable value J_n (the residual current). In Chapter V we shall analyze the possible cause of this current and the losses associated with it. Inasmuch as this current is concentrated closer to the edge of the anode, we call it the edge current, and the losses associated with it are called the edge losses. The corresponding efficiency will be denoted η_n. If η_a, η_k, and η_n differ little from unity, then the electronic efficiency η_e can be assumed equal to their product.

To determine the anode losses we must know the kinetic energy with which the electrons strike it. The electron velocity has two components, $\dot{z}_0$ due to motion in the static fields and $\dot{\bar{\alpha}}$ due to the oscillations. But it is obvious from (3.38) that we are free to neglect the phase velocity $\dot{A} + i\dot{B}$ due to the alternating field.

If the planotron operates under the resonance conditions (2.18), then according to (2.20) the radius a of the orbits is constant and therefore the average kinetic energy with which the electron started its path

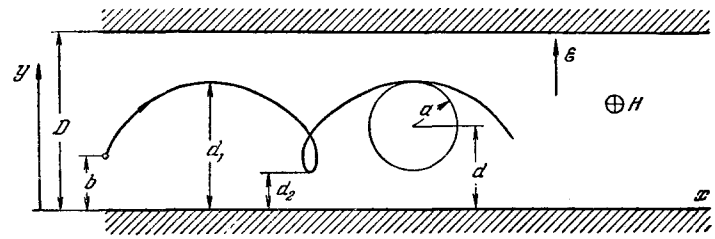

FIG. 6

towards the anode from the supply plane B = d will remain constant over the entire path. Thus, the kinetic energy of the electron is determined by the constant acceleration f_{0y} in accord with the usual equations (1.03)

$$\left.\begin{aligned} \ddot{x} - \Omega\dot{y} &= 0, \\ \ddot{y} + \Omega\dot{x} &= f_{0y}. \end{aligned}\right\} \qquad (4.02)$$

The velocity components will be (if $\varphi = 0$ when $t = 0$)

$$\left.\begin{aligned} \dot{x} &= \frac{f_{0y}}{\Omega} + \Omega a \sin \Omega t, \\ \dot{y} &= \Omega a \cos \Omega t. \end{aligned}\right\} \qquad (4.03)$$

The trajectories of this motion will be cycloids or trochoids (Fig. 6). The electron moves along the circle a with angular velocity Ω, and the center of the circle moves parallel to the x axis with velocity f_{0y}/Ω. The radius a of the circular orbit and the position of the center of the orbit in the working space are determined by the initial conditions, which can be derived in the following fashion. The condition of energy conservation at any point of the trajectory has the form

$$\frac{1}{2}(\dot{x}^2 + \dot{y}^2) = f_{0y}y. \qquad (4.04)$$

Let the electron emitter be located at a distance b from the cathode and let it have the same potential as the cathode, and in addition, assume that the influence of the electric field component parallel to the x axis on the motion of the electron can be neglected on the segment of path near the emitter. Then, integrating the first equation of (4.02) and assuming that the initial velocity of the electron on the emitter is zero, we obtain

$$\dot{x} = \Omega(y - b) \qquad (\dot{x} = 0 \text{ when } y = b). \qquad (4.05)$$

Let us find under what values $y = d_1$ and $y = d_2$ the velocity y vanishes. For this purpose we substitute x from formula (4.05) into (4.04). For the sought values of y we obtain the quadratic equation

$$(y - b)^2 = \frac{2f_{0y}}{\Omega^2}y. \qquad (4.06)$$

Introducing for the sake of brevity the symbol

$$\delta = \frac{f_{0y}}{\Omega^2} \qquad (4.07)$$

and solving (4.06), we obtain two roots

$$\left.\begin{aligned} d_1 &= \delta + b + \delta\sqrt{1 + \frac{2b}{\delta}}, \\ d_2 &= \delta + b - \delta\sqrt{1 + \frac{2b}{\delta}}, \end{aligned}\right\} \qquad (4.08)$$

from which we obtain the radius of the orbit

$$d = \frac{d_1 - d_2}{2} = \delta\sqrt{1 + \frac{2b}{\delta}} \qquad (4.09)$$

and the ordinate of the plane in which the centers of the orbits move (supply plane),

$$d = \frac{d_1 + d_2}{2} = \delta + b. \qquad (4.10)$$

From these expressions we see that the trajectory depends on the position of the emitter relative to the cathode. If b is positive (the emitter is above the cathode, Fig. 7a), we obtain an elongated cycloid. When b = 0, when, as is customary, the emitter is on the surface of the cathode, we obtain a normal cycloid (Fig. 7b). If b is negative, then the emitter is located below the surface of the cathode and a foreshortened cycloid is obtained (Fig. 7c), and finally, in the limiting case when

$$b = -\frac{\delta}{2} = -\frac{f_{0y}}{2\Omega^2}, \qquad (4.11)$$

we obtain in place of a trochoid a straight trajectory (Fig. 7d), since a = 0 and the electron moves parallel to the x axis with the drift velocity f_{0y}/Ω. Thus, the form of the trajectory is very sensitive to the position of the emitter relative to the cathode.

The kinetic energy of the electron moving along the trajectory will have a maximum at the point $y = d_1$ farthest from the cathode plane. From relation (4.04) it follows that the kinetic energy of the electron at the point $y = d_1$ is equal to $mf_{0y}d_1$; this is precisely the energy with which it arrives at the anode during the generation mode. The energy which the electron obtains from the constant field along the entire path from the cathode to the anode is equal to $mf_{0y}D$. It follows therefore that the relative anode losses are

$$1 - \eta_a = \frac{d_1}{D}. \qquad (4.12)$$

For small values of b (compared with δ) we obtain from (4.07) the approximate formulas

$$\left.\begin{aligned} d_1 &= 2(\delta + b), \\ d_2 &= \frac{b^2}{2\delta} \end{aligned}\right\} \qquad (b < \delta). \qquad (4.13)$$

Substituting the value of d_1 into (4.12) we obtain an expression for the relative anode losses at small values of b:

$$1-\eta_a=2\frac{\delta+b}{D} \qquad (b<\delta). \tag{4.14}$$

Under practical conditions d_1 is equal to several tenths of a millimeter, therefore even a small rise of the electron-emitter surface above the cathode surface greatly decreases the efficiency of the process.

If the emitter is located in the plane of the cathode, as is the case in ordinary magnetrons with oxide cathodes, then b = 0 and the trajectory will be a normal cycloid (Fig. 7b). In this case the losses are equal to

$$1-\eta_a=2\frac{\delta}{D}. \tag{4.15}$$

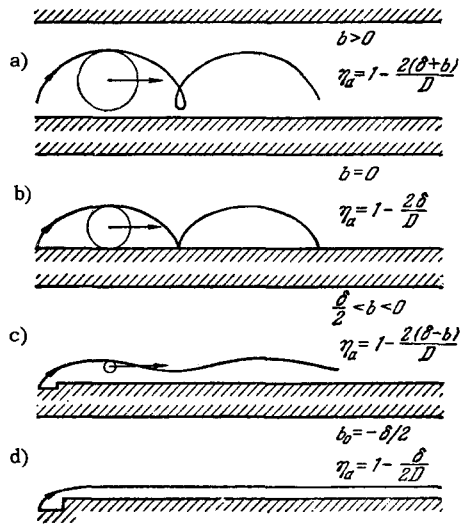

FIG. 7

When the emitter is located deeper (b < 0), the losses will decrease according to (4.14) (Fig. 7c). The limiting value for the negative values of b is $-\delta/2$; when $b=-\delta/2$ the motion of the electrons will follow a line parallel to the cathode plane (Fig. 7d). In this case the electron velocity will be minimal and the anode losses will also be minimal

$$1-\eta_a^{\max}=\frac{1}{2}\frac{\delta}{D} \qquad \left(b=-\frac{\delta}{2}\right). \tag{4.16}$$

Comparing the last two expressions, we see that in the second case the losses are one quarter as large as in the first, and the efficiencies differ greatly from each other.

The reason for this difference is obviously that when the electrons move from an emitter which is recessed in the cathode, the trajectories of motion are linear and there is no orbital kinetic energy connected with the circular motion of the electron, so that its entire kinetic energy is determined by the square of the drift velocity. Consequently the anode losses given by (4.16) are the smallest possible.

The velocity of electrons moving along a normal cycloid at a point farthest away from the cathode is twice as large and the kinetic energy is four times as large as in "pure drift." It follows from (4.14) that any rise of the emitter above the cathode surface increases the losses. By locating the emitter below the surface of the cathode the rotational motion of the electrons is decreased, which not only increases the anode efficiency but also other losses, which will be referred to later.

Let us introduce in (4.07) the field in place of the acceleration and let us use the resonance condition (2.24); we then obtain

$$\delta=\frac{m}{e}\frac{2cl}{H\lambda}, \tag{4.17}$$

and the optimal efficiency will be

$$\eta_a^{\max}=1-\frac{m}{e}\frac{cl}{\lambda DH}. \tag{4.18}$$

This relation makes it possible to estimate the maximum efficiency of the planotron in a given mode. We note that the anode efficiency of the planotron increases with increasing magnetic field at which the electronic process takes place.

The optimal depth of the emitter is, in accordance with (4.11),

$$b_0=-\frac{\delta}{2}=-\frac{m}{e}\frac{cl}{\lambda H}. \tag{4.19}$$

It must be pointed out that this value is inaccurate, for in the derivation of expression (4.05) for $\dot{x}$ we assumed that there is no x-component of the electric field along the electron path. Actually this condition is not realizable exactly, and therefore expression (4.19) must be regarded as an approximation. Experiment shows that for a successful choice of the form of the recess for the emitter the experimental value of b_0 agrees closely with the calculated one. It is easy to establish experimentally the optimal conditions, since this is simply effected by choosing the magnetic field.

It would be interesting to investigate the influence of the form of the recess on the trajectory of the electrons, and particularly find forms at which the electrons move in the working space without orbital motion if possible. Apparently the most effective will be an investigation of the electron trajectories, since the difficulties in the mathematical analysis are aggravated here by the influence of space charge, which has a high density near the cathode.

The orbital motion of the electrons can also affect the anode losses in the following manner. It was shown in Chapter II that in double resonance (2.21), when $\Omega = \omega$, the radius of the electron orbit does not remain constant. It is seen from (2.23) that, depend-

ing on the value of the phase gA + 2φ, the rate of change of the orbit $\dot{a}$ can be either positive or negative. Therefore part of the electrons will strike the anode with an increased radius and consequently with an increased kinetic energy, which will give rise to additional losses. The other part, which will arrive with decreased radius, will bring less kinetic energy and decrease the losses. It is easy to show that in the final analysis this will lead to an increase in the losses, since the derivative $\dot{a}$, as can be well seen from the third equation of (2.23) is proportional to a and therefore the kinetic energy of the electrons increases on the average. Consequently, when the angular frequencies Ω and ω coincide, a certain decrease in generator efficiency is observed in experiment.

Resonances of the type (2.21) manifest themselves relatively weakly because the electrons cover the distance from the cathode to the anode in a small number of cycles and the radius of the orbit does not have a chance to increase noticeably. The principal means of decreasing the losses connected with resonances of the type (2.21) is to use a recessed emitter, which reduces the electron orbital motion to a minimum.

It must be noted that the conditions (2.17) do not exhaust all the possibilities, since it can be shown that the higher spatial harmonics in the expansion of the potential (2.04), can also resonate. But such effects can be regarded as small and I believe that at the present stage of the study of the planotron they can be disregarded.

The reason for the cathode losses follows also from the previously considered (Chapter II, p. 787) mechanism of phase focusing of the electron orbits near the cathode. These losses are due to the kinetic energy brought by the electrons returning to the cathode.

The electrons returning to the cathode are those whose phase gA lies in the range from $\pi/2$ to $3\pi/2$ (Fig. 8) and "there is not enough space" for the orbits to pass into the tongues. The center of the electron orbit, which lies in the supply plane B = d with phase coordinate gA_0 should go over into a tongue along the stream line shown dashed in Fig. 8. At the point $gA = \pi/2$ this trajectory will be closest to the cathode. If the distance from this point to the cathode is smaller than the radius a of the orbit, then there is enough room in the orbit and the electron will reach the cathode. Thus, the limiting trajectory for the electron entering into the tongue will be determined, in accordance with (2.26), by the expression

$$\operatorname{sh} gB \sin gA = \operatorname{sh} ga. \tag{4.20}$$

The point with coordinates $A = A_0$ and $B = d$ (on the supply plane) will lie on this trajectory, and therefore

$$\sin gA_0 = \frac{\operatorname{sh} ga}{\operatorname{sh} gd}. \tag{4.21}$$

In view of the smallness of the quantities ga and gd,

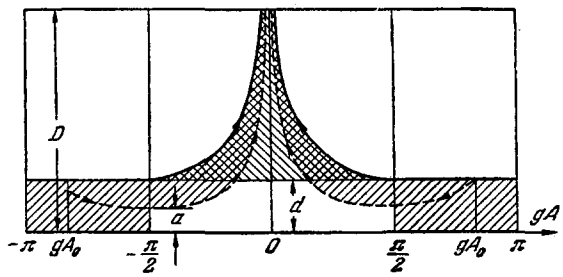

FIG. 8

we obtain for the limiting phase the expression

$$gA_0 = \pi - \arcsin\frac{a}{d}, \tag{4.22}$$

where the arcsine is taken in the first quadrant.

It is seen from Fig. 8 that if we put the total number of electrons starting from the cathode in the right half of the tongue proportional to π, then gA_0 electrons will enter the tongue, and $\pi - gA_0$ return to the cathode. Thus, we find that the ratio of the cathode current J_k to the working (anode) current J will be

$$\frac{J_k}{J} = \frac{\pi - gA_0}{gA_0} = \frac{\arcsin\frac{a}{d}}{\pi - \arcsin\frac{a}{d}}. \tag{4.23}$$

Each electron returning to the cathode absorbs from the oscillations an energy proportional to the path d – a, and each electron striking the anode will give up an energy proportional to B. It follows therefore that the relative losses due to the return of the electrons to the cathode are

$$1 - \eta_k = \frac{J_k}{J}\,\frac{d-a}{D}. \tag{4.24}$$

Substituting the value of J_k/J from (4.23) we obtain ultimately

$$1 - \eta_k = \frac{d}{D}\left(1 - \frac{a}{d}\right)\frac{\arcsin\frac{a}{d}}{\pi - \arcsin\frac{a}{d}}. \tag{4.25}$$

From this expression and from (4.23) we see that the losses due to the reverse current are wholly dependent on the type of the trajectory along which the electrons move. The cathode losses are zero ($\eta_k = 1$) in two cases:

$$\begin{aligned} &1)\quad a = d, \qquad J_k = J, \\ &2)\quad a = 0, \qquad J_k = 0. \end{aligned} \tag{4.26}$$

In the first case the trajectory is a normal cycloid, and in the second the radius of the orbit is a = 0. Only in the second case is there no backward current.

Figure 9 shows the dependence of J_k/J on 1 – a/d, calculated from formula (4.23). Figure 10 shows the function

$$\left(1 - \frac{a}{d}\right)\frac{\arcsin\frac{a}{d}}{\pi - \arcsin\frac{a}{d}}, \tag{4.27}$$

which is contained in formula (4.25) for the cathode

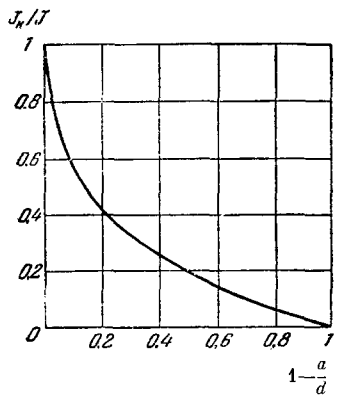

FIG. 9

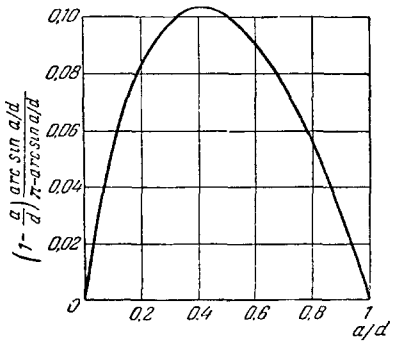

FIG. 10

losses. It is seen from Fig. 10 that the losses have a maximum when $a \approx 0.4d$.

The cathode losses are always smaller than the anode losses. Indeed, from (4.12) and (4.25) we obtain

$$\frac{1-\eta_k}{1-\eta_a} = \frac{d_2}{d_1} \frac{\arcsin\frac{a}{d}}{\pi - \arcsin\frac{a}{d}}, \qquad (4.28)$$

and inasmuch as the ratio d_2/d_1 is always less than unity (Fig. 6), the cathode losses are smaller than the anode losses. As is well known, the harmful influence of these losses is connected with additional heating of the emitter, which may be harmful at high power.

It follows from the foregoing that the cathode losses are always connected with the orbital motion of the electrons, and if there is no orbital motion ($a = 0$), these losses are likewise missing. All the factors which influence the orbit radius a also influence the losses. If the motion is strictly cycloidal ($a = d$), there are no cathode losses, but even small deviations from the equality $a = d$ immediately give rise to cathode losses, as can be seen from Fig. 10.

The main factor influencing the orbit radius a is the edge effect, which will be discussed in the next chapter. An increase in the radii of the orbits, occurring as a result of resonance phenomema on the edges of the cathode, can greatly increase the cathode losses just calculated. For the time being it is still difficult to take quantitative account of this factor.

5. EDGE EFFECT AND ASSOCIATED LOSSES

Ever since the study of the cutoff action of a magnetic field on a radial electron beam started in 1921, the phenomenon of residual or null current was observed even in the prototypes of the modern magnetron. This phenomenon consists in the fact that for a fixed potential difference between two coaxial cylinders or between two planes, there is a definite value of the magnetic field, directed perpendicular to the static electric field, which twists the electron trajectories in such a way, that the anode current stops flowing. The magnetic field at which the electrons cannot reach the cathode is called the "cutoff magnetic field." Experiment shows that this cutoff is never complete: between the cathode and the anode a certain current always flows, which is called either the null or the residual current.

This phenomenon is of great theoretical interest; it appears quite paradoxical, since it is contrary to the fundamental laws of electron motion. To derive the conditions for current cutoff in crossed electric and magnetic fields it is not necessary to know either the distribution of the space charges or the electron trajectories, since this condition is obtained only from the fundamental laws of dynamics, namely the conservation of the momentum (or angular momentum) and the conservation of energy. Naturally, this problem has been the subject of many papers, but so far there is not only no quantitative theory of this phenomenon, but there are not even convincing qualitative explanations.*

It is also important to understand the nature of the residual current because it has great practical significance both in magnetrons and in the planotron, inasmuch as the residual current can reach considerable magnitudes and greatly reduce the efficiency. The reason for it is that the value of the residual current apparently depends little on the generated power; some power is always lost in the maintenance of this current, and does not participate in the generation of the oscillations, thus reducing the generator efficiency. This phenomenon is particularly harmful in the generation of small amounts of power; it is quite possible that this phenomenon has so far been the principal factor interfering with the realization of magnetrons that generate continuously small power with good efficiency. In the study of the planotron it has been confirmed that this phenomenon harmfully influences the efficiency here, too.

An experimental investigation of the residual current has shown that it is concentrated on the outer edges of the cathode and its magnitude greatly increases with the radius of the electron orbits. This fact leads to the hypothesis that the residual current

*See, for example, R. L. Jepsen and M. W. Mueller, J. Appl. Phys. 22 (9), 1196-1207 (1951) and the literature cited therein.

is brought about by the interaction between the orbital motion of the electrons and the electrostatic field. Indeed, a theoretical study, by our method, of the electron motion in the absence of oscillations in resonators shows that the residual current can be explained quite simple and naturally. As experimental material is accumulated, this point of view continues to develop and its correctness becomes more probable. As will be seen from what follows, we still do not have (owing to the complexity of the mathematical problem) the ability of accurately calculating the value of the residual current, but there is already a possibility of explaining the mechanism of this phenomenon and of disclosing those factors on which the residual current depends and which essentially influence its magnitude.

Let us find, by the method developed in Chapter I, the trajectories of the electrons in an electrostatic field $\mathcal{E}$, taking into account the fact that this field has periodic irregularities due, for example, to the resonator slots in the planotron or in the magnetron. It turns out that the inhomogeneous field can influence the orbital motion of the electrons, and that the radii of the electron orbits grow and consequently the electrons can reach the anode; this indeed produces the residual current.

Let us show how the electron trajectories are calculated in this case by the averaging method. We first find the periodic electrostatic field produced by the resonator slots in the working space of the planotron. Figure 11 shows the distribution of the electrostatic force lines in the working space. In the absence of oscillations in the resonators this is the only electric field in the work space.

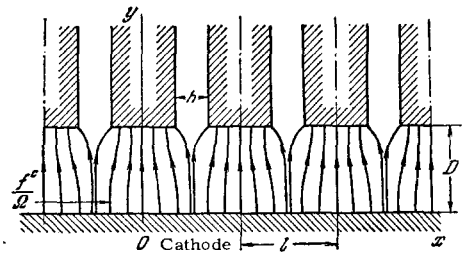

FIG. 11

We retain the previous notation which is marked on Fig. 11. The periodic electrostatic field which satisfies the two-dimensional Laplace equation can be written in the following general form:

$$\left.\begin{aligned}\mathcal{E}_x &= \sum_{n=1}^{\infty} M_n \operatorname{sh} 2ngy \sin 2ngx,\\ \mathcal{E}_y &= \mathcal{E}_y^c - \sum_{n=1}^{\infty} M_n \operatorname{ch} 2ngy \cos 2ngx.\end{aligned}\right\} \qquad (5.01)$$

We employ here the previous notation of (2.02)

$$g = \frac{\pi}{l}. \qquad (5.02)$$

The coefficients M_n, as usual, are determined from the boundary conditions. Inasmuch as in our problem it is not necessary to know the exact values of M_n, it is sufficient to assume the following simplified boundary conditions: in the plane y = D, over the entire width h of the resonator apertures, we have $\mathcal{E}_y = 0$, and on the metal teeth of the resonators $\mathcal{E}_y$ has a constant value $\mathcal{E}_1$. In the plane y = D we have, as always, $\mathcal{E}_x = 0$. We do not give the ordinary calculations and present immediately the coefficients obtained from these boundary conditions

$$M_n = (-1)^n \frac{2\mathcal{E}_1}{\pi} \quad \frac{l}{l-h} \quad \frac{\sin ngh}{n \operatorname{sh} 2ngD}. \qquad (5.03)$$

In order to change over from fields to accelerations, we use the following notation:

$$H_n = \frac{e}{m} M_n, \quad F_x = \frac{e}{m}\mathcal{E}_x, \quad F_y = \frac{e}{m}\mathcal{E}_y. \qquad (5.04)$$

The acceleration components corresponding to the n-th spatial harmonic of the electrostatic field are

$$\left.\begin{aligned}F_{nx} &= H_n \operatorname{sh} 2ngy \sin 2ngx,\\ F_{ny} &= -H_n \operatorname{ch} 2ngy \cos 2ngx.\end{aligned}\right\} \qquad (5.05)$$

Changing over to complex quantities $F_n = F_{nx} + iF_{ny}$ we obtain

$$F_n = -H_n \cos 2ngz^*, \qquad (5.06)$$

where z* is the conjugate of z, and

$$z = \bar{\alpha} + \frac{f_y^c}{\Omega} t - iae^{-i(\Omega t+\varphi)}. \qquad (5.07)$$

We use here formulas (2.12) and (2.13); a is the radius of the orbit and $f_y^c = (e/m)\mathcal{E}_y^c$ is the constant acceleration along the y axis. Substituting these quantities into (1.20) we obtain the following equations

$$\dot{\bar{\alpha}} = \frac{i}{\Omega} \sum_{n=1}^{\infty} H_n \overline{\cos 2ngz_0^*}, \qquad (5.08)$$

$$\dot{a} - ia\dot{\varphi} = -\frac{ie^{i\varphi}}{\Omega} \sum_{n=1}^{\infty} H_n \overline{\cos 2ngz_0^* e^{i\Omega t}}. \qquad (5.09)$$

Let us calculate the average value of $\cos 2ngz_0^*$, for which purpose we rewrite it in complex form:

$$\cos 2ngz^* = \frac{1}{2}\exp\left\{2ing\left(\bar{\alpha}^* + \frac{f_y^c}{\Omega} t\right) - 2ngae^{i(\Omega t+\varphi)}\right\}$$
$$+ \frac{1}{2}\exp\left\{-2ing\left(\bar{\alpha}^* + \frac{f_y^c}{\Omega} t\right) + 2ngae^{i(\Omega t+\varphi)}\right\}. \qquad (5.10)$$

We expand the exponentials in series and retain only those terms that do not vanish after averaging:

$$\cos 2ngz^* = \frac{1}{2} e^{-2ing\left(\bar{\alpha}^* + \frac{f_y^c}{\Omega} t\right)}$$
$$\times \left[1 + \sum_{m=1}^{\infty} \frac{(2nga)^m}{m!} e^{im(\Omega t+\varphi)}\right] + \ldots \qquad (5.11)$$

The averaging is carried out over the time interval $T = 2\pi/\Omega$.

The resonance condition, i.e., the condition, under which terms which do not depend explicitly on the time exist, has the form

$$2ng\frac{f_y^c}{\Omega} = m\Omega \qquad (m = 1, 2, \ldots). \tag{5.12}$$

When this relation is satisfied we obtain

$$\overline{\cos 2ngz_0^*} = \frac{1}{2}\frac{(2nga)^m}{m!}e^{-i(2ng\bar{\alpha}^* - m\varphi)}. \tag{5.13}$$

The right half of (5.09) is calculated analogously, and under the same resonance condition (5.12) we have

$$e^{i\varphi}\overline{\cos 2ngz_0^* \cdot e^{i\Omega t}} = \frac{1}{2}\frac{(2nga)^{m-1}}{(m-1)!}e^{-i(2ng\bar{\alpha}^* - m\varphi)}. \tag{5.14}$$

Substituting these expressions into (5.08) and (5.09) we obtain

$$\dot{A} + i\dot{B} = -\frac{H_n}{2\Omega}\frac{(2nga)^m}{m!}e^{-2ngB}e^{-i(2ngA - m\varphi)}, \tag{5.15}$$

$$\dot{a} - ia\dot{\varphi} = i\frac{H_n}{2\Omega}\frac{(2nga)^{m-1}}{(m-1)!}e^{-2ngB}e^{-i(2ngA - m\varphi)}, \tag{5.16}$$

from which we see that

$$\dot{A} + i\dot{B} = i\frac{2nga}{m}(\dot{a} - ia\dot{\varphi}). \tag{5.17}$$

Separating in the latter relation the imaginary and the real parts, we obtain

$$\dot{B} = \frac{2ng}{m}a\dot{a}, \tag{5.18}$$

$$\dot{A} = \frac{2ng}{m}a^2\dot{\varphi}. \tag{5.19}$$

It follows from (5.18) that the average motion of the electron satisfies the energy conservation law. To demonstrate this, we integrate (5.18):

$$B - \frac{ng}{m}a^2 = b_0 = \text{const}. \tag{5.20}$$

Substituting the value of the coefficient at g from the resonance condition (5.12) and changing from acceleration to the field values, we obtain

$$e\mathcal{E}_y^c B - \frac{m_0}{2}\Omega^2 a^2 = \text{const}, \tag{5.21}$$

where m_0 denotes the mass of the electron (so as not to confuse it with the index m). On the left is the average potential energy of the electron during one period of revolution; it is equal to the coordinate B of the orbit center, multiplied by the charge e and by the intensity of the homogeneous field $\mathcal{E}_y^c$. The second term is the average kinetic energy of orbital motion. Consequently, Eq. (5.18) yields the energy conservation law: this shows that when the electron moves its energy does not go over into any oscillating process. Equation (5.19) relates the angular momentum $m_0a^2\dot{\varphi}$ with the velocity $\dot{A}$; it replaces the angular-momentum conservation law, which in the absence of edge resonances prevents the electrons from reaching the anode.

We have thus conservative motion. Its physical picture is as follows.

If condition (5.12) is satisfied, then a resonance sets in between the period with which the electron moves past the slots of the resonator and the period of its natural orbital revolution. Because of the resonance, the trajectory along which the electron moves begins to change and becomes either larger or smaller than the elongated cycloid. The result is a family of trochoids, in which the radius a of the orbit and the coordinate B of its center are related by Eq. (5.20), which results from the energy conservation condition. An analogous family was already obtained by us in the preceding chapter (see Fig. 7). Expression (5.20) is obtained from the previous expression (4.04) by substituting in the latter the values of the velocities $\dot{x}$ and $\dot{y}$ from (4.03) and further averaging over the time. In the preceding case, however, the trochoid was determined by the initial conditions of motion (by the value of b) and remained the same, but here the trochoid varies continuously.

Let us consider in greater detail the resonance condition (5.12). By virtue of the fact that according to (5.03) and (5.04) we have

$$H_n \sim \frac{1}{n \operatorname{ch} 2ngD}, \tag{5.22}$$

the coefficients H_n decrease very rapidly with increasing n, and therefore we can confine ourselves only to an examination of the first harmonic of the acceleration, since it exerts the decisive influence. For this harmonic the resonance condition (5.12) assumes the form

$$\frac{2gf_y^c}{\Omega} = m. \tag{5.23}$$

Let us show that under real operating conditions, regions where condition (5.23) is satisfied must exist both in the planotron and in the magnetron along the edges of the working space. On approaching the edges of the cathode (Fig. 12) the vertical component of the electrostatic field $\mathcal{E}_y^c$ and the acceleration corresponding to it gradually decrease. The electrons drifting along the cathode form a plane cloud, in which an exchange force is effective and repels the electrons to the edges of the working space. Because of this force, the charge density in the cloud is redistributed over the plane of the cathode in such a way, that the forces brought about by the space charges are compensated for over the entire surface of the cathode by the horizontal component $\mathcal{E}_x$ of the external electrostatic field. It follows therefore that the electron cloud has a density that drops off along the edges; this is shown in Fig. 12, which shows schematically the transverse cross section of the working space.

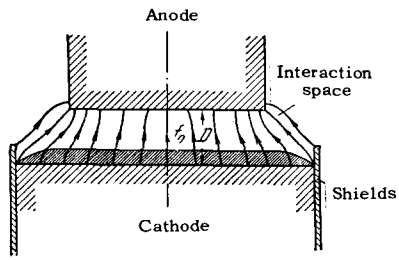

FIG. 12

The electrostatic field $\mathcal{E}_y^c$ and the corresponding acceleration f_y^c will have in the center of the working space, on the large part of the transverse cross section, practically constant values $\mathcal{E}_{0y}$ and f_{0y}, which are determined by the resonance conditions (2.18), which guarantee the most effective generation of the oscillations. Towards the edges, the acceleration f_y^c decreases and at the very edge, where the barriers are located, the acceleration f_y^c dropped to zero (Fig. 12). Thus, the acceleration f_y^c varies between the limits

$$0 \leqslant f_y^c \leqslant f_{0y}. \tag{5.24}$$

Eliminating the value of g from expressions (5.23) and (2.18), we obtain the condition of edge resonance in the form

$$\frac{f_{yl}^c}{f_{0y}} = \frac{\Omega}{\omega}\frac{m}{2}. \tag{5.25}$$

Formulas (5.24) and (5.25) show that subject to the condition

$$\omega < \Omega < \frac{3}{2}\omega \tag{5.26}$$

there are on the edges of the cathode, on each side, two regions where the edge resonances take place (for m = 1 and m = 2). With increasing Larmor frequency Ω, the number of edge resonances will increase. Under the condition

$$\frac{1}{2}\omega < \Omega < \omega \tag{5.27}$$

only one edge resonance is possible. If the magnetic field is so small that $\Omega < \omega/2$ there will be no resonance. This case has no practical significance, for at small magnetic fields corresponding to such a mode the anode efficiency, as shown in the preceding chapter, becomes small.

In practice, planotrons and magnetrons usually operate in modes with $\Omega > \omega$, i.e., in the presence of at least two edge resonances. Therefore under the operating conditions there exist at each edge of the cathode regions in the electron cloud, where the radius of the electron orbits changes as a result of the edge resonance, and the trochoidal trajectories are gradually deformed.

In order to investigate this deformation in greater detail, let us consider the electron trajectories under resonance conditions. We separate the real and imaginary parts in Eqs. (5.15) and (5.16), and thus obtain four equations [confining ourselves to the case n = 1, i.e., taking into account only the first term in the series of (5.03)]:

$$\dot{A} = -\frac{H_1}{2\Omega}\frac{(2ga)^m}{m!}e^{-2gB}\cos(2gA - m\varphi), \tag{5.28}$$

$$\dot{B} = \frac{H_1}{2\Omega}\frac{(2ga)^m}{m!}e^{-2gB}\sin(2gA - m\varphi), \tag{5.29}$$

$$\dot{a} = \frac{H_1}{2\Omega}\frac{(2ga)^{m-1}}{(m-1)!}e^{-2gB}\sin(2gA - m\varphi), \tag{5.30}$$

$$a\dot{\varphi} = -\frac{H_1}{2\Omega}\frac{(2ga)^{m-1}}{(m-1)!}e^{-2gB}\cos(2gA - m\varphi). \tag{5.31}$$

Let us find the trajectory of the center of the electron orbit; we are essentially interested in the quantity B, the distance from the center of the orbit to the surface of the cathode. Its minimum value is $b_0 = f_y^c/2\Omega^2$, determined by an expression analogous to (4.19) and valid for all motions under which the kinetic energy is accumulated only at the expense of the electric-field potential in the working space. From the value of B we determine, using (5.20) and (5.23), the radius of the orbit

$$a^2 = \frac{m}{g}(B - b_0) = \frac{2f_{yl}^c}{\Omega^2}(B - b_0), \quad b_0 = \frac{l}{\pi}m. \tag{5.32}$$

The critical value B_c at which the electron strikes the anode is given by the condition

$$B_c = D - a. \tag{5.33}$$

The last two expressions enable us to calculate the critical value of B_c. From (5.28)—(5.31) we see that if an electron appears in the supply plane B = d, then its subsequent fate depends not only on the value of the phase coordinate gA at the initial instant of motion, but also on the phase φ on the circular orbit. In order to include the motion of electrons with all possible initial phases, it is sufficient to introduce the summary phase

$$\mu = 2gA - m\varphi \tag{5.34}$$

and consider μ within the limits $-3\pi/2 \leq \mu \leq \pi/2$. We also introduce the function

$$\nu = 2gB - m\ln a. \tag{5.35}$$

We obtain

$$\dot{\mu} = 2g\dot{A} - m\dot{\varphi} = -\frac{gH_1}{\Omega}\left[\frac{(2ga)^m}{m!} - \frac{m}{m-1}\frac{(2ga)^{m-2}}{(m-2)!}\right]e^{-2gB}\cos\mu,$$

$$\dot{\nu} = 2g\dot{B} - m\frac{\dot{a}}{a} = \frac{gH_1}{\Omega}\left[\frac{(2ga)^m}{m!} - \frac{m}{m-1}\frac{(2ga)^{m-2}}{(m-2)!}\right]e^{-2gB}\sin\mu,$$

from which follow the simple relations

$$\left.\begin{aligned}\dot{\nu} &= -\dot{\mu}\,\mathrm{tg}\,\mu,\\ \nu &= \ln\cos\mu + \mathrm{const.}\end{aligned}\right\} \tag{5.36}$$

Using (5.32), we obtain an expression for the sought trajectory

$$\left(\frac{B_0 - b_0}{B - b_0}\right)^{m/2} = e^{-2g(B-B_0)}\frac{\cos\mu}{\cos\mu_0}, \tag{5.37}$$

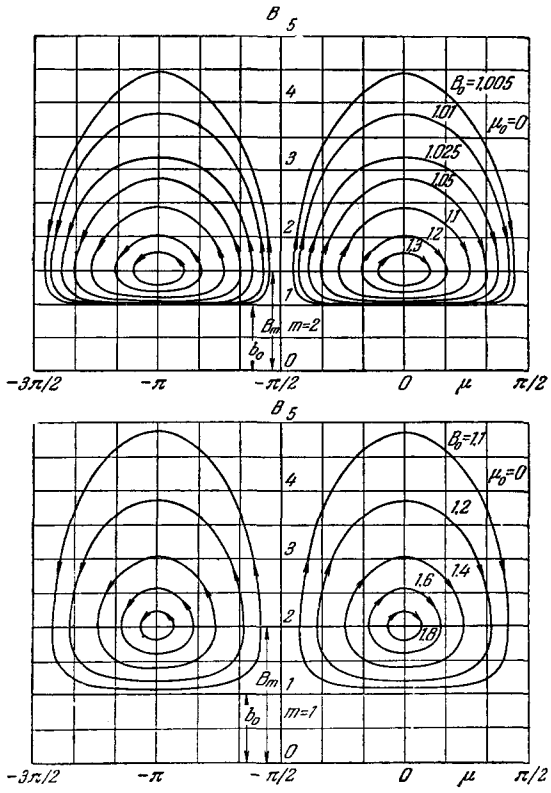

FIG. 13

where B_0 and μ_0 are the initial values of B and μ.

Figure 13 shows two families of these trajectories, calculated for values m = 1 and m = 2; we see that they have a closed character. Differentiating the preceding expression, we can show that the point which is encompassed by all the closed trajectories has coordinates

$$\mu = 0,\ \pm\pi,\ \pm 2\pi,\ \ldots\quad B = B_m = \frac{1}{mg} + b_0 = \frac{l}{\pi}\left(\frac{1}{m} + m\right). \tag{5.38}$$

On the horizontal line passing through these points lie the points of inflection of all the curves. All the curves are bounded from below by the horizontal $B = b_0$ and are not bounded at all from above, so that when $B_0 \to b_0$ the curve becomes more and more stretched in the direction of the B axis. We see that we have here also a phenomenon analogous to phase focusing, since the centers of the electron orbits gather into tongues, but above the horizontal line $B = B_m$ the tongues diverge (Fig. 13). These tongues of course pertain to the phase space (μ, B) which is connected in a complicated fashion with the actual space. In the actual space there will be no periodic concentration of electrons along the A axis. The only electrons whose orbits will increase and which move towards the anode will be those whose initial phase is in the interval $0 < \mu_0 < -\pi$. The closer this initial phase is to $-\pi/2$ (see Fig. 13), the more stably does the electron move to the anode. Another part of the electrons will move towards the cathode, and the radii of their orbits will decrease.

The results obtained explain the appearance of the residual current. Inasmuch as the acceleration f_y^c on the edge where the resonance causing the residual current occurs is not connected with the acceleration f_{0y} in the center of the working space, which is determined by the resonance conditions that ensure generation of oscillations, the two resonant processes can occur independently of each other. The residual current is produced along the edges of the working space, in strips where conditions (5.12) are satisfied, and since it does not participate in the generation process it only decreases the generator efficiency. To calculate the residual current it is necessary to know both the width of the strip of the electron cloud along the edge of the cathode, from which the electron can be drawn into the tongues, and the density of the electron charge in the cloud. These quantities are unknown and at the present time we do not know how to calculate them.

The phenomena in the electron cloud should also become more complicated because of the transverse motion of the electrons, because of which the electrons will continuously enter into the resonant bands and leave them. In spite of the fact that the change in the electron-orbit radii occurs in narrow strips along the edges of the working space, owing to the transverse motion of the electrons it will extend over the entire space. Thus, a variety of orbit radii will be produced in all of the working space and the kinetic energy of the orbital motion will increase on the average. It was shown in the preceding chapter that this leads to a deterioration of the anode efficiency and increases the inverse current to the cathode.

Experiments which we carried out with the planotron have shown that the cathode can become strongly heated even in the absence of oscillations in the resonators. In some such cases our calorimetric measurements have shown the power delivered to the anode to be comparable with the power delivered to the cathode. This shows that the electrons return to the cathode with increased energy, which in some of our experiments amounted to approximately 10%, on the average, of the voltage between the cathode and the anode (for example, with 4900 V applied the average energy of an electron returning to the cathode was 460 eV). Consequently, the motion of the electrons in the working space is not conservative, for in conservative motion relation (5.21) holds true and the electron cannot return to the cathode with an excess kinetic energy. In the absence of oscillations in the system, the cathode can be heated only in the case when energy exchange can occur between the circular motions of the electrons, an exchange which can be compared with the ordinary temperature equalization which occurs as a result of exchange of kinetic energy between molecules.

Thus, the primary cause of the residual current lies in the resonance on the edges of the working space. Because of this resonance, the motion of the

electrons is along deformed trochoids, belonging to one family, but having different kinetic energies. Therefore the summary kinetic energy of the electron cloud increases. Because of the interaction between the electrons moving in the cloud with different kinetic energies, the summary kinetic energy becomes equalized and therefore the trochoids no longer belong to the previous families. This enables the electrons to return to the cathode with an excess of kinetic energy and to heat the latter.

The explanation offered above for the residual current discloses a perfectly definite path for further both theoretical and experimental study of this interesting and important phenomenon, and at the same time permits an explanation of many known phenomena, particularly the phenomenon wherein an increase in the residual current is always accompanied by an increase in the reverse current (the current from the emitters to the cathode).

A reduction in the residual current is important to the effective operation of planotrons and magnetrons. The means for combatting the residual current follows directly from an analysis of factors which determine the value of $\dot{B}$ in accordance with Eq. (5.29). At a given width of the electron cloud and for a given density of the space charge, the value of the edge effect, and consequently of the residual current, will be proportional to $\dot{B}$. We denote the proportionality coefficient by K, and then the residual current will be

$$J_n = K\dot{B} \tag{5.39}$$

and the corresponding relative edge losses will be

$$1-\eta_n = \frac{J_n}{J} = \frac{K\dot{B}}{J}, \tag{5.40}$$

where J is the anode current.

In some of our experimental planotrons the losses due to the edge effect reached such a magnitude, that self-excitation of the generator stopped. To avoid this, it is necessary to choose correctly the parameters of the working space of the planotron. It follows from Eq. (5.39) for $\dot{B}$ and from expression (5.03) for H_1 that the value of the zero current is greatly influenced by the ratio D/l (D is the width of the working space and l the period of the structure). The larger this ratio, the smaller the residual current. However, it is impossible to increase this ratio above a certain limit, for this entails a sharp increase in the critical Q_c, which according to formula (3.37) is proportional to sinh 2gD.

The value of $\dot{B}$ decreases also with the ratio a/l, so that the smaller the initial orbit of the electrons entering into the working space, the smaller the residual current. Thus, the reverse current (like the anode and cathode losses) should decrease when the electron emitter is placed below the cathode level (see Chapter IV). This conclusion was confirmed in our experiments with the planotron. The reverse current should also decrease if one chooses a working space of such form, that the coefficient H_1, which determines the amplitude of the first harmonic of the acceleration in accord with (5.04), decreases. The value of H_1 depends on the shape of the outer edges of the anode, which must be made as even as possible so as not to increase the periodic inhomogeneities of the electrostatic field.

Finally, the last and most obvious and real method of combatting edge losses (something impossible in the case of low power) is to use as wide a working space as possible, for which the ratio of the perimeter to the area is smaller. This leads to a decrease in the relative losses due to the residual current. It is obvious that the fraction of residual-current losses decreases with increasing generated power, and thus the overall efficiency is improved.

One can point to still another cause of the residual current. It is well known that when the magnetic field cuts off the current, the electron cloud at the cathode reaches a density such that the space-charge field near the electron emitter compensates for the external electric field. It is easy to calculate the cloud density and to show that even at noticeable values of the residual current the electrons must execute a large number of revolutions about the cathode. Many manufacturing irregularities occur on the surface of the cathode and the anode, or else the working gap boundaries are not perfectly parallel; all this influences the inhomogeneity of the electric field. The inhomogeneity of the field caused by these factors can always be expanded into a Fourier series, and under certain conditions resonance arises with the orbital motion of the electrons. Because the electrons execute a large number of revolutions about the cathode even in the presence of small perturbing irregularities, the radii of the orbits will unavoidably grow and this will lead to the appearance of at least a small residual current. This apparently explains why it is impossible in practice to produce sufficiently homogeneous conditions for the electron motion, such that the magnetic field be capable of completely cutting off the electron current in accordance with the laws governing the motion of electrons in crossed fields.

In multicavity magnetrons as well as planotrons, the cavities necessary for the generation produce a strong periodic inhomogeneity of the electrostatic field, so that the residual current and the phenomena associated with it are large. From (5.29) and (5.30) it is seen that owing to the factor $\exp(-2gB)$ the derivatives $\dot{B}$ and $\dot{a}$ have the largest value at small values of B, i.e., near the cathode. This means that the initial changes in the radii of the electron orbits are easiest to produce. Therefore even small periodic irregularities in the working space, not sufficient to produce a large residual current by themselves, can strongly influence the initial spread in the electron-orbit radii. In the same manner, all irregularities in

the electric field, even very small ones, once they result in a small but well concentrated variation in the field at a distance comparable with the pitch of the trochoids, cause the orbit radii to increase and this, as shown earlier, influences adversely the quality of the device. It is therefore necessary to watch the surface finish of the cathode, which must be as perfect as possible.

VI. THEORY OF THE MAGNETRON

There is an extensive literature devoted to the magnetron, and its characteristics are known for a wide range of wavelengths. We therefore consider it of interest to compare where possible the theoretical characteristics, obtained with the aid of our method, with the experimental data.

The calculation of the electron trajectories in a magnetron is a more complicated problem than that in the planotron, for in the magnetron we deal with motion of electrons not in a plane-parallel electrostatic field, but in an annular gap with a radial electrostatic field. As will be shown below, there is no simple solution to the problem of the motion in the static fields of a magnetron, and the problem must be solved from the very outset by perturbation theory, which makes the analysis of the processes in the magnetron more complicated than in the planotron.

The electronic mechanism in the magnetron and in the planotron is the same, but the curvature of the working space can modify somewhat this mechanism and introduce new features, particularly in the ratio of the influence of the space charges. If the number of magnetron cells is increased and the gap between the anode and the cathode is made small compared with the radius of the cathode, then, as will be shown at the end of the chapter, its characteristics will approach more and more the characteristics of the planotron.

The principal symbols are indicated in Fig. 14. The inside and outside radii of the working space are denoted by r_1 and r_2 respectively, the gap between the anode and cathode is denoted by D, the mean radius by $\bar{r}$, and the number of resonator cavity pairs by p (the total number of cavities is frequently denoted in the literature by N). These quantities are related by the following simple expressions:

$$\left.\begin{aligned} D &= r_2 - r_1, \quad \bar{r} = \frac{r_1 + r_2}{2}, \\ N &= 2p, \qquad \vartheta_p = \frac{2\pi}{p}. \end{aligned}\right\} \tag{6.01}$$

An investigation of the trajectories in the magnetron is carried out in the same way as in Chapter II for the planotron. We start with the determination of the analytic expression for the alternating electric field E, produced by the resonators, and the acceleration corresponding to it

$$F = \frac{e}{m} E. \tag{6.02}$$

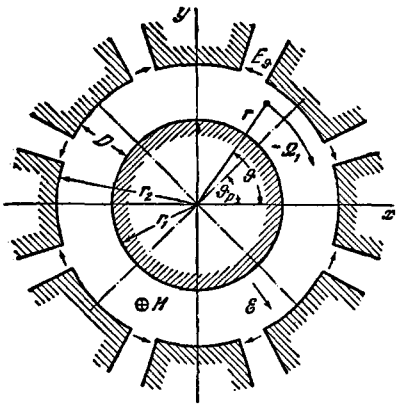

FIG. 14

The angular frequency of the oscillations in the resonator will as before be $\omega = 2\pi c/\lambda$. In view of the fact that the wavelength λ is much larger than the distance $r_2\vartheta_p$ between cavities (this condition is satisfied for the planotron, too) we use in place of the wave equation (2.03) simply the Laplace equation. In cylindrical coordinates this equation has the form

$$r\frac{\partial}{\partial r}\left(r\frac{\partial \Phi}{\partial r}\right) + \frac{\partial^2 \Phi}{\partial \vartheta^2} = 0, \tag{6.03}$$

where Φ is the scalar potential. The general solution of this equation in cylindrical coordinates, with period ϑ_p in the angle ϑ, has the form

$$\Phi = \sum_{m=1}^{\infty} M_m (z^{\pm mp} + z^{*\pm mp}), \tag{6.04}$$

where

$$z = re^{i\vartheta}, \quad z^* = re^{-i\vartheta}. \tag{6.05}$$

The calculation of the expansion coefficients M_m, and also further derivations, become much simpler if we introduce the following elementary functions, which we designate by sir and cor (radial sine and cosine):

$$\operatorname{sir}(x^n) = \frac{x^n - x^{-n}}{2}, \quad \operatorname{cor}(x^n) = \frac{x^n + x^{-n}}{2}. \tag{6.06}$$

The use of these functions greatly simplifes the calculations in cylindrical coordinates, inasmuch as sir and cor are natural generalizations of the hyperbolic functions sinh and cosh which are suitable for the case of rectangular coordinates. As will be shown below, many expressions for the motion of the electron in the cylindrical case can be directly obtained from the planar case by replacing sinh and cosh by sir and cor. At the end of the chapter we shall show that in the limiting case of a magnetron with a large number of cavities these expressions become equivalent. Inasmuch as the functions sir and cor are specially adapted for the solution of cylindrical problems, I designated them with letter combinations which show their similarity to the hyperbolic functions, and with the letter r to indicate their relationship to the

Table I

$$\operatorname{cor}(x)=\frac{1}{2}\left(x+\frac{1}{x}\right), \qquad \operatorname{sir}(x)=\frac{1}{2}\left(x-\frac{1}{x}\right),$$

$$\operatorname{cor}\left(\frac{1}{x}\right)=\operatorname{cor}(x), \qquad \operatorname{sir}\left(\frac{1}{x}\right)=-\operatorname{sir}x,$$

$$\cos x=\operatorname{cor}(e^{ix}), \qquad \sin x=-i\operatorname{sir}(e^{ix}),$$

$$\operatorname{ch} x=\operatorname{cor}(e^{x}), \qquad \operatorname{sh} x=\operatorname{sir}(e^{x}),$$

$$\frac{d}{dx}\operatorname{cor}(x^n)=\frac{n}{x}\operatorname{sir}(x^n), \qquad \frac{d}{dx}\operatorname{sir}(x^n)=\frac{n}{x}\operatorname{cor}(x^n),$$

$$\operatorname{cor}(xy)=\operatorname{cor}(x)\operatorname{cor}(y)+\operatorname{sir}(x)\operatorname{sir}(y),$$

$$\operatorname{cor}\left(\frac{x}{y}\right)=\operatorname{cor}(x)\operatorname{cor}(y)-\operatorname{sir}(x)\operatorname{sir}(y),$$

$$\operatorname{sir}(xy)=\operatorname{sir}(x)\operatorname{cor}(y)+\operatorname{cor}(x)\operatorname{sir}(y),$$

$$\operatorname{sir}\left(\frac{x}{y}\right)=\operatorname{sir}(x)\operatorname{cor}(y)-\operatorname{cor}(x)\operatorname{sir}(y),$$

$$\operatorname{sir}(x)\operatorname{cor}(y)=\frac{1}{2}\left[\operatorname{sir}(xy)+\operatorname{sir}\left(\frac{x}{y}\right)\right],$$

$$\operatorname{cor}(x)\operatorname{cor}(y)=\frac{1}{2}\left[\operatorname{cor}(xy)+\operatorname{cor}\left(\frac{x}{y}\right)\right]$$

$$\operatorname{sir}(x)\operatorname{sir}(y)=\frac{1}{2}\left[\operatorname{cor}(xy)-\operatorname{cor}\left(\frac{x}{y}\right)\right],$$

$$\operatorname{cor}^2(x)+\operatorname{sir}^2(x)=\operatorname{cor}(x^2), \qquad \operatorname{cor}^2(x)-\operatorname{sir}^2(x)=1,$$

$$2\operatorname{cor}(x)\operatorname{sir}(x)=\operatorname{sir}(x^2), \qquad \operatorname{cor}(x)+\operatorname{sir}(x)=x.$$

Equation satisfied by the cor and sir functions:

$$x\frac{\partial}{\partial x}\left(x\frac{\partial\theta}{\partial x}\right)-n^2\theta=0, \qquad \begin{cases}\theta=\operatorname{cor}(x^n),\\ \theta=\operatorname{sir}(x^n).\end{cases}$$

radius vector. Formal operations with sir and cor are very similar to operations with the trigonometric functions, and are therefore very easy to remember. The operations most frequently employed are listed in Table I. The conversion from trigonometric functions to sir and cor is given by the following simple formulas

$$\sin nx=-i\operatorname{sir}(e^{inx}), \qquad \cos nx=\operatorname{cor}(e^{inx}). \tag{6.07}$$

Plots of sir(x) and cor(x) is given in Fig. 15.

The functions $\operatorname{sir}(x^n)$ and $\operatorname{cor}(x^n)$ are solutions of the well known differential equation

$$\left(x\frac{\partial}{\partial x}\right)^{2p}y=n^{2p}y. \tag{6.08}$$

These functions greatly abbreviate and simplify the derivations.

The solution of the Laplace equation in a form

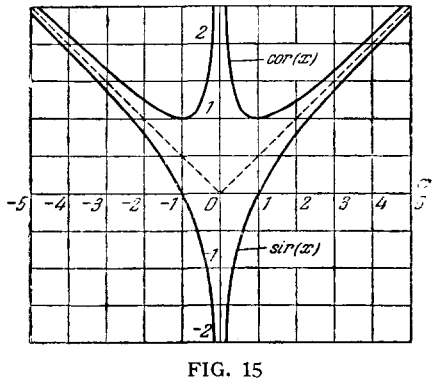

FIG. 15

suitable for our boundary conditions will have the form

$$\Phi=\sum_{m=1}^{\infty}M_m\operatorname{sir}\left(\frac{r}{r_1}\right)^{mp}\cos mp\vartheta. \tag{6.09}$$

To determine the coefficients M_m we introduce boundary conditions with the same simplifications as in the planar case when solving the Laplace equation (2.07). With allowance for Fig. 14, these can be written in the form

$$\left.\begin{aligned} &E_\vartheta=0 && r=r_1, && \\ &E_\vartheta=0 && r=r_2 && 0<\vartheta<\frac{\vartheta_p-\vartheta_h}{2},\\ &E_\vartheta=E_1=\text{const} && r=r_2 && \frac{\vartheta_p-\vartheta_h}{2}<\vartheta<\frac{\vartheta_p+\vartheta_h}{2}\end{aligned}\right\} \tag{6.10}$$

etc., recognizing that the neighboring resonators oscillate in phase opposition (π mode). We denote by ϑ_p the period of the anode structure with respect to the angle ϑ, i.e., the angle subtended by one period of the anode block at the center of the magnetron; ϑ_h denotes the angle subtended by the cavity slot.

Employing the ordinary method, we obtain the following expression for the potential

$$\Phi=\frac{4E_1r_2}{\pi p}\sum_{n=1}^{\infty}(-1)^{n+1}\frac{\sin\frac{(2n-1)\,p\vartheta_h}{2}}{(2n-1)^2\operatorname{sir}\left(\frac{r_2}{r_1}\right)^{(2n-1)p}}\times\operatorname{sir}\left(\frac{r}{r_1}\right)^{(2n-1)p}\sin(2n-1)\,p\vartheta. \tag{6.11}$$

This expression goes over into (2.08) if sir and cor are replaced by sinh and cosh.

We further confine ourselves to inclusion of the first spatial harmonic (n = 1) in formula (6.11). We introduce the notation

$$U=\frac{e}{m}\frac{4E_1}{\pi}\frac{\sin\frac{p\vartheta_h}{2}}{\operatorname{sir}\left(\frac{r_2}{r_1}\right)^p}. \tag{6.12}$$

Then the first harmonic can be written in the form

$$\frac{e}{m}\Phi=\frac{Ur_2}{p}\operatorname{sir}\left(\frac{r}{r_1}\right)^p\sin p\vartheta. \tag{6.13}$$

The acceleration components will be

$$\left.\begin{aligned}F_\vartheta&=\frac{1}{r}\frac{\partial}{\partial\vartheta}\left(\frac{e}{m}\Phi\right)\sin\omega t,\\ F_r&=\frac{\partial}{\partial r}\left(\frac{e}{m}\Phi\right)\sin\omega t.\end{aligned}\right\} \tag{6.14}$$

According to Table I, formula (6.13) can be rewritten in complex form

$$\frac{e}{m}\Phi=\frac{Ur_2}{2p}\left[\operatorname{sir}\left(\frac{z}{r_1}\right)^p+\operatorname{sir}\left(\frac{z^*}{r_1}\right)^p\right]. \tag{6.15}$$

Comparing this expression with (1.34) we obtain the complex acceleration F, due to the variable electric field in the working space of the magnetron,

$$F=\frac{Ur_2}{z^*}\operatorname{cor}\left(\frac{z^*}{r_1}\right)^p\sin\omega t. \tag{6.16}$$

The electrostatic field between two coaxial cylinders has a radial direction and a value

$$\mathscr{E}=\frac{V}{r\ln\frac{r_2}{r_1}}, \tag{6.17}$$

where V is the potential difference and r_1 and r_2 the radii of the cylinders. The complex acceleration due to this field in the working space of the magnetron is equal to

$$f=\frac{K}{z^*}, \tag{6.18}$$

where

$$K=\frac{e}{m}\frac{V}{\ln\frac{r_2}{r_1}}. \tag{6.19}$$

Under the influence of the acceleration f, the center of the circular orbit of the electron will drift around the cathode and the drift velocity will decrease with increasing radius. If we substitute the acceleration f into the fundamental equation of motion (1.06), it turns out that it has no exact solution in a sufficiently simple form which permits subsequent account of the high frequency field. Therefore, in order to find the motion in the electrostatic field we employ our approximate method, where we use the third fundamental case (1.09). In this case we resolve the acceleration (6.12) into two components

$$f=f_0+\Delta f, \tag{6.20}$$

where the acceleration f_0 is equal to

$$f_0=Cz, \tag{6.21}$$

and

$$\Delta f=\frac{K}{z^*}-Cz, \tag{6.22}$$

while the fundamental equation of motion (1.06) has the form

$$\ddot{z}+i\Omega\dot{z}=Cz+\Delta f. \tag{6.23}$$

Thus, the acceleration Cz determines the motion in accordance with formula (1.09), while the additional acceleration Δf changes only the parameters α and β. Thus, in first approximation, the motion of the electrons follows the epitrochoid

$$z=\alpha e^{-i\Omega_1 t}+\beta e^{-i\Omega_2 t}, \tag{6.24}$$

where

$$\left.\begin{aligned}\Omega_1&=\frac{\Omega}{2}\left(1-\sqrt{1-\frac{4C}{\Omega^2}}\right),\\ \Omega_2&=\frac{\Omega}{2}\left(1+\sqrt{1-\frac{4C}{\Omega^2}}\right).\end{aligned}\right\} \tag{6.25}$$

The motion when α = const and β = const consists in the center of the circular orbit moving around the cathode with angular velocity $-\Omega_1$ along a circle with radius R = | α |. The electrons revolve around this center with angular velocity $-\Omega_2$ along a circle of radius a = | β |. The perturbation of this motion under the influence of the additional acceleration Δf will be calculated from Eq. (1.22), where we put Δf for F. We then obtain

$$\dot{\bar{\alpha}}=-\frac{i}{\sqrt{\Omega^2-4C}}\overline{\left(\frac{K}{z_0^*}-Cz_0\right)e^{i\Omega_1 t}}. \tag{6.26}$$

Averaging and separating the imaginary and real parts we obtain

$$\left.\begin{aligned}\dot{\theta}&=-\frac{1}{\sqrt{\Omega^2-4C}}\left(\frac{K}{R^2}-C\right),\\ \dot{R}&=0,\ \bar{\alpha}=Re^{i\theta}.\end{aligned}\right\} \tag{6.27}$$

Analogously, we obtain an equation for $\bar{\beta}$, from which we find

$$\left.\begin{aligned}\dot{\varphi}&=\frac{1}{\sqrt{\Omega^2-4C}}\left(\frac{K}{a^2}-C\right),\\ \dot{a}&=0,\ \bar{\beta}=ae^{i\varphi}.\end{aligned}\right\} \tag{6.28}$$

Let us determine now the constant C in the expression (6.21) for the acceleration f_0. In order to obtain the best approximation, it is necessary to choose the value of C such that the average value of the difference Δf over the extent of the working space $r_1 < r < r_2$ be as small as possible. Using (6.22), we set the average value equal to zero

$$\int_{r_1}^{r_2}\left(\frac{K}{r}-Cr\right)dr=0,$$

hence

$$C=\frac{e}{m}\frac{2V}{r_2^2-r_1^2}. \tag{6.29}$$

Indeed, the average value of Δf is zero when the po-

tential difference V in (6.29) is equal to the potential difference in (6.19). A definite connection is then established between K and C. If we denote by r_0 the value of the radius vector at which $\Delta f = 0$, i.e., $f = f_0$, then

$$r_0^2 = \frac{r_2^2 - r_1^2}{2 \ln \frac{r_2}{r_1}} \text{ and } K = Cr_0^2. \tag{6.30}$$

Replacing K by C, we transform (6.27) into

$$\dot{\theta} = -\frac{C}{\sqrt{\Omega^2 - 4C}} \left(\frac{r_0^2}{R^2} - 1 \right). \tag{6.31}$$

The angular velocity at which the center of the circular orbit of the electron revolves under the influence of the acceleration f will be $-\Omega_1 + \dot{\theta}$, and depends therefore on R; it has a maximum value at the cathode and decreases as it approaches the anode. For this reason, the resonance between the oscillations of the cavities and the motion of the electrons is possible only for electrons which run around the cathode at some single value of R. Therefore the generation of oscillations in the magnetron is possible only because of phase focusing. Phase focusing in the high-frequency field maintains the correct phase of the centers of the electron orbits (which have different radii), around the cathode, resulting in a phasing velocity that changes the angular velocity of the revolution of the electrons around the cathode in the required direction.

It follows from these considerations that the trajectories of the electrons must be calculated in two stages. We first calculate the trajectories of the electrons under the influence of the acceleration $f_0 + F$, where f_0 is given by (6.21) and F by (6.16), the latter being due to the alternating electric field of the cavities. We then investigate the effect of the perturbation Δf on the motion obtained in this manner and obtain the trajectories of interest to us by the method given at the end of Chapter I.

Let us find the motions of the centers of the electron orbits under the influence of the acceleration $f_0 + F$. Using Eqs. (1.22) we obtain

$$\dot{\bar{\alpha}} = -\frac{iUr_2}{\sqrt{\Omega^2 - 4C}} \frac{1}{z_0^*} \operatorname{cor} \left(\frac{z_0^*}{r_1} \right)^p \sin \omega t e^{i\Omega_1 t}. \tag{6.32}$$

In the averaging we express sin ωt in terms of sir, using Table I, and obtain under the averaging sign the following expression:

$$\frac{1}{2} \frac{1}{z_0^*} \left\{ \operatorname{sir} \left[\left(\frac{z_0^*}{r_1} \right)^p e^{i\omega t} \right] - \operatorname{sir} \left[\left(\frac{z_0^*}{r_1} \right)^p e^{-i\omega t} \right] \right\}.$$

In order for the expression

$$\left(\frac{z^*}{r_1} \right)^p e^{i(\Omega_1 - \omega)t} = \frac{(\alpha e^{i\Omega_1 t} + \beta e^{i\Omega_2 t})^p}{r_1^p} e^{i(\Omega_1 - \omega)t}$$

to contain a term that does not depend on the time, it is necessary to satisfy the equality

$$\omega = p\Omega_1 + m\sqrt{\Omega^2 - 4C}, \tag{6.33}$$

where m = 0, 1, 2, ...

This is the resonance condition, and it interests us when m = 0, inasmuch as we have then $\dot{\bar{\beta}} = 0$, as in the planotron, and consequently the radii of the electron orbits remain constant. Substituting the value of Ω_1 from (6.25) into the resonance condition, we obtain for m = 0

$$\omega = \frac{p\Omega}{2} \left(1 - \sqrt{1 - \frac{4C}{\Omega^2}} \right). \tag{6.34}$$

In this case after averaging Eq. (6.32) assumes the form

$$\dot{\bar{\alpha}} = \frac{Ur_2}{2\sqrt{\Omega^2 - 4C}} \frac{1}{\bar{\alpha}^*} \operatorname{sir} \left(\frac{\bar{\alpha}^*}{r_1} \right)^p. \tag{6.35}$$

Using the rules for the differentiation of the cor function we can also write

$$\dot{\bar{\alpha}} = \frac{Ur_2}{2p\sqrt{\Omega^2 - 4C}} \frac{d}{d\bar{\alpha}^*} \operatorname{cor} \left(\frac{\bar{\alpha}^*}{r_1} \right)^p. \tag{6.36}$$

Comparing the right half of this equation with (1.35), we obtain the stream function for the velocity $\dot{\bar{\alpha}}$. After simple transformation we obtain

$$\Psi = \frac{Ur_2}{2p\sqrt{\Omega^2 - 4C}} \operatorname{sir} \left(\frac{R}{r_1} \right)^p \sin p\theta. \tag{6.37}$$

The trajectories are determined by the equation Ψ = const; when sir is replaced by sinh they go over into the trajectories (2.25), previously obtained for the planar case. The values of the phase velocities are obtained by differentiating the stream function

$$\left.\begin{aligned} \dot{\theta} &= -\frac{1}{R} \frac{\partial \Psi}{\partial R} = -\frac{Ur_2}{2\sqrt{\Omega^2 - 4C}} \frac{1}{R^2} \operatorname{cor} \left(\frac{R}{r_1} \right)^p \sin p\theta, \\ \dot{R} &= \frac{1}{R} \frac{\partial \Psi}{\partial \theta} = \frac{Ur_2}{2\sqrt{\Omega^2 - 4C}} \frac{1}{R} \operatorname{sir} \left(\frac{R}{r_1} \right)^p \cos p\theta. \end{aligned}\right\} \tag{6.38}$$

Let us proceed now to the second part of the problem—the calculation of the perturbation due to the acceleration Δf. For this purpose, in accordance with Eq. (1.32), we introduce in place of $\Delta C/\sqrt{\Omega^2 - 4C}$ the quantity $\dot{\theta}$ from (6.27); we then obtain

$$\left.\begin{aligned} \dot{\theta} &= -\frac{1}{\sqrt{\Omega^2 - 4C}} \left[\frac{Ur_2}{2R^2} \operatorname{cor} \left(\frac{R}{r_1} \right)^p \sin p\theta' + C \left(\frac{r_0^2}{R^2} - 1 \right) \right], \\ \dot{R}' &= \dot{R}. \end{aligned}\right\} \tag{6.39}$$

The phase velocity R remains the same as before. It is easy to see that the perturbed phase velocities determine as before potential flows. The stream function of this flow is

$$\Psi' = \frac{1}{2\sqrt{\Omega^2 - 4C}} \left\{ \frac{Ur_2}{p} \operatorname{sir} \left(\frac{R}{r_1} \right)^p \sin p\theta - Cr_0^2 \left[\ln \left(\frac{R}{r_0} \right)^2 - \left(\frac{R}{r_0} \right)^2 \right] \right\}. \tag{6.40}$$

Putting Ψ′ = const, we obtain the sought-for trajectory of the center of the electron orbit. If the motion is subject to condition (6.34), then $\dot{a} = 0$ and the radius of the circular orbit remains unchanged. The angular orbital velocity of the electron will be Ω_2'

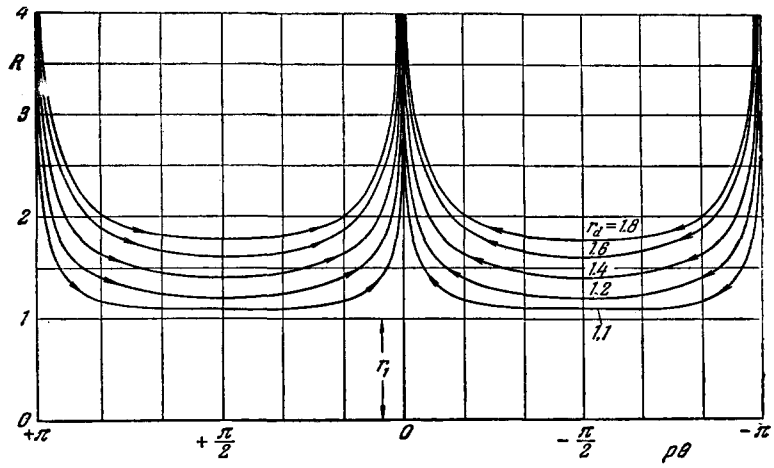

FIG. 16

$= -\Omega_2 + \dot{\varphi}$ where $\dot{\varphi}$ is determined by (6.28) and (6.30); therefore

$$\Omega_2' = -\left[\frac{\Omega}{2} + \frac{1}{2}\sqrt{\Omega^2 - 4C} + \frac{C}{\sqrt{\Omega^2 - 4C}}\left(\frac{r_0^2}{a^2} - 1\right)\right]. \quad (6.41)$$

As can be seen, Ω_2' is independent of R and therefore the phase φ and the radius a can have arbitrary values specified by the initial conditions. Consequently, the motion of the center of the electron orbit follows the trajectory Ψ' = const, which rotates in phase space with angular velocity $-\Omega_1$ around the origin. The center of the electron orbits move in this phase space with velocities $\dot{\theta}'$ and R', determined by Eqs. (6.39). The electrons revolve around the centers with angular velocity Ω_2'.

We have thus obtained a complete analytic solution for the motion of the electron in the working space of the magnetron. We do not investigate the entire electronic process in detail, as we did for the planotron. From expression (6.40) we can readily calculate all the electron trajectories; this problem is somewhat more complicated (compared with the planotron) but perfectly feasible. We merely point out that the magnetron has certain singularities compared with the planotron, as follows from the expressions obtained for the trajectories. In the case of oscillations of large intensity, when U is large and the second term in the right half of (6.40) is small compared with the first, the trajectories will approach those of the unperturbed motion, determined by the equation Ψ = const, where Ψ is given by (6.37). The corresponding family of trajectories in the $p\theta$, R phase plane is shown in Fig. 16. The individual trajectories of this family are characterized by different values of the radius R when $p\theta = \pm\pi/2$.

If we assume that the cylindrical surface $R = r_d$ is the supply surface (see Chapter II), then we can readily obtain the distribution of the electrons in the interaction space of the magnetron. As can be seen from Fig. 16, the motion of the centers of the electron orbits has the same tongue-like character as in the planotron (see Fig. 2), and consequently the results pertaining to the stability of the process, obtained in Chapter III for the planotron, are applicable also to the magnetron. The difference between the two devices arises when it is necessary to take into account the second term in the expression for Ψ'. Indeed, the trajectories Ψ' = const are no longer symmetrical but curved, owing to the acceleration Δf due to the inhomogeneity of the electrostatic field. These trajectories have a character reminiscent of the previously obtained perturbed trajectories in the plantron (see Fig. 4). They can be investigated in the same manner, so that we confine ourselves here only to mentioning the final results of interest to us.

It is seen from (6.40) that for specified magnetron dimensions the difference between the trajectories Ψ' = const and the trajectories Ψ = const depends only on the ratio U/C, i.e., on the ratio of the alternating electric field to the static field. When $U < U_c$ the trajectory Ψ' = const loses its tongue-like character and becomes a wavy line which runs around the cathode; then oscillation becomes impossible.

The critical value of U_c can be determined directly from the first equation of (6.39). Let us assume that the centers of the circular electronic orbits are generated on the supply surface $R = r_d$, and then the most important is phase focusing on this surface, which is realized by the first term in the expression for $\dot{\theta}'$, proportional to U; the second term, proportional to C, counteracts the phase focusing. When $U = U_c$, $R = r_d$, and $p\theta = -\pi/2$, these terms should add up to zero (see Chapter III), and then the motion loses its tongue-like character when $U < U_c$. We thus obtain a critical value

$$U_c = \frac{C}{r_2}\frac{r_0^2 - r_d^2}{\cos\left(\frac{r_d}{r_1}\right)^p}, \quad (6.42)$$

from which it is seen that the closer the radius of the supply surface r_d is to the radius r_0 given by (6.30), the smaller U_c.

The existence of a critical oscillation intensity in the magnetron, below which generation is impossible, is of interest primarily from the point of view of self-excitation of oscillations. Indeed, for generation it is essential that the intensity of the oscillations exceed the critical intensity. The initial oscillations, as is well known, are due to fluctuations in the electron cloud blanketing the cathode. Tentative calculations have shown that in this way one can hardly excite any oscillations with intensity above critical. It seems to us that a way out of this contradiction must be sought in the influence of the space charge on the self-excitation process. There is no doubt that because of the edge effect and the interaction between the circular orbits of the electrons, described in the preceding chapter, the interaction space becomes filled with electrons drifting on orbits of different radii. It can be shown that the space charges produced by the presence of the electron orbits in the working space will modify the electrostatic field in such a way, that its inhomogeneity along the radius will contribute to the motion of the centers of the electron orbits around the cathode with constant angular velocity. This will make the self-excitation of the oscillations easier.*

It is seen from (6.42) that the dimensions of the working space influence the value of U_c. With decreasing gap D of the working space ($D/r_1 \to 0$), r_0 tends to r_1, in accordance with (6.30), and U_c decreases. The smaller U_c, the easier it is for the magnetron to become self-excited. Inasmuch as the oscillating process occurs when $U > U_c$, the trajectories in the generation mode always have a tongue-like character. As follows from the foregoing analysis, under all conditions the phase velocities $\dot{\theta}'$ and $\dot{R}'$ are potential and solenoidal, so that all the conclusions concerning the uniform filling of the tongues with orbit centers, the mechanism of phase stability, the possibility of inverting the generation process to obtain direct current, etc., which were drawn from the analysis of the electronic processes in the planotron, remain wholly in force also for the magnetron.

In order to obtain the pattern of the motion of the electrons in the working space of the magnetron, we have calculated the trajectories of the orbit centers for $r_1 = 1$, $r_2 = 3$, $r_d = 1.2$, $p = 4$, and for the critical intensity of oscillations (6.42). The corresponding tongues are shown in Fig. 17 in cylindrical coordinates; the tongues proper, i.e., the regions where the centers of the electron orbits move, are shown shaded. If the electrons are emitted from the cathode surface, then the radius of the electron orbits will be $a = r_d - r_1$. For these initial conditions thinner lines, which indicate the boundaries within which electron motion occurs, are shown alongside the tongues. Inasmuch as we know the values of $\dot{R}'$, $\dot{\theta}'$, Ω_1' and Ω_2' we can

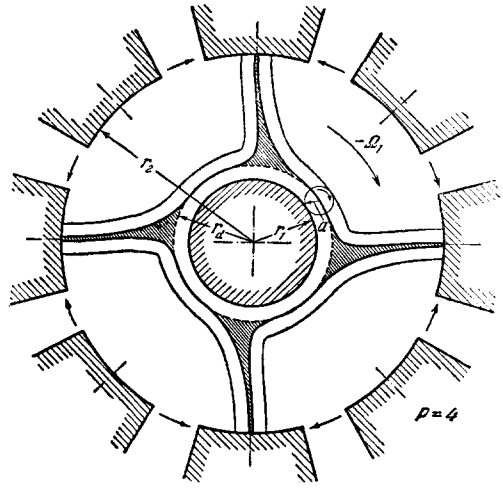

FIG. 17

readily plot the trajectories of the individual electrons.

Such trajectories are of no particular interest, since to calculate the characteristics of an electronic device it is necessary to know only the limits of all possible electron trajectories. In order to obtain these limits, at one time a calculation was undertaken of the individual electron trajectories by numerical integration, as described in an American paper "Magnetrons,"* and the boundaries of the tongues were obtained from them (see Fig. 15 of this paper). Comparing these numerical results with ours we see that they are in good agreement. A shortcoming of this numerical method is not that it calls for calculations which can be performed only with electronic digital computers, but that the trajectories obtained in this way do not make it possible to derive the required magnetron characteristics, for example to determine the space charge density, the critical U_c, the critical Q_c, the critical power P_c, etc.

Let us determine now the wavelength given by the condition (6.34). Inasmuch as the quantity $4C/\Omega^2$ under the square root is usually small, we obtain from (6.25) by expansion

$$\Omega_1 = \frac{C}{\Omega}, \tag{6.43}$$

$$\omega = \frac{pC}{\Omega}. \tag{6.44}$$

The quantity C is given by expression (6.29); changing over to wavelengths, we obtain

$$\lambda = \frac{2\pi H \bar{r} D}{pV}, \text{ where } \bar{r} = \frac{r_1 + r_2}{2}. \tag{6.45}$$

The cited paper gives the characteristics of several American magnetrons, in the wavelength range from 40 to 1.25 cm. The data which we need on these magnetrons are listed in Table II. The wave-

*See also the footnote on p. 791.

*Fisk, Hagstrum, and Hartman, Magnetrons, Bell Sys. Tech. J. 25 (2), 167-348 (1948).

Table II

$\bar{r}=\frac{r_1+r_2}{2}$, $D=r_2-r_1$, $N=2p$,

$\lambda=\frac{4\pi H\bar{r}D}{NV}$, $1-\eta_a=\frac{2mc^2}{e}\frac{V}{H^2D^2}$

Type	4j42	4j51	728Aj	5j23	4j2630	4j2125	5j22
λ (exptl), cm	43	32.1	32.1	28.6	24	22.8	23.4
λ (theoret), cm	47	29	32	31	21	24	26
$1-\eta_e$ (exptl), %	68	35	35	42	54	47	42
$1-\eta_a$ (theoret), %	21	19	18	21	20	20	25
p/S_a, kW/cm²	0.75	0.7	5.5	3.7	9.4	9.6	11.2

Type	718AyEy	714Ay	706AyGy	720AE	4j4547		
λ (exptl), cm	10.7	9.1	9.8	10.7	10.7		
λ (theoret), cm	12.6	11.2	9.2	11.2	9.4		
$1-\eta_e$ (exptl), %	47	47	45	32	32		
$1-\eta_a$ (theoret), %	24	25	24	23	17		
p/S_a, kW/cm²	13,6	14.5	15.5	44.0	61.1		

Type	2j4850	2j5560	4j52	4j50		3j21	
λ (exptl), cm	3.3	3.2	3.2	3.3		1.25	
λ (theoret), cm	3.57	3.30	3.56	3.44		1.47	
$1-\eta_e$ (exptl), %	48	50	31	34		63	
$1-\eta_a$ (theoret), %	28	48	38	29		40	
p/S_a, kW/cm²	17	40	45	110		100	

lengths calculated from formula (6.45) are also given in Table II; they agree sufficiently well with the experimental data. The existing discrepancies must apparently be attributed to the inaccuracy in the data pertaining to the dimensions of the working space of the magnetron. The principal source of this inaccuracy is the fact that temperature deformations occur during the course of operation both in individual parts of the device and in the fastenings connecting them. Calculations show that this inaccuracy alone is insufficient to explain the discrepancy between the theoretical and experimental data.

Let us calculate the anode losses. These, as is well known, are due to the kinetic energy with which the electron arrives at the anode. Inasmuch as both angular velocities with which the electron arrived at the anode are known, this kinetic energy will be, neglecting the velocities $\dot{R}'$ and $\dot{\theta}'$,

$$W_a=\frac{m}{2}(\Omega_1 r_2+\Omega_2 a)^2. \tag{6.46}$$

If the electrons are emitted from the surface of the cathode, then the radius of the orbit of the electron is determined from the initial conditions on the cathode. When $r = r_1$ the velocity of the electron is equal to zero and inasmuch as the angular velocities Ω_1 and Ω_2 remain constant during the course of motion, we have at the surface of the cathode

$$\Omega_1 r_1=\Omega_2 a \tag{6.47}$$

and formula (6.46) assumes the form

$$W_a=\frac{m}{2}\Omega_1^2(r_1+r_2)^2=2m\Omega_1^2\bar{r}^2. \tag{6.48}$$

Substituting the values of Ω_1 and C from (6.43) and (6.29) we obtain after simple transformations

$$W_a=\frac{2mc^2V^2}{H^2D^2}. \tag{6.49}$$

The total potential energy acquired by the electron on passing through the working space is

$$W=eV, \tag{6.50}$$

from which we obtain an expression for the relative anode losses:

$$1-\eta_a=\frac{W_a}{W}=\frac{2mc^2}{e}\frac{V}{H^2D^2}. \tag{6.51}$$

The quantities calculated from this expression are also given in Table II. The difference between the total losses obtained from experiment and the calculated anode losses can be attributed to the edge losses. As can be seen, this difference is always positive, and its value depends on the type of magnetron.

It was shown in the preceding chapter that the edge losses depend little on the power drawn, so that the larger the generator power the smaller their share in the total losses. Therefore they manifest themselves more in magnetrons, which operate with smaller load per unit surface. In the last row of Table II are listed the powers drawn per unit magnetron surface; it is seen from these data that the larger this power, the smaller the difference between the calculated anode losses and the total losses de-

termined from experiment. In short-wave magnetrons, where the power drawn is up to 100 kW/cm^2, this difference is small.

We could continue our investigations along the same path as for the planotron, and consider the influence of space charges in the magnetron, determine its maximum power, critical Q, etc. However, the results obtained above illustrate sufficiently well the effectiveness of the method developed above for the study of electronic processes in the magnetron. Further study of the magnetron characteristics must be based on material well verified by experiment, specially obtained to check the theoretical conclusions.

The power magnetron for continuous operation is of interest in high-power electronics. Such a generator is quite feasible, but in order to dissipate the heat due to the losses it must have large dimensions. This will cause it to contain a large number of cavities, and the cylindrical working gap with large radius of curvature will be narrow. The characteristics of such a device can be calculated, with accuracy fully adequate for practical purposes, using the simple formulas derived in the preceding chapters for planotrons. The expressions obtained for a magnetron of large dimensions should in the limit go over into the expressions derived for the planotron.

Let us show, in particular, that the magnetron stream function (6.40) goes over into the planotron stream function (3.02) when the number of cavities in the magnetron is increased. Indeed, then

$$\left.\begin{aligned} &\frac{R}{r_1}\to 1, \quad R-r_1\to B,\\ &\ln\frac{R}{r_1}=\frac{R}{r_1}-1-\frac{1}{2}\left(\frac{R}{r_1}-1\right)^2+\ldots\to\frac{B}{r_1}. \end{aligned}\right\} \tag{6.52}$$

The period of the planotron structure is $l = \pi/g$, therefore

$$\frac{2\pi r_1}{p}\to 2l=\frac{2\pi}{g}, \quad \frac{p}{r_2}\to g. \tag{6.53}$$

Using the connection between the functions sir and sinh (see Table I) we have

$$\mathrm{sir}\left(\frac{R}{r_1}\right)^p=\mathrm{sh}\left(p\ln\frac{R}{r_1}\right)\to\mathrm{sh}\frac{pB}{r_1}=\mathrm{sh}\,gB. \tag{6.54}$$

We also obtain

$$p\theta=\frac{p}{r_1}r_1\theta\to gA, \tag{6.55}$$

$$\sin p\theta\to\sin gA. \tag{6.56}$$

The additional term in (6.40) will tend to a constant value as $R/r_0 \to 1$, so that formulas (6.54), (6.56), and (6.40) will yield in the limit as $R/r_1 \to 1$ the same functional dependence of the stream function on gA and gB as formulas (3.02) and (3.09) for the planotron.

Therefore the expressions which we obtain for the critical values of the current, power, and Q, and also for other characteristics of the planotron, should yield (upon making the indicated substitutions) the correct order of magnitude even for small magnetrons. We have performed such calculations; their results also agree perfectly satisfactorily with the experimental data which were used above. Thus, even with this crude comparison we obtain agreement between the theoretical deductions and experiments.

VII. EXPERIMENTAL INVESTIGATION OF THE ELECTRONIC PROCESSES IN THE PLANOTRON

The initial task of our experiments was a study of the mechanism of the electronic processes which occur in the constant magnetic field, so as to use them in high-power electronics.

We chose to investigate the planotron. The theory of the phenomena occurring in the planotron, which was described in the preceding chapters, was developed in close connection with our experimental research, so that if we were to treat the problem chronologically, it would be necessary to describe the theory and the experiment in parallel, and not separately as we are doing it.

We started our experimental work with a planotron which we manufactured by the very simple means corresponding to the technical capabilities at our disposal. To obtain a homogeneous magnetic field we used a solenoid with inside diameter of 10 cm, in which a magnetic field up to 1,000 Oe could be obtained, and the dimensions of our first planotrons were chosen with this in mind.

A schematic diagram of the planotron with which we began our experiments is shown in Fig. 18, which also shows the principal electric circuit, while Fig. 19 shows a photograph of this device, already mounted in its holder. The resonant system (1), as can be seen from Fig. 18, is made up of 14 U-shaped resonators,

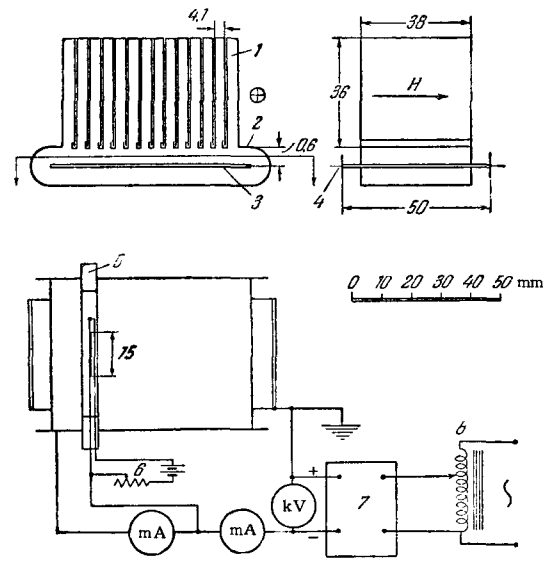

FIG. 18

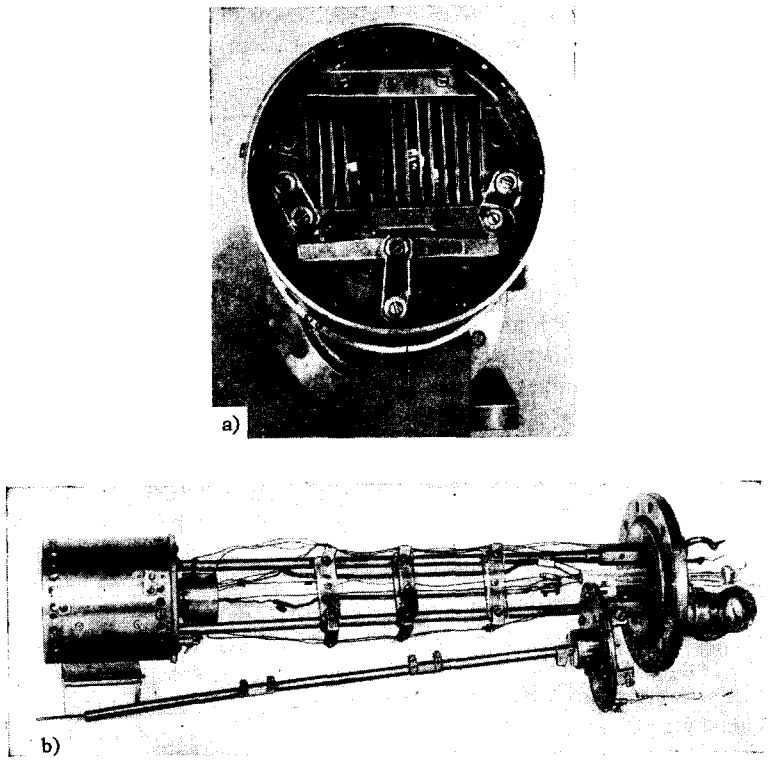

FIG. 19

made of bent copper foil 0.35 mm thick and held together by crimps on the ends. Their dimensions are indicated in the figure. The height of the working space was 0.6 cm; on the edges and on the side opposite the apertures of the resonators the height was limited by a solid wall (2) made of the same bent copper foil. The cathode was a copper plate (3) 2 mm thick, with protective shields (4) on its sides to prevent the electrons from leaving the interaction space laterally under the influence of their space charge. The electron emitter was a thoriated tungsten wire 0.12 mm in diameter with working length of about 1.5 cm; the emitter was mounted on a plate (5) which could be moved out from the cathode side. This plate was insulated from the cathode by a layer of mica on each side. This made it possible to measure the current from the emitter and the current to the cathode plate separately. The emitter was heated by a storage battery (6) the current from which was controlled with a rheostat. The insulation of the cathode (not shown in the figure) was by means of braces made of mica strips, on which the cathode plate was hung like a suspension bridge. The tube was placed in a container made of brass tubing. A vacuum was produced by an ordinary diffusion pump. To supply the direct current a small rectifier unit was used (7) with voltage up to 4 kV at 100 W. The voltage was regulated with a Variac (8).

The presence of electromagnetic oscillations in the system was detected and their intensity measured with a thermocouple of simple construction; it proved to be very convenient at the very start and we are still using it. Such a thermocouple is shown in Fig. 20 and consists of two identical plates (4) made of copper foil 3—4 mm wide and 0.15 mm thick. Each of the plates is cut in such a way that a very narrow strip (0.5—0.7 mm wide) is formed on the end. One plate is placed on the other in such a way that the narrow ends form a fork (2) and the ends of a copper-constantan or chromel-alumel thermocouple (TC) are clamped in the bent ends of the fork. The thickness of the thermocouple wires ranged from 10 to 30 microns with a total length of 4—5 mm. Both copper plates are clamped in a holder (3), made of beryllium-bronze foil (0.3 mm thick); the thermocouple holder is secured to the body of the planotron (1). The insulation between the holder and both copper plates was provided by a thin bent sheet of mica. The thermo-

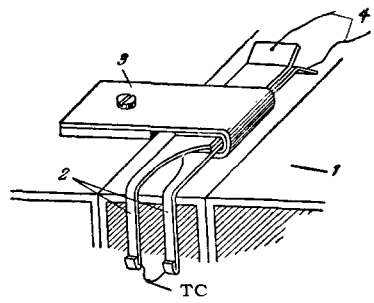

FIG. 20

couple is placed near the resonator in such a way that the magnetic field produced by the oscillations penetrates through the area of the fork (2).

The operating principle of such a thermocouple is obvious. The fork and the thermocouple together form the inductive part of the resonant circuit, the capacitive part being produced by the copper plates with the copper liners, clamped by the holder (3). This results in a tank circuit of relatively short oscillations period and large damping, so that the heating of the thermocouple can be regarded as proportional to the magnetic-field energy at constant frequency. Inasmuch as the area formed by the fork amounts to only a few square millimeters, this device operates more like a probe, since it influences the field little and does not affect the oscillation in the resonator. The ends of the thermocouple (4) are connected to a low-resistance short-period galvanometer (period 0.3 sec). The magnetic field of the galvanometer is chosen such that the entire system is critically damped. The resonant frequencies can be readily determined with the aid of such a thermocouple. By placing such thermocouples in various parts of the device we could determine the distribution of the oscillation energy in various locations of the planotron.

When we started these experiments, as was already indicated in Chapter III (see p. 791), it was not quite clear from general theoretical considerations whether a self-excited oscillating system could be produced in such a device. Our first task was therefore to ascertain whether self-excitation of such systems is possible.

The first experiments with the model planotron started in April of 1950, and immediately gave affirmative results. It turned out that the planotron, in spite of its simple construction, is readily self-excited; at an emitter current of 6 milliamperes and 1.04 kV a clear-cut resonance was observed and the galvanometer deflection indicated the presence of strong oscillations in the resonators. In subsequent experiments we measured the frequency by piping the oscillations to the outside with a waveguide and found the wavelength to be approximately 20 cm. To check whether these oscillations were actually produced by the resonators, metallic plates were inserted in the resonators; these should have decreased the wavelength and experiment confirmed this fact.

It was observed in the very first experiments that the onset of oscillations is very sensitive to the position of the electron emitter relative to the cathode plane. It turned out that even a small rise (several tenths of a millimeter) of the emitter above the cathode plane made self-excitation of the planotron impossible. Further observations have shown that the planotron operates best when the emitter is somewhat below the cathode plane. These observations served as the starting point for the development of the theory which takes into account the initial emission conditions and their influence on the electronic processes in the planotron. Further experiments and theoretical studies have led to the anode-loss theory which we have developed in Chapter IV (see p. 795) and following).

Even this simple planotron has shown that oscillations were produced at magnetic field values below critical when the emitter is recessed in the cathode. As is well known, at an above-critical magnetic field the height d_1 of the cycloidal electron trajectories should be lower than the height D of the working space (see Fig. 7), and then the anode efficiency is positive in accord with (4.12). The condition

$$d_1 = D \tag{7.01}$$

yields in accordance with (4.15) and (4.17) for the critical field a value

$$H_c = \frac{4m}{e}\frac{lc^2}{\lambda D}, \tag{7.02}$$

if the emitter is on the cathode plane. From the theory presented in Chapter IV it follows that when the emitter is recessed below the cathode plane the critical field can be reduced to $H_C/4$. All this indicates the significance of careful mounting of the emitter relative to the cathode plane. In later planotron constructions, provision was made for a special tension device for the emitter to keep it from bending as a result of the electrostatic and electrodynamic forces, and also to compensate for its thermal expansion. In subsequent planotron models it was possible to reduce appreciably both the operating magnetic field and the electronic losses.

The next observations made with this simple device have shown that the residual current is connected with processes that occur on the edges of the cathode. The copper or brass parts became partially covered after the experiment by dark spots due to a light deposit of copper oxide. These spots were observed following the flow of electric current, and their origin is easy to explain. The vacuum always contains some oxygen molecules which become ionized by electron impact. These ions diffuse to or are attracted by the copper surfaces and inasmuch as they are in a chemically active state, they form surface oxides. The spots therefore gave an idea of the electron distribution in the planotron. Upon disassembling the planotron we invariably observed, regardless of whether or not oscillations were produced, that on each side of the copper plate of the cathode there is formed a colored strip with a blurred edge facing the center. It followed therefore that the residual current flows along the edges of the working space. This pointed the way towards its theoretical explanation, which we developed in Chapter V.

During the study of this simple device the features of the electronic processes in the planotron were clearly disclosed: first—the possibility of self-excitation of such a system; second—the exceedingly

strong influence of the position of the supply plane (relative to the cathode plane) on the efficiency of the electronic process; third—the connection between the residual current and edge effects on the cathode and the high energy of the electrons returning to the cathode. However, such a device is of course not suited to determine the power characteristics. In particular, this planotron had the shortcoming that it overheated after 10 or 15 minutes, and it was necessary to wait about an hour before the experiments could be resumed. We had placed thermocouples on the body and on the cathode in order to follow their heat rise. It was observed that the cathode heating varied from experiment to experiment; this was principally connected with the recession of the emitter, which again pointed out the connection between all these phenomena and the character of the cycloid along which the electrons moved, and served as the starting point for the development of the loss theory developed in Chapters IV and V.

For further verification and development of the theory, we constructed a few other simple types of planotrons, which we describe briefly, mentioning only the problems solved by these devices.

It was of interest to ascertain the number of resonators of which the planotron could consist. For this purpose it was necessary to lengthen the planotron, so that the solenoid had to be replaced by an electron magnet. It was specially constructed and had the following main characteristics: number of turns—5,892, resistance—27.5 ohms; more than 50,000 ampere turns could be obtained at a power of 3 kW. The space between the poles was rectangular in form, 25 cm long and either 3, 5, or 8 cm high (as desired). The distance between poles was 4, 5, or 6 cm: accordingly, the maximum magnetic field was 4.5, 3.75, or 3.50 kOe. The homogeneity of the field without shims was ±(1—2)%. With shims it was possible to improve the homogeneity by a factor of three or four, which was sufficient. The magnet is shown on the photograph (Fig. 21), which shows also the entire experimental setup.

A photograph of the next planotron which we constructed is shown in Fig. 22. This planotron has precisely the same construction as the first, and is made up of simple U-shaped resonators, also made

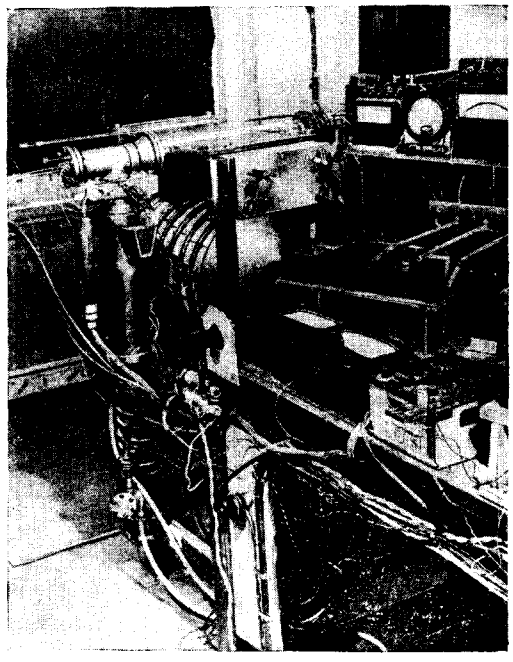

FIG. 21

of copper foil, except of smaller dimensions, and the number is increased from 14 to 97. The resonators are 12.6 mm high and 19.6 mm wide, with the total length of all resonators being 202 mm at a pitch l = 2.08 mm. The height of the working gap varied from 1.5 to 3.0 mm. The cathode was made as before of a copper plate. The emitter was again a thoriated tungsten wire with the same dimensions as in the preceding device. The emitter was installed on the cathode opposite the sixth resonator. Thermocouples were placed over the entire length of the instrument (the 10th, 24th, 55th and 82nd resonators) to determine the intensity of oscillation at these points.

The planotron was constructed with as high a precision as possible, although all the resonators were bent by hand on patterns. All the parts were outgassed in a vacuum furnace. The mountings and reinforcements were made of beryllium bronze. Experiment has shown that this planotron also generated successfully, and was even easier to self-excite than the preceding one, and furthermore over a wider range of voltages (from 2 to 5 kV at a suitable magnetic field).

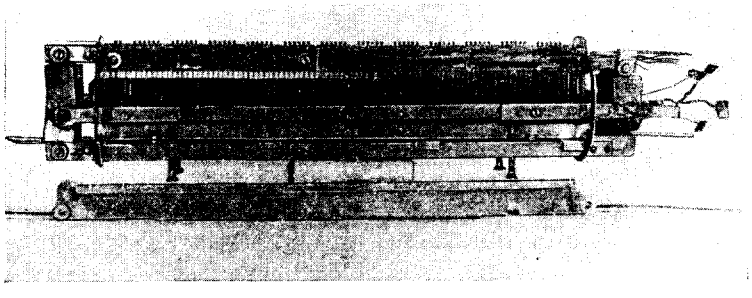

FIG. 22

The wavelength was not specially measured, but calculations showed it to be about 7 cm.

The experiments with this device have also confirmed that its operation is influenced by the height of the emitter above the surface of the cathode. If it was placed slightly outside the cathode or was recessed to a depth much larger than b_0 [Chapter IV, formula (4.19)], the self-excitation of the device became very difficult, large losses appeared, and the cathode overheated. All these phenomena were in agreement with the theory of losses in the planotron which we developed. The edge losses and the residual current were large in this tube; this caused it to become rapidly heated and thus greatly hindered the experiments.

In addition to solving the self-excitation problem for such a long planotron, we also investigated with the same tube the degree of coupling between the oscillations of the resonator system, namely whether the entire system of resonators oscillated as a whole. This was verified using four thermocouples arranged along the resonator system in the following manner. One thermocouple was connected to one galvanometer and any one of the remaining three could be connected at will to a second galvanometer. Both galvanometers had identical characteristics. The light beams of both galvanometers were projected along-side on a single scale. By varying the planotron mode we checked to see whether one beam followed the other. These experiments have shown quite definitely that even the beams from the extreme thermocouples followed each other and the oscillation energy was evenly distributed over the entire system of the resonators. We could therefore conclude the presence of a sufficiently strong electromagnetic coupling between the resonators. The supply conditions in this planotron were inconvenient, since only one emitter was placed on the cathode.

The subsequent work was connected with a study of the resonant system of the planotron. It constituted a system made up of a large number (say, n) resonators, which could oscillate relative to one another at different phases. This system thus has n degrees of freedom and a spectrum of n frequencies. The lowest frequency usually corresponds to an oscillation such that any two neighboring resonators oscillate in phase opposition; as in a multi-cavity magnetron, we have called these π oscillations. Obviously, depending on the intensity of the electric field $\mathscr{E}_{0y}$ in the working gap, it is necessary to choose for a fixed magnetic field H such an electron drift velocity, at which any of the n modes will be excited. This can actually be observed in the experiment.

The theory of excitation of any one of these modes can be simply developed in analogy with the theory described for the π mode in Chapter II. For this purpose it is merely necessary to obtain for the scalar potential Φ an expansion corresponding to expression (2.08).

In order to decrease the number of degrees of freedom of the resonant system, and also in order to raise the Q of the oscillating system, the latter can be constructed as shown in Fig. 23a. The resonator cavity (3) and the oscillating system are enclosed in a housing (2). The oscillations are detected through transverse slots cut in the upper part of the housing.* The electric oscillations of the resonators are coupled with the working space under the cathode (5) through a grid in which, as can be seen from the figure, three neighboring slots oscillate in phase and the fourth, which is at the midpoint, oscillates in phase opposition. By suitably expanding the potential Φ it is possible to show (by the same method as in Chapter II) that such a system will generate effectively.

The resonator housing was cooled in this plantron with running water (tube 4). The entire system was placed in a quartz bulb (1). A photograph of this device is shown in Fig. 23b. Experiment has shown that oscillations were easy to produce at a frequency that remained stable without jumping to neighboring frequencies corresponding to other modes.

The closed resonant system coupled with the working space by means of a reticular wall turned out to be the most effective resonant system for the planotron†.

It must also be pointed out that the oscillations could be excited in the system described not only at definite values of the electric field $\mathscr{E}_{0y}$ and magnetic field H, corresponding to the principal mode ($m_2 = 0$) when the drift velocity of the electrons is determined by relation (2.17), but also at other values of m_2, in agreement with the theory. Experiment has shown that the efficiency of excitation decreases in this case, as also follows from the theory. Thus, all the results of the experimental study of the processes in the planotron were in good agreement with the theory presented above. To investigate the power characteristics of closed oscillating systems of this type, experiments must be carried out with a device in which suitable pick-off of high frequency power is provided and effective cooling is produced. It can be seen beforehand that the indices will be lower than those attained in the magnetron (Chapter VI).

In conclusion, mention should also be made of a few features of the experimental techniques. The photograph (Fig. 21) shows the setup for the investigation of the planotron operation. Like the magnetron,

*By suitably placing these slots and by making the planotron sufficiently wide it is possible to produce through the quartz tube an intense well-directed radiation of high frequency oscillations from its entire length into the free space.

†The calculation of the oscillations in such systems and the method of placing the partitions in them is the subject of the article referred to in the introduction (see p. 777).

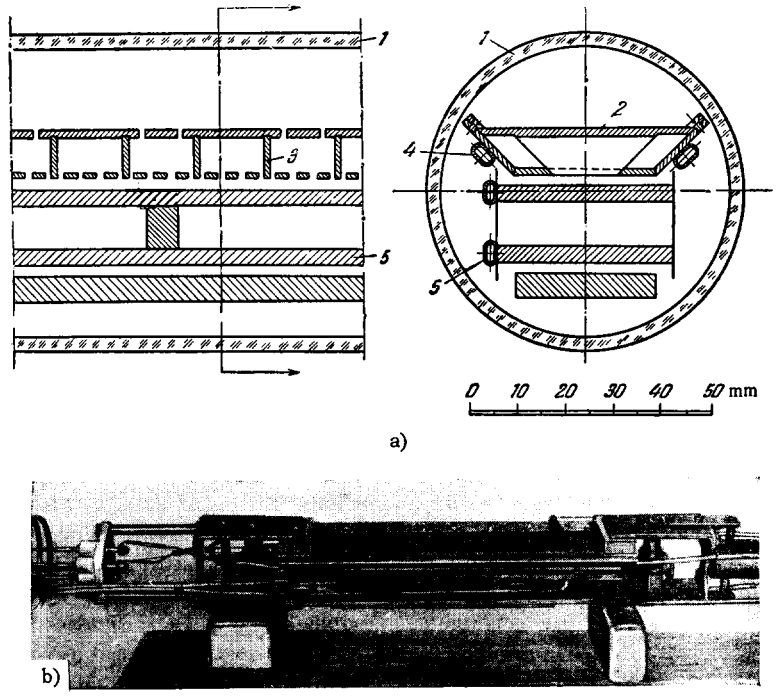

FIG. 23

the planotron generates stably and quietly in its working mode only in good vacuum (10^{-6}—10^{-7} mm Hg) and if all the surfaces, particularly in the interaction space, are well outgassed. Therefore, for the planotron to operate stably it is necessary that all parts be outgassed first in a vacuum furnace. In addition, even after assembly, it is conditioned prior to the experiment for several hours at 450°C, by small porcelain heaters (with a total power of 200 watts) attached to the planotron cathode. All metal parts of the planotron are made either of copper (M-I) or of beryllium bronze. The insulation is porcelain or quartz. When the planotron is heated to 450°C it is necessary that its construction provide for free expansion of the main parts relative to one another.

Even after thorough preliminary outgassing, an arc may be produced in the operating space and damage the planotron during startup. The following precautions are therefore necessary. The high voltage is first applied to the planotron through a chopper, which operates 50 times a second with a duty ratio 1/6. We also developed a high speed switch for turning on the high voltage. This switch is actuated by a thyratron ignited by the current flowing through the planotron and acting on the thyratron grid. The accuracy with which the limiting current flowing through the planotron was adjusted was several milliamperes, and the switching speed was one hundredth of a second.

As regards the manufacture of the planotron itself, particular attention must be paid to good contacts in the resonator, where the high frequency currents flow. Practice has shown that only silver soldering in vacuum can provide the required contact conductivity between the metallic parts.

In the last planotron, running water was used to cool not only the body but also the cathode. An independent cooling system for the body and for the cathode made it possible to separate the cathode losses from the total losses and to determine them by measuring the amount of heat carried away. In addition, knowing the total power supplied, we could determine the generated power and consequently the overall efficiency of the installation from the difference between the heat supplied and the heat carried away by the water. The efficiencies of various planotrons were close to the efficiencies that can be attained in magnetrons (see Chapter VI).

The operating efficiency of the planotron, like that of the magnetron, depends on the precision with which it is manufactured, particularly on the extent to which the dimensions of the working space and of the resonators can be maintained constant. The precision which we attained in the vital places reached several hundredths of a millimeter. Greater difficulties arose in connection with the need of establishing accurately the working plane of the emitter relative to the cathode plane. Depending on the operating mode, the depth of the emitter b_0 fluctuated between 0.2 and 0.5 mm (see Chapter V). A method for adjusting the emitter was developed, making it possible to hold these quantities to within several per cent. The most successfully operating were emitters made of tungsten wire; their position was fixed as accurately as possible by a specially developed spring tension mechanism.

Finally, a setup was developed making it possible to rotate the entire device in vacuum between the poles of the electromagnet so as to make the magnetic field precisely parallel to the plane of the cathode. This position was established by determining the minimum reverse (residual) current.

The procedures described were developed gradually, as the need arose. After all these improvements were made, we obtained a system with good operating stability.

VIII. LARMOR ORBIT IN HIGH-FREQUENCY FIELD

A distinguishing feature of the mechanism of generation in the planotron and in the magnetron is the fact that the resonant process is due to uniform "drift" of the electron cloud in the oscillating electromagnetic field, which has a periodic structure along the path of the cloud. Thus, in these processes, in order to produce the drift of the electron cloud it is necessary to employ crossed static electric and magnetic fields.

As shown in the preceding chapter, the effectiveness of the resonance is closely connected with the process of formation of the electron tongues. It turned out that this formation was hindered by the motion of the electrons along the circular orbits with Larmor frequency, a motion superimposed on the drift. This not only blurs the outline of the tongue, but in addition produces extraneous resonant effects, which give rise to losses. The most unpleasant resonances are those on the edges of the cathodes, which produce the harmful residual current. Therefore for effective generation in a planotron or a magnetron it is necessary that the radii of the Larmor orbits be as small as possible.

This raises the natural question of whether there are electronic processes in which the orbital Larmor motion can be employed. For this purpose this motion should be investigated in greater detail, as will be done now.

A distinguishing property of the Larmor motion is that the angular frequency of revolution Ω is independent of the radius of the orbit a (this, of course, is valid in the prerelativistic region, which is of interest to us). This property of the Larmor motion makes it possible to realize stable resonant processes over the entire volume of the electron gas without formation of electron clusters, something which may find independent application in electronics.

Using the averaging method developed in Chapter I, we investigate the effect of an alternating electromagnetic field on the Larmor motion of electrons, regarding it as a perturbation of the first fundamental case of motion given in expression (1.07). In the simplest case it is easy to show that when the electric field is plane and oscillating ($E_x = 0$, $E_y = E_0 \sin \omega t$), its resonant action on the motion of the electrons reduces merely to a change in the radius α of the Larmor orbit. The sign and magnitude of this variation are determined by the phase difference between the field, which oscillates with angular frequency ω, and the circular motion, which has a Larmor frequency Ω. Thus, the process is trivial and of no interest to us. But when the electric field is not homogeneous in space, then in addition to the change in the electron orbits there is also a displacement of the orbit centers, and motion of this type is already of interest in itself. To investigate such processes we choose the simplest form of an alternating electric field produced between coaxial cylinders; it turns out that it displays sufficiently well the properties of the resonant processes of this type. It is easy to see that in the case of necessity the same method of investigation can be extended to include also more complicated field configurations.

We assume that there is no electrostatic field, and that the alternating electric field has only one radial component, the value of which in the interaction space between the cylinders is inversely proportional to the distance r from the center. In the ordinary representation the field is written in the form

$$E_r = \frac{E_0 r_1}{r} \sin \omega t. \qquad (8.01)$$

According to (1.11), the acceleration F in the complex representation is

$$F = \frac{U(e^{i\omega t} - e^{-i\omega t})}{iz^*}, \qquad (8.02)$$

where

$$U = \frac{e}{m} \frac{E_0 r_1}{2}. \qquad (8.03)$$

The interaction space and the notation are shown in Fig. 24. The electric oscillations occur in a space bounded by radii r_1 and r_2, while the electron e revolves in an orbit with radius a, the center of which is located at a distance R from the origin O. The phase angles φ and θ are reckoned from the horizontal axis. The angle between the radius vectors a

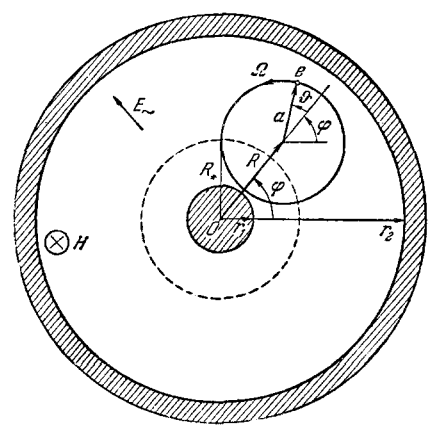

FIG. 24

and R will be denoted by ϑ, where

$$\vartheta = \theta - \varphi. \tag{8.04}$$

In the space between the coaxial cylinders two types of electron motion are possible. In the former type of motion a < R and the orbit does not enclose the origin O. In the second case a > R and the orbit encloses the center O. We shall start with an analysis of the first type.

Substituting in (1.18) the high frequency acceleration (8.02) we obtain

$$\left.\begin{aligned} \dot{\bar{\alpha}} &= -\frac{U\,(\overline{e^{i\omega t} - e^{-i\omega t}})}{z_0^*}, \\ \dot{\bar{\beta}} &= \frac{U\,(\overline{e^{i\omega t} - e^{-i\omega t}})\,e^{i\Omega t}}{z_0^*}. \end{aligned}\right\} \tag{8.05}$$

Using the notation in (1.23), we carry out the expansion

$$\frac{1}{z^*} = \frac{1}{Re^{-i\theta} + ae^{-i(\varphi - \Omega t)}} = \frac{e^{i\theta}}{R}\sum_{n=0}^{\infty} p^n e^{in(\vartheta + \Omega t)}, \tag{8.06}$$

where

$$p = -\frac{a}{R}, \quad -p < 1. \tag{8.07}$$

The resonance conditions have the form

$$\omega = n\Omega, \tag{8.08}$$

where the necessary averaging time is determined by the smallest frequency and is equal to

$$T = \frac{2\pi}{\omega}. \tag{8.09}$$

We then obtain after averaging, according to formulas (1.18)

$$\left.\begin{aligned} \dot{\bar{\alpha}} &= -\frac{U}{\Omega}\frac{p^n}{R}e^{i(\theta + n\vartheta)}, \\ \dot{\bar{\beta}} &= \frac{U}{\Omega}\frac{p^{n-1}}{R}e^{i(\varphi + n\vartheta)}. \end{aligned}\right\} \tag{8.10}$$

Let us replace the velocities $\dot{\bar{\alpha}}$ and $\dot{\bar{\beta}}$ in accordance with (1.23) and separate the real and imaginary parts; we then finally obtain the fundamental equations of electron motion in resonance

$$\left.\begin{aligned} \dot{R} &= \frac{U}{\Omega}\frac{p^n}{R}\cos n\vartheta, \\ \dot{\theta} &= \frac{U}{\Omega}\frac{p^n}{R^2}\sin n\vartheta, \\ \dot{a} &= \frac{U}{\Omega}\frac{p^n}{a}\cos n\vartheta, \\ \dot{\varphi} &= \frac{U}{\Omega}\frac{p^n}{a^2}\sin n\vartheta. \end{aligned}\right\} \tag{8.11}$$

In the integration of these equations we introduce the following initial conditions

$$a = a_0,\ \varphi = \varphi_0,\ R = R_0,\ \theta = \theta_0,\ \vartheta = \vartheta_0 = \theta_0 - \varphi_0 \text{ when } t = 0. \tag{8.12}$$

From the first and third equations of (8.11) we obtain

$$R\dot{R} - a\dot{a} = 0, \tag{8.13}$$

which gives the first integral of motion

$$R^2 - a^2 = R_0^2 - a_0^2 = R_*^2 = \text{const}. \tag{8.14}$$

Thus, the difference in the squares of the radii always remains constant; this means that the orbit never crosses the center, inasmuch as the condition R > a is satisfied all the time if it is satisfied at the initial instant d = 0. The radius R is always larger than the radius R_* to which the center of the orbit tends when the orbit contracts to a point:

$$a \to 0, \quad R \to R_*. \tag{8.15}$$

From the second and fourth equation of (8.11) we obtain

$$a^2\dot{\varphi} - R^2\dot{\theta} = 0. \tag{8.16}$$

This expression shows that the difference in the sectorial velocities of the electron on the orbit and of the center of its orbit remains constant. This is a kind of angular-momentum conservation law in phase space.

By virtue of the circular symmetry of the alternating electric field, its effect on the orbital motion of the electron is completely determined by the phase angle ϑ alone (8.04). Let us calculate now the difference $\dot{\vartheta} = \dot{\theta} - \dot{\varphi}$. Substituting the values of $\dot{\theta}$ and $\dot{\varphi}$ from (8.11) and using (8.14) and (8.16), we obtain

$$\dot{\vartheta} = -\frac{U}{\Omega}\frac{R_*^2}{a^2R^2}p^n \sin n\vartheta. \tag{8.17}$$

Combining this equation with the first equation of (8.11) we obtain

$$\dot{\vartheta}\operatorname{ctg} n\vartheta = -\frac{R_*^2\dot{R}}{(R^2 - R_*^2)R}. \tag{8.18}*$$

Integrating this equation, introducing the inital conditions (8.12), and using relation (8.14), we obtain

$$\left(\frac{a}{R}\right)^n \sin n\vartheta = \left(\frac{a_0}{R_0}\right)^n \sin n\vartheta_0, \tag{8.19}$$

which enables us to plot the trajectories in the phase space (a, nϑ). For this purpose we change over to rectangular coordinates

$$x = \frac{a}{R_*}\cos n\vartheta, \quad y = \frac{a}{R_*}\sin n\vartheta,$$

and obtain

$$\frac{a^2}{R_*^2} = x^2 + y^2, \quad \sin n\vartheta = \frac{y}{\sqrt{x^2 + y^2}}, \quad \frac{R^2}{R_*^2} = 1 + x^2 + y^2. \tag{8.20}$$

Putting further

$$\left(\frac{a_0}{R_0}\right)^n \sin n\vartheta_0 = \sin n\vartheta_a, \tag{8.21}$$

the equation of the trajectory assumes the form

$$y^2(x^2 + y^2)^{n-1} = (1 + x^2 + y^2)^n \sin^2 n\vartheta_a. \tag{8.22}$$

In the simplest case when n = 1 this equation becomes

$$y = \pm\sqrt{1 + x^2}\operatorname{tg}\vartheta_a, \tag{8.23}\dagger$$

*ctg = cot.
†tg = tan.

and we obtain a simple hyperbola with asymptotes that make angles $\pm \vartheta_a$ with the x axis.

Figure 25 shows the families of hyperbolas for resonance n = 1 at a fixed initial value a_0, but for different initial angles ϑ_0, so that all the possible initial values of the phase angle ϑ_0 lie in the initial circle of radius a_0. The trajectories break up into two identical families, symmetrical about the horizontal line y = 0. Using (8.17), we have designated (with arrows) the direction of motion on the trajectories. From the directions of the arrows it is seen that the sign of the velocity $\dot{a}$ depends on the initial angle ϑ_0; it is seen from Fig. 25 that all the trajectories for which $\pi/2 < \vartheta_0 < 3\pi/2$ decrease in radius as they move to a minimum value a_{min}, which when x = 0 lies on the intersection between the vertical axis and the trajectory. After intersecting the vertical axis, the radius begins to increase continuously. From (8.23) we obtain

$$a_{\min} = R_* \operatorname{tg} \vartheta_a. \tag{8.24}$$

The second part of the electrons with initial angles $-\pi/2 < \vartheta_0 < \pi/2$ increases in radius from the very start of the motion. The increase in the orbit radius a is actually limited by the dimensions of the working space, so that it continues until the electron collides with the outer cylinder of radius r_2. The largest possible values of a_{max} determined by this limitation are obtained from the relation

$$r_2 = R_{\max} + a_{\max}. \tag{8.25}$$

Using (8.14) we obtain for the largest possible values of a_{max} and R_{max}

$$a_{\max} = \frac{r_2^2 - R_*^2}{2r_2}, \quad R_{\max} = \frac{r_2^2 + R_*^2}{2r_2}. \tag{8.26}$$

Figure 25 shows the trajectories of motion for n = 1. It is easy to show, however, that for other values n the trajectories plotted in phase space with polar coordinates (a, $n\vartheta$) will be very similar to the trajectories given in Fig. 25. In the polar coordinates

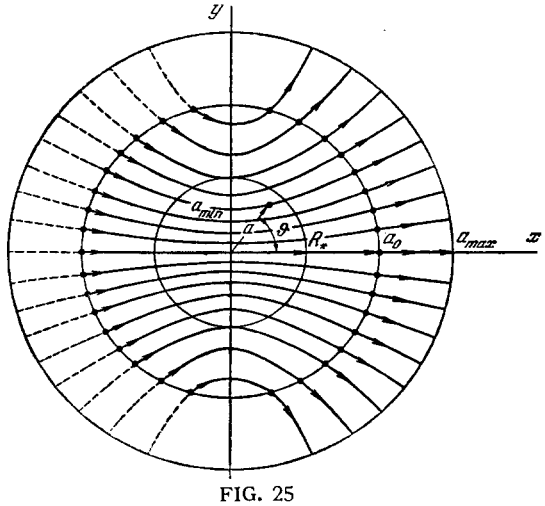

FIG. 25

(a, ϑ), the trajectories for the n-th resonance fill 2n sectors, in each of which there are identical trajectory families, similar to those shown in Fig. 25, but with the angle scale shrunk by a factor n.

Figure 25 shows an interesting singularity of the electron motion: they are repelled, as it were, from the internal cylinder, and in final analysis all tend to the outer cylinder, which they strike. The characteristic feature of the resonant action of the alternating electric field on the orbital motion of the electrons is that the centers of the Larmor orbits move into a region of lower field intensity. This process will occur even if the field has a more complicated structure than the radially symmetrical field considered above.

It is easy to see that the process will be accompanied by absorption of energy from the high-frequency field. Neglecting small phase velocities, we obtain for the electron kinetic energy the simple expression

$$W = \frac{m}{2} \Omega^2 a^2, \tag{8.27}$$

and therefore when $\dot{a} > 0$ the kinetic energy will increase at the expense of the energy of the alternating electric field, and when $\dot{a} < 0$, it will be transferred to the field. Let us assume that N electrons are formed per unit time in the interaction space for a specified value of initial radius a_0 and for arbitrary values of the initial angle ϑ_0. Then the electron critical energy will increase per unit time by an amount

$$P = N \frac{m}{2} \Omega^2 (a_{\max}^2 - a_0^2). \tag{8.28}$$

This power will be supplied by the alternating electric field and will be dissipated in the form of heat on the walls of the outside cylinder which the electrons strike. Thus, the presence of Larmor electron orbits with frequencies corresponding to resonance leads to absorption and dissipation of the field energy. The absorption of electromagnetic energy at resonance is a characteristic feature of Larmor orbits, so that their presence in an inhomogeneous oscillating field leads to losses. This property explains the reduced efficiency of planotrons and magnetrons when the Larmor frequency or its harmonic coincide with the fundamental frequency of the resonator field. Then the losses can occur not only in the working space, but the electrons can pass through the slots in the anode block into the cavities and there they can absorb energy by the mechanism just described.

The radius of some of the electrons with phase angles ϑ_0 between $\pi/2$ and $3\pi/2$, decreases at the start of the motion to a value a_{min}, and the electrons thus transfer part of their kinetic energy to the oscillation. The question arises whether this phenomenon can be utilized.

By modulating the initial phase angles ϑ_0 of the electrons entering into the interaction space, and by

extracting them at the proper time from the space, it is possible to effect generation, but it is difficult to visualize how to construct a simple device which will operate effectively as a generator. One cannot exclude the possibility that such a process (with low efficiency) takes place under natural conditions. If the electron orbit originates on the surface of the outer cylinder (this may be a secondary electron), and if the electrons are emitted with initial phase ϑ_0, at which their radius increases, they will immediately return to the wall of the cylinder without absorbing a noticeable energy from the field. But in the case of phase angles that lead to a reduction in the radius a of the orbit, the electrons will continue their motion without obstacle and their energy will be transferred to the alternating field. The radius will then start increasing again and resume its initial value, the electron will return to the outer cylinder, but if the electron moving along the magnetic field goes out of action sooner, striking the end boundary of the working space, then electromagnetic oscillations will be generated (in the final analysis). It is easy to see that the effectiveness of such a process will be very small but apparently fully adequate to explain the usual presence of weak oscillations with Larmor frequency has already been spectrum.

The intense resonant absorption of electromagnetic energy by an electron gas, which was analyzed here, can be used in practice in those cases when it is required to produce along the path of radio waves propagating in a waveguide a strong narrow-band absorption, corresponding to the Larmor frequency or its harmonic. It is possible that processes connected with Larmor motion can be utilized for isotope separation. The idea of a method for isotope separation using resonance with the Larmor frequency has already been proposed (see, for example, "Atomic Energy" by H. D. Smyth, where it is pointed out that J. Slepian did work in this field). Our analysis permits a quantitative study of the mechanism of processes of this type for the separation of isotopes and the determination of the best parameters of the equipment.

Isotopes can be separated in accordance with the scheme shown in Fig. 26. A constant magnetic field is produced by a solenoid (1); to make the field homogeneous over the major part of its length, the solenoid has more turns and iron discs (3) on the ends (2). The high-frequency electric field is produced in the working space between the coaxial cylinders (4) and (5). The oscillations are produced by generator (6). The ions of various isotopes will move along the Larmor orbits in place of the electrons. They enter into the working space from an emitter (8) and are accelerated by a dc voltage source (7). The circular orbits of the ions, which are formed at the emitter, move in the working space parallel to the cylinder axis toward the other end and, in the final analysis, the ions that are in

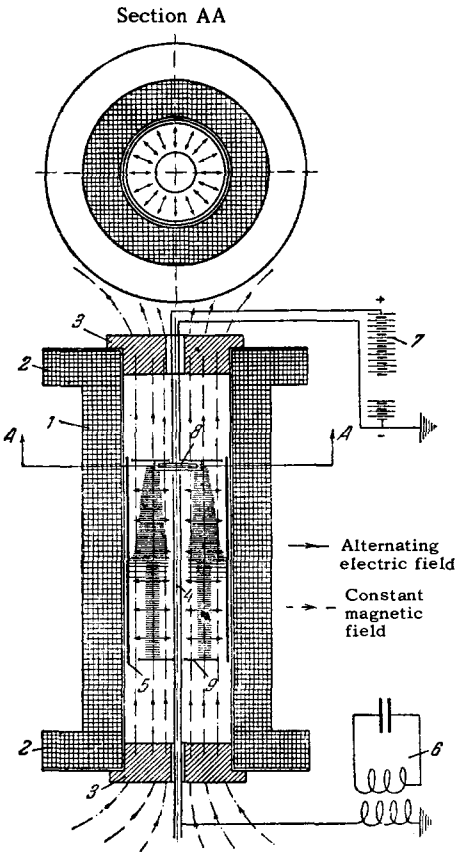

FIG. 26

resonance with the alternating electric field will gain kinetic energy of orbital motion along the path. Their radii therefore increase and they strike the wall of the outside cylinder (5), where they remain. The orbits of ions of different mass and of different Larmor frequency, for which the resonant condition is not satisfied, will not change noticeably in radius and will move along the magnetic field, so that they can reach the end discs (9) on which they settle. The separation process consists in having ions with different masses settle in different places—on the cylinder or on the end discs.

The frequency of the electromagnetic field ω is chosen such that only the orbits of the ions of one isotope enter in resonance with this frequency and only their radius increases. The separation method has that advantage that the yield does not depend on the degree of ionization of the atoms, for according to (1.02) the Larmor frequency is a multiple of the charge. Therefore if the resonance condition (8.08) is satisfied for a singly-charged ion, it will be satisfied also for multiply charged ions, but the resonance will occur simultaneously at several values of n; they will strike the same surface of the outside cylinder.

Inasmuch as the Larmor frequency of the ions in the same magnetic fields is many thousands of times

lower, and the radii of the orbits are many times larger than in the case of electrons, the apparatus for the separation of the isotopes, shown in Fig. 26, has large dimensions. For these processes, the frequency in ordinary magnetic fields, correspond to the 100-meter band. We have described only the general scheme of the device, but actually it is necessary to develop many details, for example, to produce an accelerating electric field in the working space between electrodes (8) and (9); it is important to develop an emitter capable of producing ion orbits with specified initial conditions. The construction of such an emitter is a difficult design problem.

The analysis of this method of isotope separation raises a few interesting problems; we merely point the way towards their solution but do not discuss the process in detail here. As in all electronic processes, the decisive factor in their efficiency is stability against perturbations. In this case we can investigate the perturbations in the same way as for the planotron and magnetron. The perturbing factor can be either the inhomogeneity of the magnetic field or additional orbit precession due to the electrostatic field of the space charge. The perturbation can be taken into account in the same manner as in (1.32), by regarding this perturbation as an additive action of a supplementary angular velocity $\Delta\Omega$ on the phase velocity $\dot{\varphi}$ of the ion in the circular orbit. The inhomogeneity of the magnetic field is determined by the value of the relative perturbation

$$\gamma = \frac{\Delta\Omega}{\Omega}. \tag{8.28'}$$

Let us introduce the perturbing angular velocity $\Delta\Omega = \gamma\Omega$ into the fourth equation of (8.11), obtaining the equation of the perturbing motion

$$\dot{\varphi} + \gamma\Omega = \frac{U}{\Omega a^2} p^n \sin n\vartheta. \tag{8.29}$$

Inasmuch as to maintain the character of motion the perturbing velocity $\gamma\Omega$ must be smaller than $\dot{\varphi}$, the stability of motion is determined by the condition

$$|\dot{\varphi}| > |\gamma|\Omega. \tag{8.30}$$

If we take in this condition the maximum amplitude $|p_0|$, we obtain

$$\frac{U}{\Omega^2}\frac{|P_0|^n}{a_0^2} > |\gamma|. \tag{8.31}$$

On the other hand, it is necessary that the motion be not so stable that orbits of isotopes with neighboring Larmor frequencies be subject to the resonant action. This action should be such that an increase in the radius a for the isotopes be smaller than the limiting radius a_{max}, so that these ions do not settle on the outside cylinder.

To consider the perturbed motion of the ions it is necessary to calculate their trajectory in the phase space (a, ϑ). For this we must solve the equations

$$\left.\begin{aligned} \dot{\vartheta} &= -\frac{U}{\Omega}\frac{R_*^2}{a^2R^2}p^n \sin n\vartheta + \gamma\Omega, \\ \dot{R} &= \frac{U}{\Omega}\frac{1}{R}p^n \cos n\vartheta, \quad a = \sqrt{R^2 - R_*^2}. \end{aligned}\right\} \tag{8.32}$$

We introduce the notation

$$x = R^2, \quad b = R_*^2, \quad y = \sin n\vartheta. \tag{8.33}$$

We then obtain a first-order linear equation

$$\frac{dy}{dx} + \frac{nby}{2x(x-b)} = (-1)^n \frac{n\gamma\Omega^2}{2U}\left(\frac{x}{x-b}\right)^{\frac{n}{2}}. \tag{8.34}$$

Solving this equation by the usual method with the previous initial conditions, we obtain after returning to the initial variables

$$\left(\frac{a}{R}\right)^n \sin n\vartheta = \left(\frac{a_0}{R_0}\right)^n \sin n\vartheta_0 + (-1)^n \frac{n\gamma\Omega^2}{2U}(a^2 - a_0^2). \tag{8.35}$$

We see from this formula that at sufficiently large a (when $a/R \approx 1$) the term containing the perturbation becomes the principal one and determines the character of the motion. It is easy to see that in this case the trajectory changes from a hyperbola with branches that go to infinity into a closed curve. Thus, the radius a will have a finite limit.

If the atomic weight of the separated isotope is M, while $M \pm \Delta M$ is the atomic weight of the neighboring isotope, then the trajectory of the orbit of the neighboring isotope is obtained from formula (8.35) by putting

$$\gamma = \frac{\Delta M}{M}. \tag{8.36}$$

It is seen from (8.35) that in order for one of the orbits of the next isotope not to have $a > a_{max}$, it is perfectly sufficient to satisfy the condition

$$\frac{\Delta M}{M} > \frac{4U}{n\Omega^2(a_{max}^2 - a^2)}, \tag{8.37}$$

which is obtained if the absolute value of the term containing the perturbation in (8.35) is set equal to 2 for $a = a_{max}$. This important condition, necessary for the separation, at the same time limits the amplitude of the alternating electric field, which reduces the productivity of this separation method. It is important to note that operation at higher harmonics ($n > 1$) makes it possible in accordance with (8.37) to employ larger values of U.

In order to visualize the perturbation of the trajectories, let us trace them in phase space (a, ϑ) as shown in Fig. 27 for $n = 1$. The quantity

$$B = \frac{2U}{n\Omega^2 R_*^2} \tag{8.38}$$

will be called the stability factor; we put $B/\gamma = 6$ in Fig. 27. As can be seen from this figure, the trajectories, which are now closed, are symmetrical about the vertical axis $\vartheta = \pm\pi/2$. A study of these trajectories makes it possible to determine more accurately

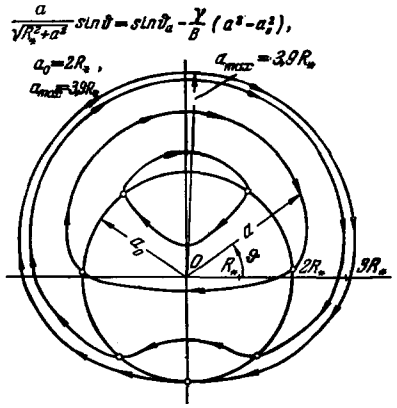

FIG. 27

the stability conditions, which were approximately given by formula (8.37).

In Fig. 27 we put $a_0/R_* = 2$ and $B/\gamma = 6$, and obtained $a_{max}/R_* = 3.9$, whereas the estimate leading to formula (8.37) was based on $a_{max}/R_* = 4$.

On the basis of the material presented we can if necessary carry out a similar complete numerical analysis of the processes which are essential in this isotope separation method, as was done in the preceding chapters for electronic processes in planotrons and magnetrons.

In conclusion we consider cursorily motion of the second type, when the electron orbits enclose the origin. In this case we obtain in place of conditions (8.07)

$$a > R, \quad -p = \frac{a}{R} > 1. \tag{8.39}$$

Then in the averaging we employ in place of the expansion (8.07) the formula

$$\frac{1}{z^*} = \frac{e^{i(\varphi-\Omega t)}}{a} \sum_{n=0}^{\infty} p^{-n} e^{-in(\vartheta+\Omega t)}. \tag{8.40}$$

Proceeding as before, we obtain under the same resonance condition the equations

$$\left.\begin{aligned} \dot{R} &= \frac{U}{\Omega}\frac{p^{-n}}{R}\cos n\vartheta, \\ \dot{\theta} &= -\frac{U}{\Omega}\frac{p^{-n}}{R^2}\sin n\vartheta, \\ \dot{a} &= \frac{U}{\Omega}\frac{p^{-n}}{a}\cos n\vartheta, \\ \dot{\varphi} &= -\frac{U}{\Omega}\frac{p^{-n}}{a^2}\sin n\vartheta. \end{aligned}\right\} \tag{8.41}$$

Introducing the previous initial conditions (8.12), we obtain

$$a^2 - R^2 = a_0^2 - R_0^2 = a_*^2, \quad a^2\dot{\varphi} - R^2\dot{\theta} = 0, \tag{8.42}$$

where a_* is the final value of a, equal to the minimum radius.

The motion is investigated in the same way and in final analysis it can be shown that the electrons, as in the preceding case, will draw energy from the field, increase their radii a, and strike the body of the cylinder. The phase diagram is similar to that shown in Fig. 25, but refers not to the radius a but to the radius R of its center.

It is easy to see that this case can be obtained from the preceding one by replacing n in all the expressions by −n.

In conclusion it can be pointed out that motion in which the orbits enclose the center of the working space are difficult to realize in experiment. Motion of this type is presently encountered in practice in cyclic accelerators.

IX. PROSPECTS OF HIGH-POWER ELECTRONICS

The theory developed by us and the experiments described point to the promising nature of electronic processes in high-power energetics.

The theory shows that high-efficiency high-power generators for microwave frequencies are feasible. Generators of the planotron and magnetron type, which have the same excitation mechanism, apparently point the way towards the development of high-power electronics. We consider most promising the development of such methods for the generation of microwave power, in which the oscillations are excited directly in the waveguide. This is accomplished by strong coupling between the oscillations in the working gap of the planotron or the magnetron and the oscillations in the waveguide. An example of a generator operating on this principle is the planotron shown in Fig. 23.

For the development of high-power electronics it is essential to learn how to use planotrons and magnetrons which operate in the inverted mode, i.e., which transform the high-frequency power into dc. The feasibility of such inversion was considered theoretically in Chapter II, where it was shown that this process will be just as stable and as effective as the direct process, wherein microwave oscillations are generated.

In order to outline more specifically the ways towards realization of high power processes, which make use of the advantages of microwave frequencies, I present here a few characteristic examples of such power processes and will sketch a possible scheme for their realization. These examples, of course, must be regarded only as tentative and possible solution schemes, but not as specific designs.

One important and interesting problem in high-power electronics is the transmission of electric energy over waveguides. Unlike transmission over wires, the energy flux does not come in the waveguide from outside the wire, but from inside the tube.

The technical advantages of power transmission by waveguide are obvious. Modern high-voltage ac or dc transmission lines have many known shortcomings, due to their open character. They can be damaged by lightning discharges, overvoltages can arise, corona

discharge may be produced, etc. This does not occur when power is transmitted in waveguides, since the entire process occurs in a tube which can be buried underground. Of course, from the point of view of safety, transmission in tubes also offers many advantages.

It is well known that in any electric transmission line the energy flux comes from outside the conductor. The maximum power which can be transmitted along the line is determined by the integral of the Poynting vector

$$P = \frac{c}{8\pi} \int [\mathbf{EH}]_z \, dS, \qquad (9.01)^*$$

where c is the velocity of light, **E** and **H** the amplitudes of the electric and magnetic field intensities in the transverse cross section (z = const) of the transmission line, and dS an area element of this cross section outside the metal. In order to transmit large power, the field intensity must be made as large as possible. In practice **E** is limited by the dielectric strength of air. In an ordinary transmission line the most dangerous breakdown location is the surface of the wire itself, where **E** reaches its maximum value; transmission lines must therefore use wires of large cross section. The same expression (9.01) holds true for power transmission over waveguides, so that for large amounts of power **E** will also have to be large. Inside a waveguide, however, the field is distributed more uniformly over the cross section than in the case of a cylindrical wire, so that breakdown is more difficult. This uncovers the possibility of transmitting large power in waveguides of small cross section.

For example, if we allow a five-fold safety factor in the dielectric strength of air, assuming the permissible field intensity to be 6,000 V/cm, we obtain from (9.01) that one square meter of waveguide can carry as much as a million kilowatts.

Another advantage of the waveguide is that the question of insulation is completely eliminated in spite of the high voltage. All this makes a waveguide a reliable means of transmission of high power.

The economy of this transmission method is less obvious. This question is connected, first, with the energy factors of the planotrons or magnetrons connected at the terminals of the transmission line. On the transmitting end of the transmission line the planotron will transform direct current into high frequency; on the receiving end, the planotron will transform the high frequency into direct current. The planotron operating characteristics have been discussed in the earlier chapters, and there are grounds for predicting theoretically that with time its efficiency will become sufficient for economic operation of transmission lines.

*[EH] = E × H.

With respect to the losses in the transmission line itself, we are faced with great difficulties in principle. Owing to the skin effect, current at high frequencies flows through a thin layer on the wall of the waveguide. On the one hand this is an advantage, for thin metallic coverings may be sufficient, but on the other hand such current flow is accompanied by large ohmic losses. By way of an example let us take a rectangular waveguide of height b and let us transmit through it an energy in the H_{10} mode. We then find that if the waveguide walls are copper covered, the initial transmitted power P_0 will attenuate along the length L in accordance with the formula

$$P = P_0 \exp\left\{-\frac{6{,}1 \cdot 10^{-5}}{\sqrt{\lambda}} \frac{L}{b}\right\}, \qquad (9.02)$$

where λ is in centimeters. It follows from this expression that at λ = 100 cm and b = 2 meters, 10% of the transmitted power will be lost over a distance L = 32 kilometers.

In the H_{10} mode, the electric flux lines start and end on the waveguide walls, so that appreciable currents are produced in it. If we use a cylindrical waveguide in the H_{01} mode, the electric flux lines in which are closed and form rings, there will be much less current flowing in the waveguide walls and lower loss. In this case we have so to speak a freely propagating wave with axial symmetry, and the task of the currents flowing in the waveguide walls reduces to a neutralization of the tendency of the wave to move out in a radial direction. As is well known, in this case the losses in a cylindrical waveguide of radius r with copper walls are determined by the expression

$$P = P_0 \exp\left\{-\frac{3.5 \cdot 10^{-5}}{\sqrt{\lambda}} \frac{\lambda^2 L}{r^3}\right\}, \qquad (9.03)$$

where λ is again in centimeters. Unlike the preceding case, the losses here decrease sharply with decreasing wavelength. If we take by way of an example a waveguide for which r = 1 meter, then the power loss at λ = 3 cm and at a distance L = 1,000 kilometers will be merely 10%, and the power which can be transmitted over this waveguide without exceeding the permissible field intensity will amount to 4 million kW. From expression (9.03) we see that the losses decrease rapidly with increasing radius of the tube. As is well known, however, the H_{01} mode has low stability and, unlike the H_{10} mode, it can rapidly degenerate; therefore, in spite of such favorable factors, the question of its use is not so simple, since it involves the known problem of stabilizing the H_{01} mode in a cylindrical waveguide. It is easy to predict that the advantages of power transmission over waveguides will become manifest to full degree if superconductors operating at normal or near-normal temperature are developed.

Figure 28 shows schematically a waveguide transmission line and the diagram of two planotrons, one operated by a dc generator and the other feeding a dc line.

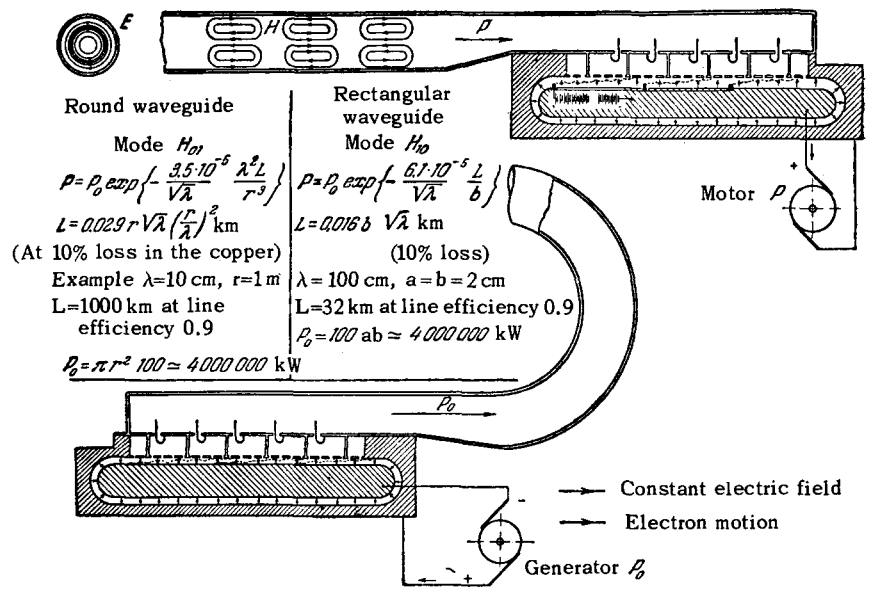

FIG. 28

At the present stage we confine ourselves only to a general description and do not stop to discuss the solution of many important technical problems necessary to realize such a transmission system, for example the matching of the load to the generator, the stability of the transmitted wave in the waveguide, etc.

It is interesting to note that if a high-power waveguide transmission line is ever realized, it will also be possible to tap electricity from it by smaller waveguides. The possibility of channelling electric energy of considerable power along uninsulated tubes can solve many important technical problems. For example, no particular difficulty is involved in using this high-frequency power for direct heating; for this purpose it needs be merely channeled through the tubes to a metallurgical furnace, where it will be absorbed and produce very high temperatures without the use of special electrodes. Electricity of sufficiently high frequency can be guided without insulation through tubes in wells to heat the ground at large depths, a procedure which can be useful in the extraction of sulfur, heavy oils, etc.

When large values of high-frequency power are used in closed buildings, it must be kept in mind that the electromagnetic oscillations can readily leak outside through very narrow slots; this is frequently a serious obstacle.

The effective generation of high frequency oscillations and the inversion of direct current uncovers the possibility of transmitting electricity through free space. The transmission scheme will of course be analogous to that considered here, except that the waveguide will be replaced by a directional beam which, as is well known, diverges little only at short wavelengths. Such a transmission system, first conceived by N. Tesla many years ago, has been under discussion for a long time. Although it is possible in principle, it entails the solution of many complicated technical problems and can therefore be realized only in those special cases, when other energy transmission methods are impossible (for example, power supply to artificial satellites).

In connection with the channelling and application of high-power microwave oscillations it is apparently advantageous to use the planotron for the conversion of one frequency to another. The possible realization of such a process is simple, and its nature is readily seen from Fig. 29. The planotron is equipped for this purpose with two independent resonant systems, each with its own natural frequency. These systems are so arranged that the interaction space of one system is a continuation of the interaction space of the other.

Let us assume that the resonator system shown on the top of Fig. 29 receives energy from a waveguide. In this case the direction of the electric field in the interaction space is such that the electrons drifting from left to right move transversely to the interaction space in a direction opposite to the constant electric field and acquire potential energy on account of the absorbed oscillation energy. When these electrons enter the lower part of the interaction space, the process reverses sign and the electrons will give up their energy to the other system of resonators, which already oscillates at the frequency of the load. Thus, energy received at one frequency will be delivered with a different frequency. Such frequency converters may assume practical significance in time, when smaller waveguide diameters are used in the couplers for the high frequency power channelling systems, and when it may become necessary to increase the frequency in order to satisfy the critical conditions

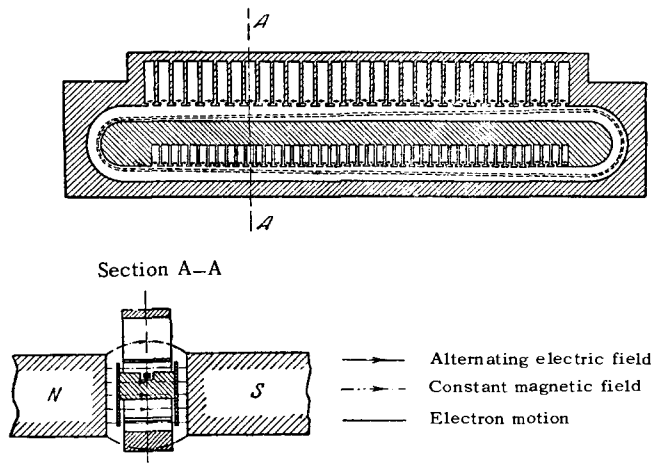

FIG. 29

imposed on the wavelength by the waveguide dimensions.

The mechanism of the electronic process in the planotron uncovers many interesting possibilities, the most promising of which we consider to be the use of the planotron as a linear accelerator. This possibility becomes quite understandable if we visualize a beam of charged particles moving over the gaps of a radiating planotron. If the distance between the gaps is reconciled with the law of motion of the particles, it is possible to choose the frequency and intensity of the mode in such a way that the particles moving over the gaps will be only under the influence of the accelerating action of the electric fields produced by the oscillations in the cavities. By varying the distance between the cavity gaps in the interaction space it is also possible to vary the drift velocity of the tongues. This can be done simply by varying smoothly the distance D between the cathode and the anode. In practice it is possible to realize such a system by various means; one is shown in Fig. 30. It is based on using two planotron resonant systems, with the accelerated beam passing through the center. The slots of the opposite ends of the resonators face both working spaces. The system has a magnetic loop in which there is no component of the magnetic field in a direction perpendicular to the motion of the particles along the line where the acceleration of the particle stream takes place. From a comparison of the operating principle of such a linear accelerator with ordinary systems we see that in this case the oscillations of the accelerating field are made coherent by a strongly coupled system of resonators, and that the energy is fed continuously along the entire path over which the acceleration takes place. Consequently, the energy supply does not become more difficult with increasing length of the accelerator, nor is the synchronism of the oscillations disturbed.

I believe that this short summary already shows that the planotron offers much promise for the realization of many fundamental problems of high-power electronics. It must be pointed out that some of the foregoing problems can also be solved successfully with the aid of a magnetron, but such a magnetron must be large and its construction would have little in common with the ordinary pulsed magnetron. The cylindrical cathode would have to be of large radius, separate emitters would be necessary, and the number of cavities would have to be large. From the magnetron theory developed in Chapter VI it follows that under such conditions the electronic process in the magnetron is practically identical with that in the

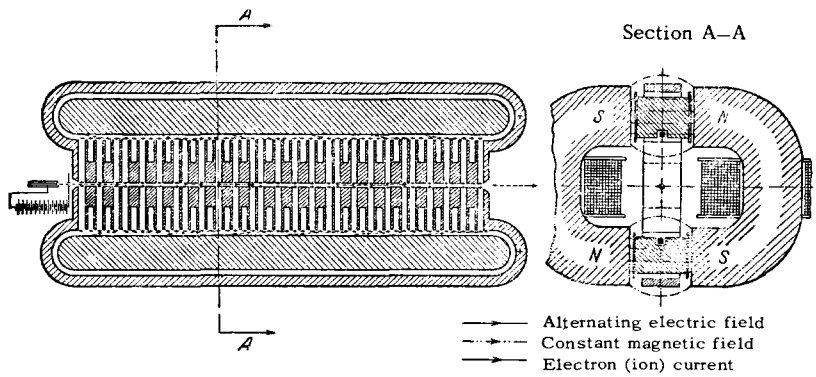

FIG. 30

planotron, and would have theoretically the same high qualities. In such high-power magnetrons, the magnetic field will be produced by a solenoid and it is possible to dispense with the iron.

The question of the use of resonant interaction between electromagnetic oscillations and electrons that revolve on Larmor orbits, as applied to high-power electronics, was already analyzed in the preceding chapter. It was shown there that these processes are little suitable for effective generation of high frequency, but may turn out to be quite useful for selective absorption of electromagnetic oscillations. As is well known, effective selective absorption of short radio waves propagating in waveguides does not have a simple solution, so that an absorbing device which operates on a new principle can prove to be useful. Such an absorbing device can be made in the form similar to the isotope separator shown in Fig. 26. The dimensions of the electron orbits are much smaller than the dimensions of the ion orbits, so that the instrument will be much smaller in size than the one for isotope separation, and will absorb short radio waves (in the centimeter and decimeter bands). The ion emitter (8) is now replaced by an electron emitter. The end disc (9) will be missing, in order to permit the instrument to be connected to a waveguide as a terminal coaxial line.

With the aid of the averaging method developed in Chapters I and VIII it is possible to show that if any oscillation mode is established in the waveguide and an electron gas is present in the magnetic field, selective absorption of the oscillations with a frequency multiple of the Larmor frequency will always occur. The prospects of the use of resonance with Larmor frequency for the separation of isotopes follows from an analysis made in the preceding chapter, and we shall not return to this problem.

The electronic processes which we have considered in the present paper have, of course, not been well studied as yet, but as they are mastered, prospects will be uncovered in high-power electronics which at present cannot be predicted. During the course of work on high-power electronics it will be necessary to solve many interesting problems, both theoretical and experimental. Further development of high-power electronics will proceed with an ever increasing rate. This will depend not only on the time necessary for the solution of the theoretical and experimental problems, but principally on the extent to which the need for solving the corresponding problems has arisen.

Translated by J. G. Adashko